COMPOSITION AND FORMATION OF THE *SACCHAROMYCES CEREVISIAE* CENTROMERIC NUCLEOSOME

By

Raymond Anthony Camahort
B.S., University of California, Santa Barbara, 2001

Submitted to the graduate degree program in the Department of Biochemistry and Molecular Biology and the Graduate Faculty of the University of Kansas in partial fulfillment of the requirements for the degree of Doctor of Philosophy

_____
Dr. Jennifer L. Gerton, Chairperson

Committee Members:

_____
Dr. Glen K. Andrews

_____
Dr. Joan W. Conaway

_____
Dr. Kenneth R. Peterson

_____
Dr. Patrick E. Fields

Date defended: 11/14/2008

The Dissertation Committee for Raymond Anthony Camahort certifies
that this is the approved version of the following dissertation:

COMPOSITION AND FORMATION OF THE *SACCHAROMYCES CEREVISIAE*

CENTROMERIC NUCLEOSOME

Committee:

_____
Dr. Jennifer L. Gerton,
Chairperson

_____
Dr. Glen K. Andrews

_____
Dr. Joan W. Conaway

_____
Dr. Kenneth R. Peterson

_____
Dr. Patrick E. Fields

Date Approved: _____

Acknowledgements

The completion of this dissertation had been a very long journey. As I reflect back upon that journey I can't help but realize all of the people in my life that have helped make this possible. I have been blessed with so many people in my life who have supported me, and even though I was by myself in the middle of the country, I never felt alone. I would like to mention a few of those people below.

- I would like to especially thank my mother Linda. If it wasn't for everything she taught me, and for and everything she sacrificed to make sure I always stayed on the right path, I would not be where I am today. I love you mom.

- I would like to thank my 3 sisters Star, Maria and Andrea, and my brother and best friend Jim White. They are more important to me then they could ever realize.

- I would like to thank my oldest and dearest friends Dan and Dane. Thank you for coming to KC to see me finish. It meant a lot. "D-Fence!"

- I would like to thank my graduate advisor Jennifer Gerton. She is one of the smartest people I know, a great mentor, and my friend. I also would like to thank her big ugly father Tom Gerton for always being there for me, and for being the second best boss I ever had.

- Finally, I would like to thank my many colleagues and collaborators at the Stowers Institute, KU Med, and elsewhere. So many people have helped me to become a better scientist, and I will always be grateful.

Abstract

The kinetochore is a complex, multi-protein structure required for proper chromosome segregation in all eukaryotes. The *Saccharomyces cerevisiae* kinetochore consists of over 65 known proteins which work in concert to facilitate equal distribution of the replicated genome. The *S. cerevisiae* CenH3 histone variant Cse4 is an evolutionarily conserved histone H3-like inner kinetochore protein that is essential for kinetochore function. Through immunopurification of Cse4 interacting proteins we have identified the previously uncharacterized protein Scm3. Here we report the characterization of *S. cerevisiae* Scm3, an essential protein with putative orthologs in fungi which possess either point or regional centromeres. We find that Scm3 localizes to all budding yeast centromeres. Construction of a conditional allele of *SCM3* has allowed us to characterize the phenotype of cells lacking Scm3. Scm3 depleted cells fail to properly localize the components of the inner kinetochore, including Cse4 and Ndc10, and arrest in metaphase with duplicated spindle poles, short spindles, and unequal DNA distribution in the daughter cells. Our data suggest that Scm3 is not an actual component of the centromeric nucleosome, but rather intimately associates with it. Additional *in vivo* and *in vitro* analysis of Cse4 reveals a single centromeric nucleosome that contains an octamer of Cse4, H2A, H2B, and H4. Based on these findings, we hypothesize that Scm3 is a novel yeast inner kinetochore protein that functions in the formation and maintenance of a segregation competent kinetochore through recruitment of the Cse4 octameric nucleosome.

TABLE OF CONTENTS

List of Figures

List of Tables

List of Appendices

CHAPTER 1.

Background and Significance

I. The Cell- The Functional Unit of all Living Organisms

In all living organisms the cell is a self-maintaining unit which carries out a number of functions essential for the organism's survival. Since the invention of the microscope in the 17th century, the structure and function of individual cells has fascinated and perplexed generations of scientists. The term "cell" was coined in 1865 by British Scientist Robert Hooke [1]. His groundbreaking work on cork cells led to the general acceptance of the cell as the smallest individual unit of life. Now, almost a century and a half later, scientists are still using the knowledge obtained from studying individual cells to further understand the complexities of basic biological processes.

One of the most important functions of the cell is to replicate and make progeny cells. This process, known as cell division, occurs in all living organisms, from the smallest single-celled bacteria to the largest creatures on Earth. In order for the cell to make an exact copy of itself, it must transfer a copy of its genetic material into the newly formed daughter cell. Armed with this genetic blueprint, the daughter cell will have the means to grow and function in the manner specific to its cell type.

1. Budding yeast as a model system

Every living organism studied can be classified into either one of two groups-

prokaryotes and eukaryotes. Prokaryotes are the simpler of the two, and consist solely of single celled organisms, including all archaea and bacteria. Prokaryotes typically have a circular DNA genome and are devoid of a nucleus or any other membrane bound organelles. Eukaryotes are more complex with the majority of species being multi-cellular. The eukaryotic genome is found within a well-defined, membrane-bound nucleus. In addition, many eukaryotic cells contain other membrane-bound organelles such as mitochondria, chloroplasts and Golgi bodies. Of the single-celled eukaryotes, one of the most thoroughly researched is a type of fungus named *Saccharomyces cerevisiae*, or as it is more commonly known, budding or baker's yeast. *S. cerevisiae* has been used in baking and fermenting alcoholic beverages for thousands of years, and more recently has been utilized as a very robust model system for studying the fundamental aspects of molecular and cellular biology. The cell cycle of a budding yeast cell is very similar to the cell cycle in humans, and therefore the basics of many cellular processes such as DNA replication, recombination, cell division and metabolism are very comparable to its human counterpart. Budding yeast can reproduce sexually or asexually and can exist in either a haploid or diploid state. In 1996, *S. cerevisiae* was the first eukaryote to have its entire genome sequenced [2]. The Yeast Genome Project revealed the budding yeast genome is composed of about 13,000,000 base pairs of DNA arranged onto 16 chromosomes, which code for approximately 6000 functional genes. This is compared to the human genome, which is estimated to contain approximately 25,000 genes, and spans over 3,000,000,000 base pairs of DNA [3]. The simplicity of the

yeast genome and the ease of genetic manipulation make it an excellent model system to study basic biological processes.

II. The Basics of Chromatin

Compared to their prokaryotic counterparts, eukaryotic genomes are very large. In order to accommodate the DNA within the confines of the nucleus, the genome is packaged in such a way that achieves a high level of compaction, while maintaining transcriptional accessibility. The cell accomplishes this feat by tightly wrapping its DNA around a protein core to form a structure called chromatin. Although eukaryotic organisms differ drastically in their appearance and cellular function, how they package DNA into chromatin remains relatively well-conserved.

1. Chromatin packaging and the histones

In all eukaryotes DNA is packaged into a higher order structure known as chromatin. Chromatin by definition is DNA in a complex with the histone proteins which forms a higher order structure. The histone proteins are an evolutionarily conserved group of proteins which interacts with DNA to form chromatin. There are four core or canonical histones: H2A, H2B, H3, and H4. Additionally there is a linker histone known as H1. For chromatin to be formed, DNA acts non-specifically with an octamer consisting of a heterotetramer of H3-H4 ($H3_2$-$H4_2$), and two heterodimers of H2A-H2B; this forms the core particle or nucleosome. The nucleosome is highly conserved between species and is composed of 146 base pairs

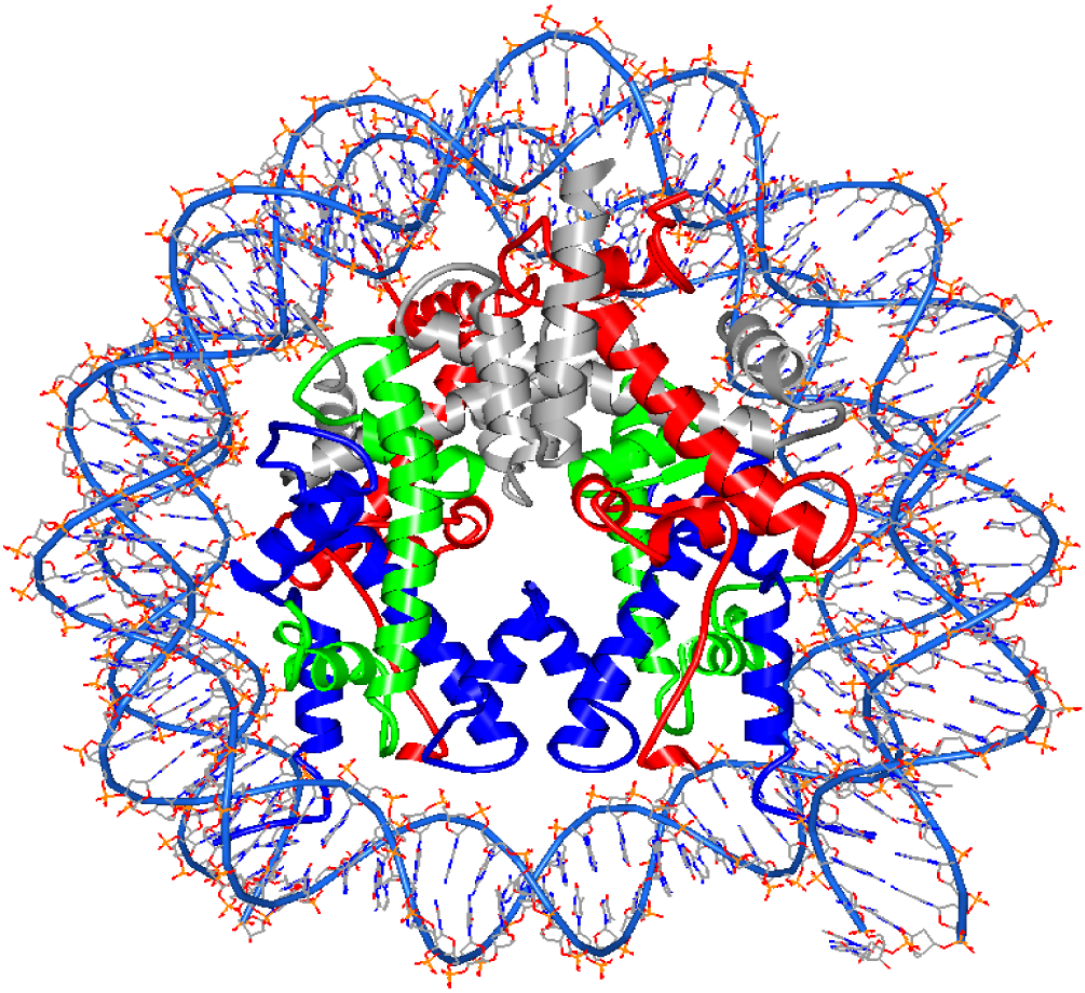

Figure 1. The Nucleosome Core Particle.
Cartoon representation of the nucleosome core particle crystal structure at 2.8 angstroms resolution. The histone proteins are each represented by ribbons and are as follows: H2A (red), H2B (silver), H3 (blue), and H4 (green). The DNA (147 bp) is represented by the light blue ribbon with each nucleotide represented by a stick figure. The image was created from NCBI PDB file 1ID3 [4] using Sirius 1.2 molecular modeling program.

of DNA wrapped 1.7 turns around a protein octamer [4] (Figure 1). The general model for nucleosome assembly is that DNA initially interacts with preassembled $H3_2$-$H4_2$ to form a tetrasome. After tetrasome formation two heterodimers of H2A-H2B interact with opposite sides of the tetramer to form the octameric nucleosome. There are a number of proteins called histone chaperones which facilitate this association of the histones with DNA (see below)

Between each nucleosome there is a length of linker DNA (~50 bp), connecting long arrays of nucleosomes. The linker histone H1, which is not well-conserved between species, functions in spacing adjoining nucleosomes. H1 helps to modulate higher order chromatin packing by providing an interaction region between adjacent nucleosomes.

Depending on the degree of packing, eukaryotic chromatin can be found in two structural varieties: euchromatin and heterochromatin. Euchromatin is the term used to describe loosely packed chromatin. Euchromatic regions of the genome are more accessible to the transcriptional machinery, and tend to be rich in actively transcribed genes. Heterochromatin on the other hand is the term used to describe tightly packed chromatin. Due to the tight packing and decreased accessibility to transcription factors, genes located in regions of heterochromatin tend to be transcriptionally silent.

In general, heterochromatin can be grouped into two types: constitutive and facultative. Constitutive heterochromatin is silenced in all cells, and is found in regions of the genome that are usually transcriptionally repressed. In budding yeast, examples of constitutive heterochromatin would be the HML/HMR silent mating type

locus, the sub-telomeric regions, and the repetitive ribosomal DNA arrays. Facultative heterochromatin differs in that it is usually not silenced in all cells at any given time. Genes in regions of facultative heterochromatin are selectively activated or silenced based on the need of the cell.

2. Histone post-translational modifications

There are a number of ways in which the transition from transcriptionally silenced heterochromatin to transcriptionally active euchromatin is achieved. The histone proteins are subjected to a number of post-translational modifications (PTMs), which in turn alter the conformation of the modified chromatin. PTM of the histones usually occurs along the amino-terminal tail which protrudes away from the face of the core particle, but can also occur at the globular core of the protein. The most well studied PTMs thought to function in the modification of chromatin structure are acetylation, methylation, and phosphorylation.

The two main PTMs involved in transcriptional activation or repression are acetylation and methylation. A number of protein complexes have been identified that have been shown to confer these specific histone PTMs. The histone acetyltranferases (HATs) function to acetylate multiple lysine residues mainly on histone H3 and H4, while the histone deacetylases (HDACs) remove acetyl groups from the histones. In budding yeast the main HAT complexes which function in chromatin remodeling are NuA4 [5] and SAGA [6], with acetylation being generally

linked to euchromatin, or transcriptionally active regions of the genome. The histone methyltranferases can add one (mono-methyl), two (di-methyl), or three (tri-methyl) methyl groups onto histones at both lysine and arginine residues. Methylation occurs on histones H3 and H4 and is generally associated with transcriptional repression. Members of the jumonji family (jmj) of proteins are the most common histone demethylases, and have been identified in many eukaryotes [7].

In addition to the modifications mentioned above, histones can also be modified by ubiquitination and sumoylation, both of which can function to facilitate further PTM of the histone N-terminal tail. Modified histone tails are thought to affect chromatin structure by two distinct mechanisms. The first mechanism suggests that the modification itself exerts its own electrostatic force upon the nucleosome, and in turn directly affects the DNA/histone interaction. The second mechanism proposes that modified histone tails are functional to recruit additional proteins which can directly cause a structural change in the histones or alter their interaction with DNA. A number of structural protein motifs have been identified which interact with modified histone residues, including bromodomains which recognize acetylated lysine residues, and chromodomains which recognize methylated lysine residues.

3. Nucleosome dynamics and chromatin remodeling

Eukaryotic chromatin is highly dynamic in regards to where and how nucleosomes are positioned on the DNA. There are a number of mechanisms which can affect the structure, positioning, and dynamics of the nucleosome. These include

chromatin remodeling complexes, transcription, and the histone chaperones. In general, how much the actual DNA sequence itself influences nucleosome positioning is a point of contention. In budding yeast some studies have estimated that upwards of 50% of the genome is specifically evolved or constrained to aid in positioning of individual nucleosomes [8, 9], while another *in vitro* study suggests that ~95% of genomic sequences do not function as a guide for nucleosome positioning [10]. Nucleosomes are deposited onto DNA in both a S phase dependent and independent manner [11]. Deposition or replacement of nucleosomes outside of S phase is usually indicative of chromatin remodeling to accommodate changes in the transcriptional program [12]. Although it is not known exactly how nucleosomes are positioned, a great deal is known about how the positioning of nucleosome can be modified to alter the accessibility of the chromatin.

One of the major classes of chromatin regulating proteins utilizes the energy from ATP hydrolysis to alter DNA/histone interactions, subsequently conferring changes in chromatin structure or nucleosome positioning. These protein complexes are known as chromatin remodeling complexes and in budding yeast include members of the Swi/Snf protein family [13]. Chromatin remodeling complexes are thought to function by two distinct mechanisms, including displacement of bulk nucleosomes through transient unwrapping of DNA from the histone octamer and translational re-positioning or sliding which changes nucleosome position on the DNA template [14].

Transcription is another major factor which influences nucleosome

positioning. Both *in vitro* and *in vivo* experiments have demonstrated that it is more difficult for RNA polymerase II (Pol II) to transcribe through a nucleosome-containing template, and doing so can actually displace nucleosomes from the highly active regulatory genes in budding yeast [15-17]. Transcription is generally believed to create nucleosome-free regions by one of two mechanisms [18]. The first mechanism involves the binding of general transcription factors (TFs) during transcription initiation. *In vivo* studies in yeast have shown that binding of TFs destabilizes pre-positioned nucleosomes at regulatory promoters [19, 20]. Additionally, genome-wide nucleosome mapping studies also reveal a correlation between known TF binding sites, and nucleosome-free regions [21]. The second mechanism of nucleosome displacement involves Pol II and transcript elongation. Several studies in yeast and in higher eukaryotes suggest a mechanism in which the elongating Pol II either partially or completely evicts nucleosomal histones [22, 23]. It is important to note that during elongation not all histones are completely disassociated from the DNA and mechanisms do exist which preferentially displace either H2A-H2B dimers or H3-H4 tetramers [24].

4. Histone chaperones

The dynamic properties of nucleosomes are achieved with the help of specialized proteins dubbed histone chaperones. Histone chaperones are a group of evolutionarily conserved proteins which facilitate both the deposition and rebuilding of nucleosomes during events such as S phase and transcription. In budding yeast a

number of chaperone proteins have been identified and characterized biochemically *in vitro* and functionally *in vivo*. The histone H3-H4 chaperones function in either one of two pathways, replication-dependent or replication-independent. The chaperone complex CAF1- facilitates loading of $H3_2$-$H4_2$ onto the DNA in a replication-dependent manner. CAF-1 physically associates with the DNA polymerase processivity clamp PCNA and histone $H3_2$-$H4_2$, allowing nucleosomes to be deposited immediately after DNA replication or DNA repair [25, 26]. The HIR complex is another evolutionarily conserved H3-H4 chaperone. HIR has been shown to function outside of DNA replication, helping to deposit or reassemble $H3_2$-$H4_2$ onto DNA during transcription and embryogenesis [27, 28].

The histone H2A-H2B chaperones assist in addition of the H2A-H2B dimer onto the pre-formed $H3_2$-$H4_2$ tetrasome. The H2A-H2B dimer is not maintained in the nucleosome with as high affinity as $H3_2$-$H4_2$, therefore H2A-H2B dimers are more dynamic and removed more readily from the nucleosome during transcription [12, 29]. The histone chaperone Nap1 is a major regulator of H2A-H2B dynamics, facilitating both the shuttling of H2A-H2B into the nucleus and its deposition into nucleosomes during S phase [30]. The FACT complex is a key histone chaperone that functions during transcription [31]. It has been observed both *in vivo* and *in vitro* that Pol II-mediated transcription removes H2A-H2B dimers from nucleosomes [15]. It is hypothesized that the FACT complex removes H2A-H2B dimers ahead of the replicating polymerase, facilitating transcription through nucleosome-dense regions. Additionally, FACT has been shown to possess chaperone activity *in vitro*, leading to

the hypothesis that FACT is necessary to re-deposit H2A-H2B dimers after Pol II has passed through a region [32].

5. Histone variants

In most eukaryotes there are multiple copies of each of the core histone genes. These genes are generally tightly regulated in a cell cycle manner, and are primarily highly expressed during S phase. The histone genes code for the majority of the histones found at nucleosomes throughout the genome. In addition to the genes that code for the core histones, there are genes which code for proteins known as histone variants. The histone variants are a group of proteins which closely resemble the core histones but have distinct biochemical properties which are thought to alter the characteristics of the nucleosome. Histone variants have been identified in all eukaryotes studies, and with the exception of H4, all core histones have identifiable variants [33]. Histone variants are usually coded for by a single gene which is expressed throughout the cell cycle, and are thought to replace their core histone counterpart to form a specialized nucleosome.

Histone variants can be species specific, or found ubiquitously in all eukaryotes, and have been implicated in regulation of multiple cellular processes including transcriptional activation and repression, formation of heterochromatic barriers, gametogenesis, and maintenance of genome stability [34-38] (Table 1). It is also important to note that in some species the predominant core histone may actually be a histone variant in another species. For example, the budding yeast core histone H3 is

actually the H3 variant H3.3 in higher eukaryotes [33].

Table 1. List of known histone variants and their function
Adapted from Kamakaka *et al*. [33].

Histone	Variant	Species	Chromatin effect	Function
H1	H10	Mouse	Chromatin condensation	Transcription repression
	H5	Chicken	Chromatin condensation	Transcription repression
	SpH1	Sea Urchin	Chromatin condensation	Chromatin Packaging
	H1t	Mouse	Open Chromatin	Histone Exchange, recombination?
H2A	MacroH2A	Vertebrate	Condensed chromatin	X-chromosome inactivation
	H2A-Bbd	Vertebrate	Open chromatin	Transcription activation
	H2A.X	Ubiquitous	Condensed chromatin	DNA repair, transcription, chr. segregation
	H2A.Z	Ubiquitous	Silenced Chromatin	Transcription repression, chr. segregation
H2B	SpH2B	Sea Urchin	Chromatin condensation	Chromatin packaging
H3	CenH3	Ubiquitous	Unknown- CEN nucleosome	Kinetochore formation, chr. segregation
	H3.3	Ubiquitous	Open chromatin	Transcription

A. The centromeric histone variant

The CenH3 histone variant is known as Cse4 in budding yeast and more generally as CENP-A in higher eukaryotes. The CenH3 variant is thought to physically replace histone H3 at centromeric nucleosome(s), and is the fundamental structural unit of the eukaryotic kinetochore. CenH3 has been shown to localize to centromeres in all eukaryotes studied and is required for proper chromosome segregation and mitotic division (for review see [39]). Structurally, CenH3 orthologs have two major domains: an evolutionarily conserved histone fold domain (HFD) and a divergent amino-terminal domain. The HFD of CenH3 orthologs has a high degree of amino acid identity to histone H3, while the amino-terminal portion of the protein can vary greatly between species (Figure 2). The N-terminal tail of yeast Cse4 is much longer than any of its eukaryotic counterparts. It is essential for Cse4

function *in vivo*, although its exact molecular function is unknown [40]. The function of the CenH3 nucleosome is highly conserved, as demonstrated by the functional complementation of RNAi-depleted CENP-A in human cells by yeast Cse4 [41].

The timing and mechanism of Cse4/CENP-A deposition varies throughout eukaryotes. In budding yeast Cse4 has been shown to be incorporated into the centromere during S-phase (see below). Cse4 bound to DNA after S-phase remains very stable throughout the remainder of the cell cycle, with new Cse4 replacing the old Cse4 during the subsequent S-phase [42]. The mechanism of targeting and incorporation of Cse4 into centromeric nucleosomes is poorly understood. In humans CENP-A is expressed during G2, after S-phase in completed [43]. CENP-A is then incorporated at the centromere during late telophase/early G1 [44]. The loading of human CENP-A requires the proteins Mis18α-β and KNL2 [45, 46]. Both Mis18α-β and KNL2 interact with the histone chaperone CAF-1, but their exact mechanism of function is unknown. The fission yeast *Schizosaccharomyces pombe* loads CENP-A (Cnp1) in two distinct pathways. The S-phase coupled Cnp1 loading pathway requires the proteins Mis6 and Ams2 for proper localization of the CenH3 variant [47]. In addition to the S-phase loading pathway, fission yeast can also load Cnp1 in a replication-uncoupled pathway during late G2 [48].

III. Mitosis and Chromosome Dynamics

In order for any cell to replicate, it must make a copy of its genome and faithfully deliver a copy of that genome to the newly formed daughter cell. This complex

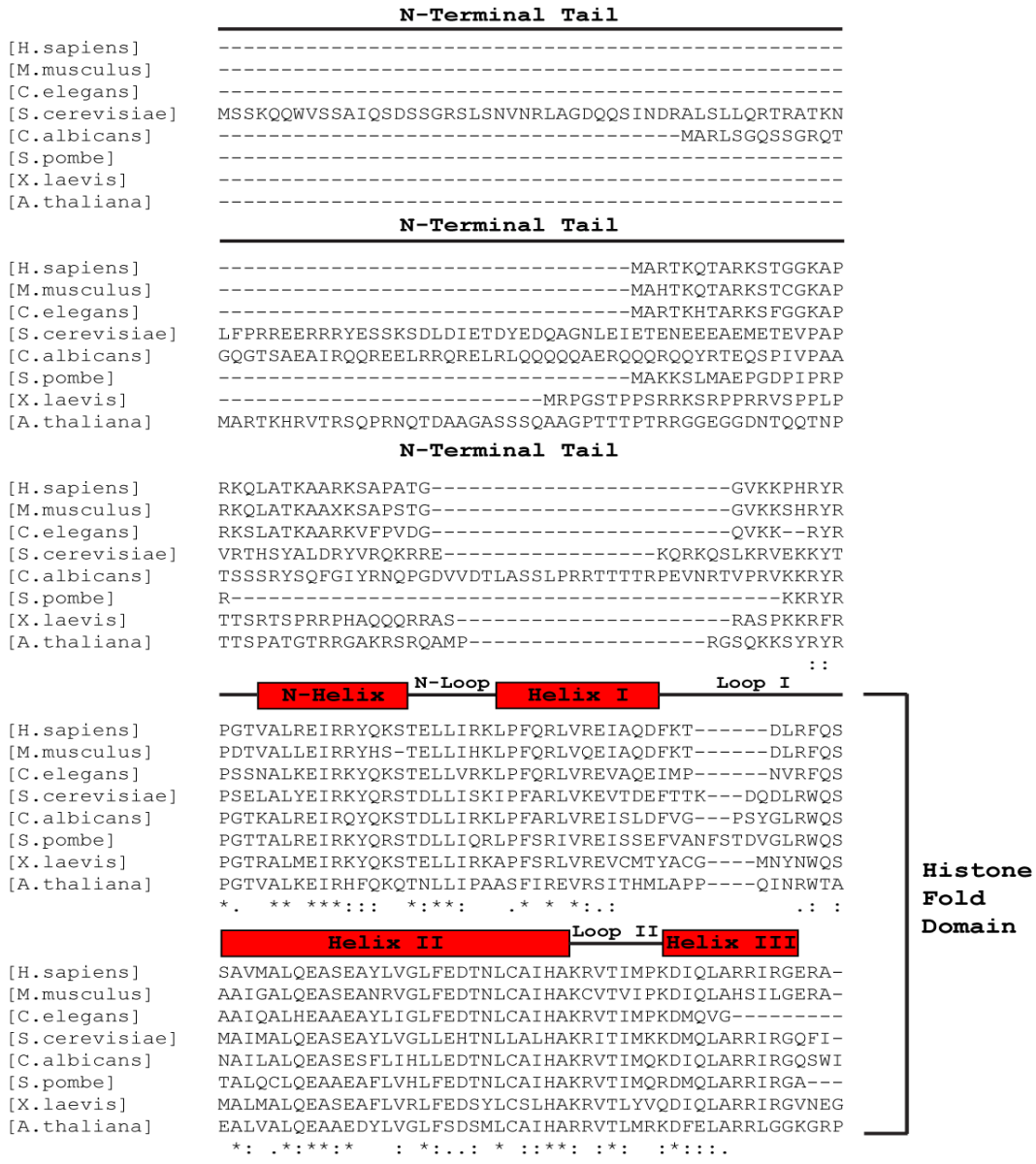

Figure 2. Multiple sequence alignment of Cse4 orthologs.
ClustalW was used to create a multiple sequence alignment of Cse4 (CENP-A) orthologs. Conserved residues which are identical in all species are marked with an asterisk. Conserved residues which exhibit strong similarity in all species are marked with a colon. Conserved residues which exhibit weak similarity in all species are marked with a period. The location of the N-terminal tail and the features of the conserved histone fold domain are indicated.

Process known as mitosis is essential for survival of any organism and involves a myriad of biological components. Since the first description of mitosis in the late 19th century, scientists have studied its complexities to gain understanding into the fundamental properties of chromosome dynamics. The primary goal of mitosis is a division of the parental cell and its genome into two daughter cells. All eukaryotic organisms undergo mitosis, and with few exceptions the process is well conserved throughout evolution. Since mitosis is such an important cellular process, it is imperative that it is carried out without error. Defects in the mitotic machinery can lead to transmission of the incorrect number of chromosomes into the daughter cell. A cell that inherits an improper number of chromosomes is referred to as aneuploid. Aneuploidy can be fatal to single-celled eukaryotes, and in humans is thought to be one of the key factors in the development of cancer [49] and Downs Syndrome [50].

1. The phases of mitosis

Mitotic division is a step-wise process and can be divided into two main phases, interphase and M phase. Interphase is relatively long when compared to M phase, and it is during this time that the cell prepares itself for the cell division. Interphase is divided into three sub-phases: first gap (G_1), synthesis (S phase), and second gap (G_2) [51]. During G_1 the cell grows and prepares for S phase, producing the proteins necessary to duplicate its genome. DNA replication occurs during S phase, resulting in the formation of a duplicate chromosome known as a sister chromatid. Concomitant with replication, the sister chromatids are held together via a

protein complex called cohesin. During G_2/Early M, the cohered sister chromatids are then aligned lengthwise along the metaphase plate in preparation for the upcoming mitotic segregation. The physical separation of the sister chromatids occurs late in M phase, during anaphase. The cell cycle then reaches its end after the completion of cytokinesis. The end product of mitosis will be a newly formed cell that is genetically identical to it progenitor.

2. Chromosome segregation

The process of physically moving a replicated genome into the daughter cell is known as chromosome segregation. Eukaryotic chromosome segregation is a fundamental and well conserved mechanism common to all species studied. There are a number of components essential to properly segregate chromosomes. The DNA component of the segregation machinery is a specialized, non-conserved sequence called the centromere. Directly over the centromere a large proteinaceous structure called the kinetochore will form. Microtubules emanating from oppositely oriented spindle poles (centrosomes) physically attach to the kinetochore. Using the energy generated by de-polymerization of the microtubules, the sister chromatids are physically separated and pulled in opposite directions. In budding yeast a single microtubule will bind at each kinetochore, while in higher eukaryotes, multiple microtubules can attach to a single chromosome. Once chromosome segregation is complete, one copy of the genome will remain in the original cell and the other copy will have been transferred into what will become the daughter cell (Figure 3).

A. Structure and function of eukaryotic centromeres

The centromere is the specialized DNA sequence which is essential for chromosome segregation in all eukaryotes. Although the mechanism of chromosome segregation is conserved between species, the actual structure and composition of the centromere is not. Eukaryotic centromeres have divergently evolved over several millions of years, and although their respective function remains the same, the actual centromeric sequence varies greatly between organisms. The purpose of the centromere is to serve as a guide for the recruitment of the kinetochore proteins to a single dedicated site on each chromosome. In order to avoid chromosome transmission defects, only one centromere must function on each chromosome during mitosis. Defects in proper centromere function or mis-localization of the kinetochore proteins can lead to aneuploidy and cell death.

Centromeres can be categorized into two groups: point centromeres and regional centromeres. In terms of sequence complexity, the point centromeres are the simplest of the eukaryotic centromeres. Point centromeres are found in many fungi, including *S cerevisiae*. The budding yeast point centromere is a 125bp consensus sequence comprised of three centromeric DNA elements (CDE I-II-III) which are conserved on each chromosome and are required for full mitotic function [52] (Figure 4A). CDEI and CDEIII are short (10-20bp) sequences conserved on each chromosome, while CDEII is an A+T rich (>90% A+T) non-conserved sequence [52]. Mutational analysis reveals that the majority of nucleotides of the CDE III

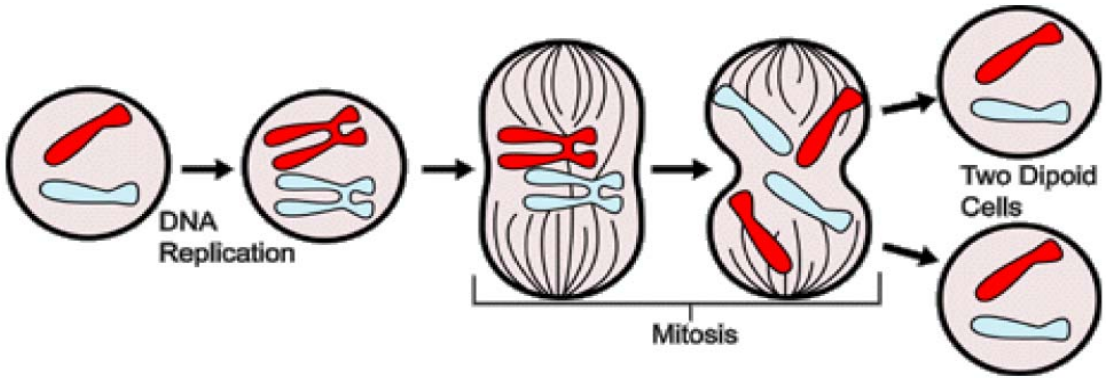

Figure 3. Mitosis and chromosome segregation
The diagram represents the process of chromosome segregation in a diploid eukaryotic cell. DNA replication occurs during S-phase of mitosis. After completion of S-phase, microtubulules attach to chromosomes via the kinetochore. At the completion of mitosis one copy of the genome will remain in the original cell and the other copy will have been transferred into what will become the daughter cell. (Reprinted with permission from NCBI, 2008).

sequence are essential for proper chromosome segregation [53]. CDE I and CDE II have less stringent sequence requirements to maintain centromere function. Single base pair deletions or insertion in CDE II are well-tolerated, and complete deletion of CDE I does not abolish mitotic segregation [54, 55].

Regional centromeres are found in certain single-celled eukaryotes and in all metazoans. Centromeres in higher eukaryotes can vary greatly in sequence composition, but all retain some type of repetitive nature. Centromeres in the fission yeast *S. pombe* are considered to be the simplest of the regional centromeres. They range from 30-110 kilobases (Kb) in length and are composed of a unique core sequence (cnt) that is flanked by a set of inner (*inr*) and outer (*otr*) repeats [56, 57] (Figure 4B). In *S. pombe* both the unique *cnt* and the repetitive dg elements of the *otr* repeats are essential for centromere function [58]. Centromeres in higher eukaryotes such as humans are much larger and more complex. Some human centromere can span megabases (Mb) of DNA [59]. In general, metazoan centromeres possess a large central core, comprised primarily of α-satellite repetitive DNA sequences. Flanking the core repeats are usually more tandem arrays of both α and γ-satellite DNA, as well as repetitive sequences which resemble transposable elements [60, 61] (Figure 4C). These large regions of pericentric DNA are heterochromatic in nature, and are essential for maintenance of centromeric identity. They are thought to function as a barrier, preventing the core repeats from events that could have a deleterious effect on centromere function, including transcription, recombination, and transposable element insertion.

B. The evolutionarily conserved kinetochore

The kinetochore is a large, multi-protein structure with an evolutionarily conserved function. Once recruited to the centromere, kinetochore proteins facilitate interaction between the chromosome and the spindle microtubules during mitosis and meiosis. Many eukaryotic kinetochore proteins have been identified to date, and in budding yeast >65 different proteins have been implicated as functional kinetochore proteins [62] (Table 2) . The kinetochore proteins are grouped into three functional groups: inner, central and outer kinetochore proteins. Kinetochore assembly is thought to be hierarchical in nature, with the initial localization of inner kinetochore proteins facilitating the recruitment of additional kinetochore proteins and protein complexes. Localization of the inner kinetochore components to the centromeric DNA is the initial step of kinetochore formation. The inner kinetochore proteins function at the interface between the kinetochore and the DNA through either a direct interaction with centromeric DNA, or via a direct interaction with other inner kinetochore proteins. In budding yeast a protein complex called CBF3 helps to specify the location of the centromere by a direct interaction with CDE II-III, while in higher eukaryotes inner kinetochore proteins have been shown to interact with the repetitive centromeric elements [63-65]. After localization of the inner kinetochore components, the proteins of the central kinetochore are recruited to the centromere via interaction with other inner kinetochore proteins. Most central kinetochore proteins are found in discrete complexes which function as a protein scaffold, physically linking the inner and outer kinetochore [62, 66, 67]. The outer kinetochore

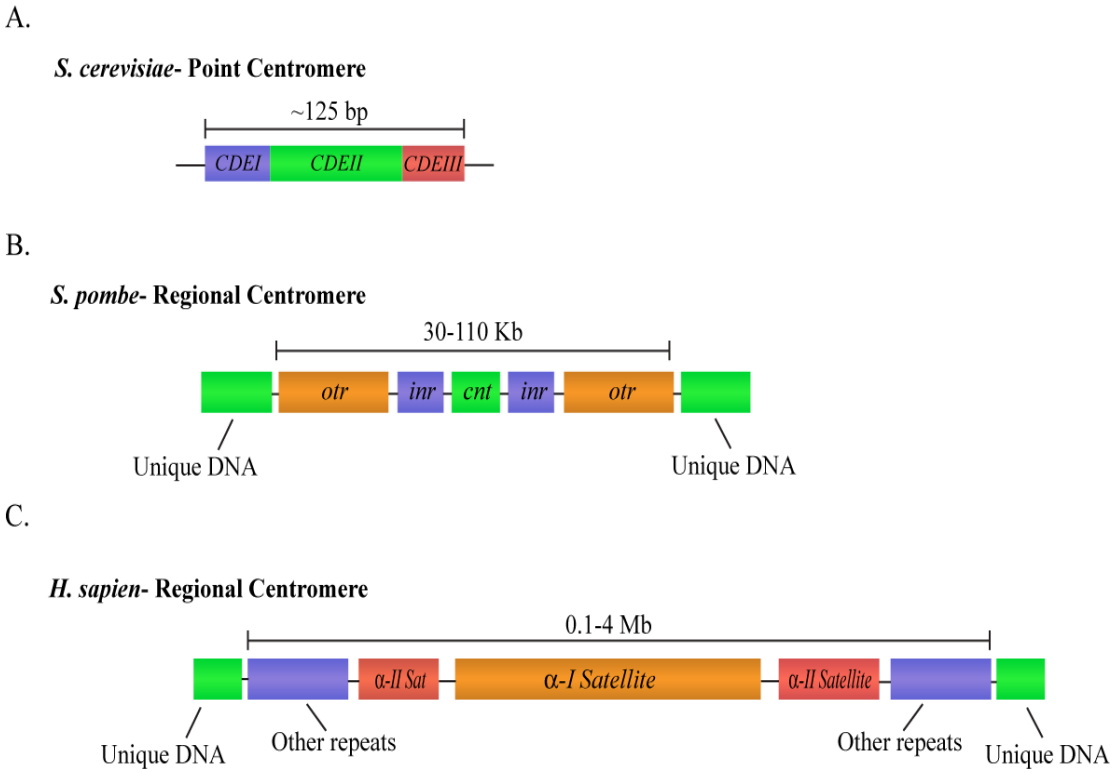

Figure 4. Eukaryotic centromeres.
The cartoon schematic represents three examples of centromeres in higher eukaryotes. A) The budding yeast "point" centromere is a 125 bp consensus sequence comprised of three centromeric DNA elements: CDE I, CDE II, and CDE III. B) Fission yeast possess the simplest of the "regional" centromeres, which range from 30-110 kb in length and are composed of a unique core sequence that is flanked by a set of inner and outer repeats. C) Some human centromeres can span megabases of DNA, and are comprised primarily of α-satellite repetitive DNA sequences.

Table 2. The evolutionarily conserved kinetochore.
Classification of budding yeast kinetochore proteins based on known function and interacting proteins. Proteins essential for viability in yeast are shown in red and those that are non-essential are shown in black. If applicable, the human homolog for each protein is listed. Adapted from Cheeseman *et al*. [62].

Inner Kinetochore	
Budding Yeast	Human
CBF3 Complex	
Ndc10	
Ctf13	
Cep3	
Skp1	
Cse4	CENP-A
Cbf1	CENP-B
Mif2	CENP-C
Scm3	

Regulatory Factors	
Budding Yeast	Human
Spindle Checkpoint	
Mad1	Mad1
Mad2	Mad2
Mad3	BubR1
Bub1	Bub1
Bub3	Bub3
Mps1	Mps1
Ipl1	Aurora kinase
Sli15	INCENP

Central Kinetochore	
Budding Yeast	Human
Ctf3 Complex	
Mcm16	
Mcm22	
Ctf3	Mis6/LRPR1
Ndc80 Complex	
Ndc80	Ndc80
Spc24	
Spc25	
Nuf2	Min-10/Mpp1
Ctf19 Complex	
Ctf19	
Mcm21	
Okp1	
Bir1	Survivin
Mtw1	
Chl4	
Mcm19	

Outer Kinetochore	
Budding Yeast	Human
Dam1 Complex	
Dam1	
Duo1	
Dad1	
Spc19	
Spc34	
Ask1	
Dad2	
Dad3	
Dad4	
Bik1	Clip-170
Bim1	EB1
Stu2	XMAP-215
Cin8	BimC kinesin
Kip3	XKCM1 kinesin
Kar3	NCD-like kinesin

contains proteins which interact with microtubules. These proteins can include motor proteins such as kinesin and dynein, and non-motor microtubule associated proteins (MAPs) which provide the attachment sites required for chromosome segregation [68, 69]. In addition to the proteins which physically link the chromosome to the spindle microtubule, the outer kinetochore is also comprised of proteins which are responsible for the regulation and maintenance of the kinetochore itself. The mitotic

spindle assembly checkpoint is a group of well-conserved proteins which ensure segregation fidelity by monitoring the proper formation and attachment of the kinetochore. In the event of a situation where segregation would be impaired, the spindle assembly checkpoint will activate, sending a signal to the cell which will halt chromosome segregation and the cell cycle. During this halt in mitotic activity, the cell can attempt to correct the defect that caused the checkpoint arrest [68]. Checkpoint activation can be induced by a number of factors including lack of microtubule attachment to the kinetochore, improperly attached microtubules, or a defect in biorientation toward opposite spindle poles [70-72].

[73]

Chapter 2.

Characterization of the Novel Kinetochore Component Scm3

I. Abstract

The kinetochore is a complex multi-protein structure located at centromeres that is essential for proper chromosome segregation. Budding yeast Cse4 is an essential evolutionarily conserved histone H3 variant recruited to the centromere by an unknown mechanism. We have identified Scm3, a new inner kinetochore protein that immunopurifies with Cse4. Scm3 is essential for viability and localizes to all centromeres. Construction of a conditional *SCM3* allele reveals that depletion results in metaphase arrest, with duplicated spindle poles, short spindles, and unequal DNA distribution. The metaphase arrest is mediated by the mitotic spindle checkpoint, being dependent on Mad1 and the Aurora kinase B homolog Ipl1. Scm3 interacts with both Ndc10 and Cse4 and is essential to establish centromeric chromatin following DNA replication. In addition, Scm3 is required to maintain kinetochore function throughout the cell cycle. We propose a model in which Ndc10/Scm3 binds to centromeric DNA which is in turn essential for targeting Cse4 to centromeres.

II. Introduction

Every time a eukaryotic cell divides, it replicates its genome and delivers a complete set of chromosomes to its daughter cell. Proper chromosome segregation is dependent on the formation of a DNA-protein complex known as the kinetochore

which attaches to microtubules to mediate the physical separation of sister chromatids. Defects in chromosome segregation can lead to aberrant cell growth, aneuploidy, improper development, and cell death. Faithful transmission of eukaryotic chromosomes requires a centromere with its associated kinetochore proteins. In *Saccharomyces cerevisiae*, the centromere is a small stretch of DNA spanning approximately 125 bp that is sufficient to support high fidelity chromosome segregation [52]. The "point centromere" of budding yeast is composed of three DNA elements (CDE I, CDE II, and CDE III), whereas centromeres of other fungi and higher eukaryotes, referred to as regional centromeres, can be comprised of up to a megabase of repetitive DNA. Although eukaryotic centromere sequences are highly variable, they are all epigenetically marked by the incorporation of the CenH3 histone variant CENP-A, which is known as Cse4 in budding yeast. This CENP-A-containing nucleosome is thought to be the chromatin scaffold on which the kinetochore is built. How this histone variant is specifically targeted to centromeres remains unclear, but factors have been identified in various higher eukaryotes that contribute to CENP-A's centromere specificity [74, 75].

Although the budding yeast centromere is a simple sequence, the kinetochore is quite complex. Through a combination of genetic and biochemical techniques, over 65 budding yeast kinetochore proteins have been identified, many of which are evolutionarily conserved from yeast to man (for reviews see [69, 76]). The kinetochore can be conceptually divided into three functional parts that are proposed to assemble hierarchically: inner, central, and outer. The inner kinetochore or DNA

binding layer is comprised of several proteins including Mif2 (CENP-C), the CBF3 complex (Ndc10, Cep3, Skp1, and Ctf13) and the CenH3 histone variant Cse4 (CENP-A), all of which are essential for kinetochore function [63, 77-79]. The central or linker kinetochore layer consists of a group of complexes (COMA, MIND, NDC80) that functions as a bridge between the outer and the inner kinetochore [66, 67, 80, 81]. The outer kinetochore is comprised of the proteins that physically bind to microtubules during mitosis, and includes 10 members of the DAM/DASH complex [82-84]. This outer layer is also associated with many of the regulatory components of the kinetochore, including the Ipl1-Sli5 kinase complex, as well as the components of the spindle assembly checkpoint which monitors proper bi-orientation and correct microtubule attachment [70, 85, 86].

In budding yeast, Ndc10 is required for the localization of all other kinetochore proteins [84, 87-89]. The binding of Ndc10 to centromeric DNA is thought to be the initial step that nucleates kinetochore formation [65]. It has been proposed that Ndc10 localizes to the centromere in two distinct modes: first, through participation in the CBF3 complex which interacts with CDEIII, and second, Ndc10 can independently bind CDEII [65, 90]. Both of these interactions are believed to occur early in S-phase, immediately following centromere replication, but the exact timing has not been determined [65, 79]. Additional loading of the CBF3 protein complex occurs throughout the cell cycle and is required for proper kinetochore function, independent of its role in recruiting other kinetochore proteins to the centromere [63]. While Ndc10 is required to localize Cse4 to centromeres in budding

yeast, these two proteins have never been shown to physically interact. This raises the question of how Ndc10 might be involved in the recruitment of Cse4 to centromeres.

Here we describe the characterization of Scm3 (Suppressor of Chromosome Missegregation), originally identified as a high-copy suppressor of a mutation to the histone fold domain of Cse4 [40]. This essential protein has putative orthologs in fungi which possess either point or regional centromeres. We find that Scm3 physically associates with both inner kinetochore components Ndc10 and Cse4, and like these proteins, localizes to centromeres. Construction of a conditional *SCM3* allele reveals that cells depleted for Scm3 fail to properly localize both Cse4 and Ndc10 to the kinetochore. Scm3 depleted cells arrest in metaphase with duplicated spindle poles, short spindles, and unequal DNA distribution. Cell cycle and spindle checkpoint experiments reveal Scm3 is essential to both establish and maintain a segregation-competent kinetochore. Based on our findings, we hypothesize that Scm3 is a novel inner kinetochore protein that functions in coupling the nucleation of the kinetochore by Ndc10 to establishment of Cse4-containing centromeric chromatin.

III. Results

1. Scm3 physically associates with both Cse4 and Ndc10

Based on the observed genetic interaction between Cse4 and Scm3 [40], we wanted to test for possible protein-protein interactions between Scm3 and inner

A.

Cse4-12Myc Immunoprecipiatations

Protein	Non-Redundant Peptides
Cse4p	K.KYTPSELALYEIR.K K.QQWVSSAIQSDSSGR.S A.IQSDSSGRSLSNVNRLAG.D Total = 52 aa/229 aa=25.8% Coverage
Scm3p	K.YESIEEQGDLVDLK.T K.LTDDEVMERHKLADE.N E.DNGHIKTLTANNSTK.D Total = 50 aa/223 aa=22.4% Coverage

Scm3-3FLAG Immunoprecipiatation

Protein	Non-Redundant Peptides
Scm3p	K.HSDCNPVHR.V K.TGEIVEDNGHIK.T K.YESIEEQGDLVDLK.T Total = 29 aa/223 aa=18.4% Coverage
Cse4p	K.YTPSELALYEIRKYQR.S Total = 18 aa/229 aa=7.9% Coverage

B.

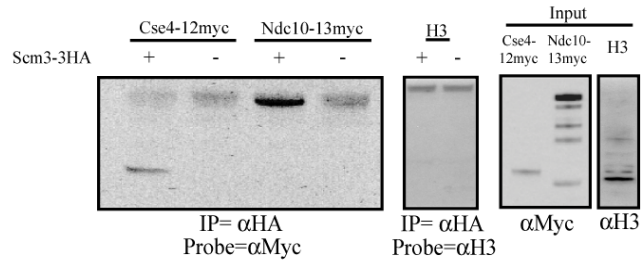

C.

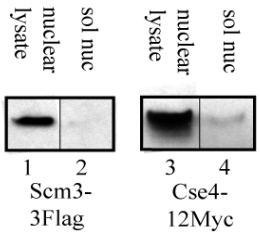

D.

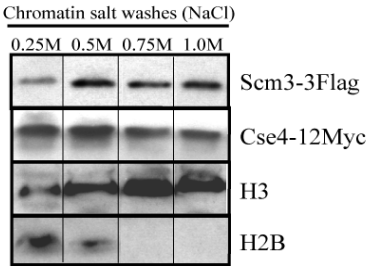

Figure 5. Scm3 interacts with inner kinetochore proteins.
A) Peptide coverage of two Cse4-12Myc immunoprecipitations and a Scm3-3FLAG immunoprecipitation analyzed by mass spectrometry. B) *In vivo* immunoprecipitation of Scm3-3HA pulls down both Cse4 and Ndc10, but fails to pull down histone H3. The αMyc and αH3 antibody hybridizes to a background band present in all HA-precipitated samples. Input controls are 0.05% of total whole cell lysate. C) Nuclear lysates were made from a strain expressing Scm3-3Flag and Cse4-12Myc. Western blotting was carried out with either αFlag antibody (lanes 1-2) or αMyc antibody (lanes 3-4). The chromatin fraction was pelleted and twice as much supernatant (soluble nuclear proteins, "sol nuc") as lysate was loaded in lanes 2 and 4. D) Equal portions of the chromatin fraction were subjected to washes of increasing ionic strength as indicated, then solubilized by treatment with MNase and analyzed by Western blotting.

kinetochore proteins. Multi Dimensional Protein Information Technology (MudPIT) mass spectrometric analysis detected three peptides of Scm3 from two independent immunopurified Cse4 preparations and Cse4 was detected in an immunopurified Scm3 preparation (Figure 5A.) Co-immunoprecipitation (co-IP) was performed from yeast whole cell extracts probing for interaction between Scm3 and Ndc10, Cse4, and histone H3. We found that Scm3 physically associates with both Ndc10 and Cse4 *in vivo* (Figure 5B). No interaction between Scm3 and histone H3 was detected (Figure 5B). Virtually all of the Scm3 and Cse4 in a nuclear lysate is chromatin associated, suggesting that these proteins may form a complex at centromeres (Figure 5C). Furthermore, Scm3 and Cse4 are very stably associated with chromatin. We performed a salt challenge experiment in which the chromatin pellet was washed with increasing concentrations of salt, solubilized by treatment with MNase, and analyzed by Western blotting. As expected, histone H2B is removed from chromatin by 0.75M salt, and histone H3 remains associated up to 1.0 M salt. Scm3 and Cse4 behave like histone H3, demonstrating a very strong association with chromatin (Figure 5D). These results suggest that Scm3 is a chromatin bound component of the inner kinetochore. However, the salt challenge experiments do not address whether Scm3 is an actual component of the centromeric nucleosome, or rather just intimately associates with it.

2. Scm3 shut-off is lethal and leads to metaphase arrest and chromosome segregation defects

We were interested in studying the effect loss of Scm3 function has on cell cycle progression and chromosome segregation. Based on data from large-scale yeast gene deletion studies, the deletion of Scm3 is lethal [91]. In order to study the function of Scm3, the endogenous copy of the gene was epitope-tagged and placed under the control of a galactose-inducible promoter ($pGAL_{1\text{-}10}$-3HA-Scm3) (Figure 6A). Expression of Scm3 from the galactose promoter should be effectively "shut-off" when cells are grown in media with glucose as the sole carbon source (YPD). Remarkably, Scm3 protein levels when expressed from the $GAL_{1\text{-}10}$ promoter are not significantly different from endogenous levels of Scm3-3HA (Figure 6B), suggesting Scm3 protein levels are tightly regulated post-transcriptionally. Western blot analysis was performed to confirm depletion of Scm3 upon switch to YPD. One hour after switching from galactose to glucose media, Scm3 is not detectable by Western blot (Figure 6C). Thus, we are reasonably certain that depletion of Scm3 has allowed us to phenocopy a null mutation. Additionally, since Scm3 is not overexpressed from the $GAL_{1\text{-}10}$ promoter, our observations cannot be attributed to a gross excess of Scm3 protein. We also examined Cse4 and Ndc10 expression in the absence of Scm3. While Scm3 is not detectable when cells are grown in YPD, levels of both Cse4 and Ndc10 remain stable (Figure 6C). This finding suggests Scm3 is not required for the stability of either Cse4 or Ndc10 protein, and any phenotype associated with Scm3 depletion is not due to lack of Cse4 or Ndc10 protein availability. Additionally both a wild-type strain and a strain containing $pGAL_{1\text{-}10}$-3HA-Scm3 grow similarly when maintained in media containing galactose ($Scm3^{on}$). No growth was observed on

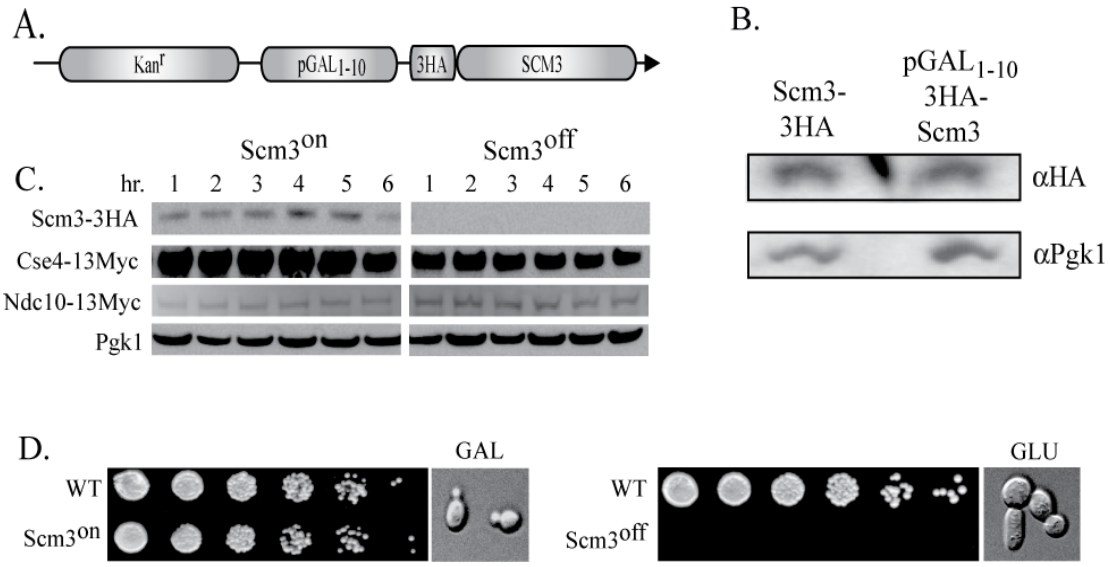

Figure 6. The effect of Scm3 shut-off on cell viability.
A) Scm3$^{on/off}$ construct. The GAL$_{1-10}$ promoter was integrated to control the expression of endogenous Scm3. B) Western analysis showing protein levels of pGAL$_{1-10}$-3HA-Scm3 as compared to Scm3-3HA expressed from its endogenous promoter. Pgk1 serves as a loading control. C) Western analysis showing levels of Scm3, Cse4, and Ndc10 in both Scm3^{on} and Scm3^{off} conditions. Scm3 protein levels are undetectable in Scm3^{off}, while Cse4 and Ndc10 levels remain unchanged. 50 micrograms of total protein were loaded per lane. Pgk1 serves as a loading control. D) Dilution assay reveals no difference in growth between a wild-type strain, and an otherwise isogenic strain containing the pGAL$_{1-10}$ promoter integrated to control Scm3 in galactose-containing media. However, in Scm3^{off} conditions, the pGAL$_{1-10}$-3HA-Scm3 strain does not exhibit any detectable growth, and arrests with large budded cells.

glucose-containing media (Scm3^{off}) (Figure 6D), an indication that we are able to recapitulate a *SCM3* null phenotype.

DAPI staining was performed to visualize DNA in Scm3^{on} and Scm3^{off} cultures. In Scm3^{on} we observe that large budded cells contain two DAPI staining foci in opposing cell bodies. This is in contrast to Scm3^{off} cells in which a single DAPI stained body is contained either entirely in one cell body, or extends across the mother-daughter neck (59% and 37% respectively) (Figure 7A). This phenotype indicates that accurate segregation of chromosomal DNA to opposite spindle poles had not occurred, with cell cycle arrest occurring sometime prior to anaphase. This phenotype is similar to that observed at the non-permissive temperature for strains with temperature sensitive mutations in either *CSE4* or *MIF2* [37, 78].

In order to visualize both spindle poles, and spindle microtubules, in Scm3^{on} and Scm3^{off}, indirect immunofluorescence was performed using antibodies against Tub1 (microtubules) and Tub4 (spindles pole bodies). In Scm3^{on}, large budded cells have normal elongated spindles of varying length (2-16μm) that span across both the mother cell and the bud. This observation is in contrast to Scm3^{off}, in which the vast majority of cells contain short spindles (96%, 1-5 μm) that either span the mother-daughter neck or reside in one cell body (Figure 7B-C). There does not appear to be a spindle pole duplication defect. Additionally, in the situation were the spindles microtubules are elongated past 5uM, we observe that the majority of cells exhibit defects in spindle morphology, including bent, and broken spindles (Figure 7D). These defects are reminiscent of those seen in strains harboring mutations in the outer

kinetochore protein Dam1, which functions in attachment of the microtubules to the kinetochore [83].

To analyze DNA content, fluorescence activated cell scanning (FACs) was performed on cells either maintained in galactose, or switched to glucose. Scm3^{on} cultures grown in galactose remain asynchronous, while cells transferred to YPD arrest within 2-3 hours with a 2N DNA content (>98%) (Figure 7E). Since the phenotypes observed for Scm3^{off} are reminiscent of those exhibited by strains with mutations to essential kinetochore proteins, we hypothesized that depletion of Scm3 was activating the mitotic spindle checkpoint. In order to verify that the metaphase arrest in Scm3^{off} is mediated by the spindle checkpoint, we deleted *MAD1*, a gene that encodes an essential spindle checkpoint component in our Scm3$^{on/off}$ background. FACs analysis was performed on cultures with Scm3^{on}-*Δmad1* and Scm3^{off}-*Δmad1*. Unlike Scm3^{off} cells, which arrest completely with 2N DNA content, Scm3^{off}-*Δmad1*cells do not arrest (Figure 7F). Instead, the culture with Scm3^{off}-*Δmad1* continues to cycle, with ploidy problems evidenced by a broadening of the 2N peak at later time points. This demonstrates that Scm3 function is required for proper chromosome segregation. Taken together, all of the above results strongly suggest that Scm3 is a novel kinetochore protein, without which the kinetochore is not fully functional and the spindle checkpoint is activated.

3. Functional Analysis of Scm3

Although Scm3 does not contain any predicted protein motifs that would

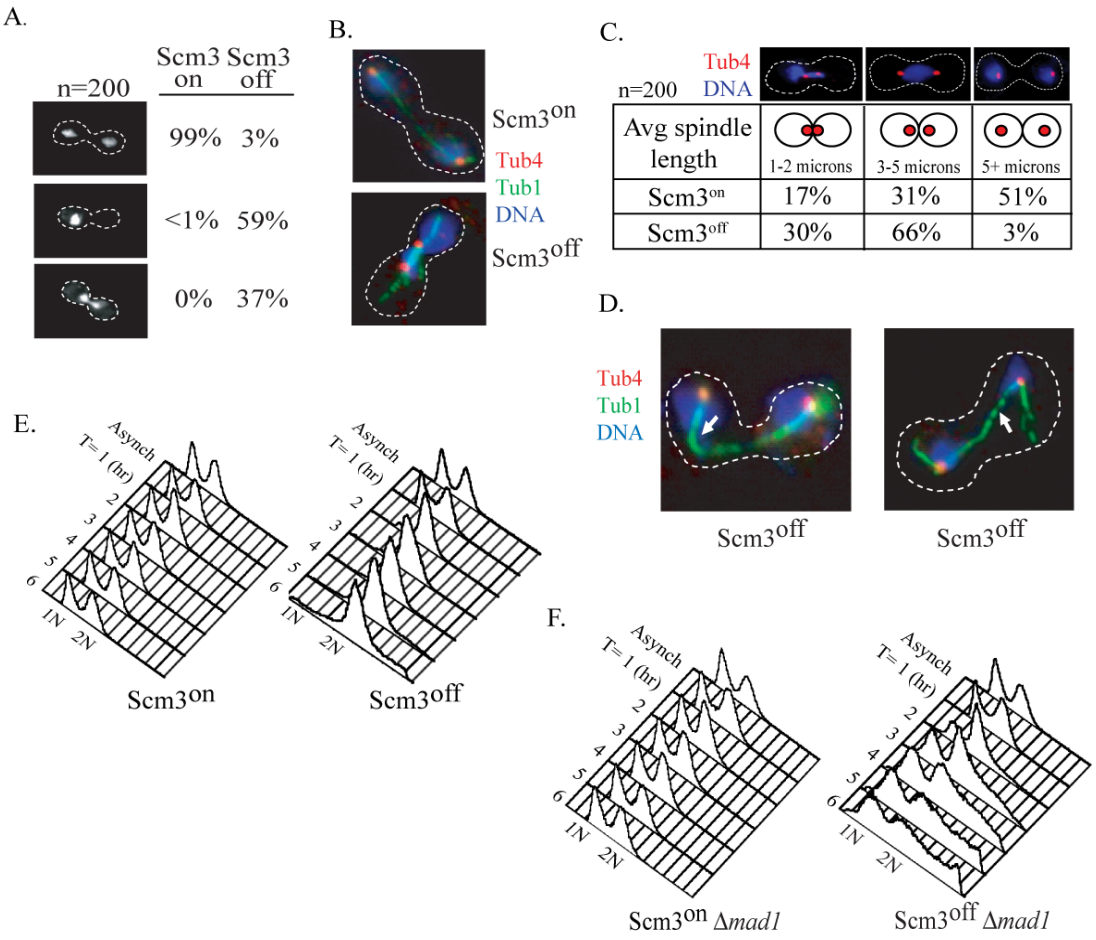

Figure 7. Phenotypic effects of the Scm3^{off} allele.
A) DAPI straining reveals the majority of DNA in Scm3^{off} cells is confined to one cell body or extends across the mother-daughter bud neck. B) Indirect immunofluorescence shows the short metaphase spindle in large budded Scm3^{off} cells. DNA is stained with DAPI (blue), spindle pole bodies are stained with antibody to Tub4 (red) and microtubules are visualized with an antibody against Tub1 (green). C) The length between spindle pole bodies (Tub4, red) was measured for 200 Scm3^{on} and Scm3^{off} cells. DNA is stained with DAPI (blue). D) The majority of Scm3^{off} cells whose distance between spindles is longer than 5 microns exhibit spindle defects. White arrows point to bent and broken spindles. Staining is the same as in (B). E) FACS analysis of asynchronous cultures switched from Scm3^{on} to Scm3^{off} shows complete arrest with 2N DNA content. F) FACS analysis shows that a strain without a functioning mitotic spindle checkpoint fails to arrest with 2N DNA content when Scm3 is shut off.

suggest its function, we have identified putative Scm3 orthologs in fungi with both point and regional centromeres (Figure 8A). Phylogenetic alignments of Scm3 reveal an evolutionarily conserved core domain (CCD) (Figure 8B). To assess the functional requirement of the Scm3 domains, we have performed domain deletion analysis focusing on both the N- and C- terminus of the Scm3 protein. Full length Scm3 protein was cloned into the high copy vector pRS423 (pRS423-Scm3Full). From this template, consecutive 25 amino acid deletions from both the N- and C-termini were constructed stopping 100 amino acids from each end of the protein. These constructs were transformed into $pGAL_{1\text{-}10}$-3HA-Scm3 and tested for growth in both $Scm3^{on}$ and $Scm3^{off}$ conditions. We find that when the endogenous Scm3 protein is shut off, and the only functional copy of *SCM3* is on the plasmid, deletion of the first 25 amino acids of the N-terminus of Scm3 (*scm3-Δ25N*) does not support growth. This is opposed to the C-terminus, where deletions of up to 75 amino acids are viable (Figure 8C). To test for essential residues of the Scm3 CCD, site directed mutagenesis was performed to selectively mutate conserved *SCM3* nucleotides. These constructs were transformed into $pGAL_{1\text{-}10}$-3HA-Scm3 and tested for growth in both $Scm3^{on}$ and $Scm3^{off}$ conditions. Using this approach, 3 essential residues (I110, I111, Y114) of the Scm3 CCD domain were identified (Figure 8D).

These results suggest that both the N-terminus and the CCD of Scm3 are required for proper protein function. To look for dominant lethality of any of these regions, clones were constructed that expressed small peptides of Scm3. The galactose inducible pESC-HIS plasmid was constructed to contain either: the N-

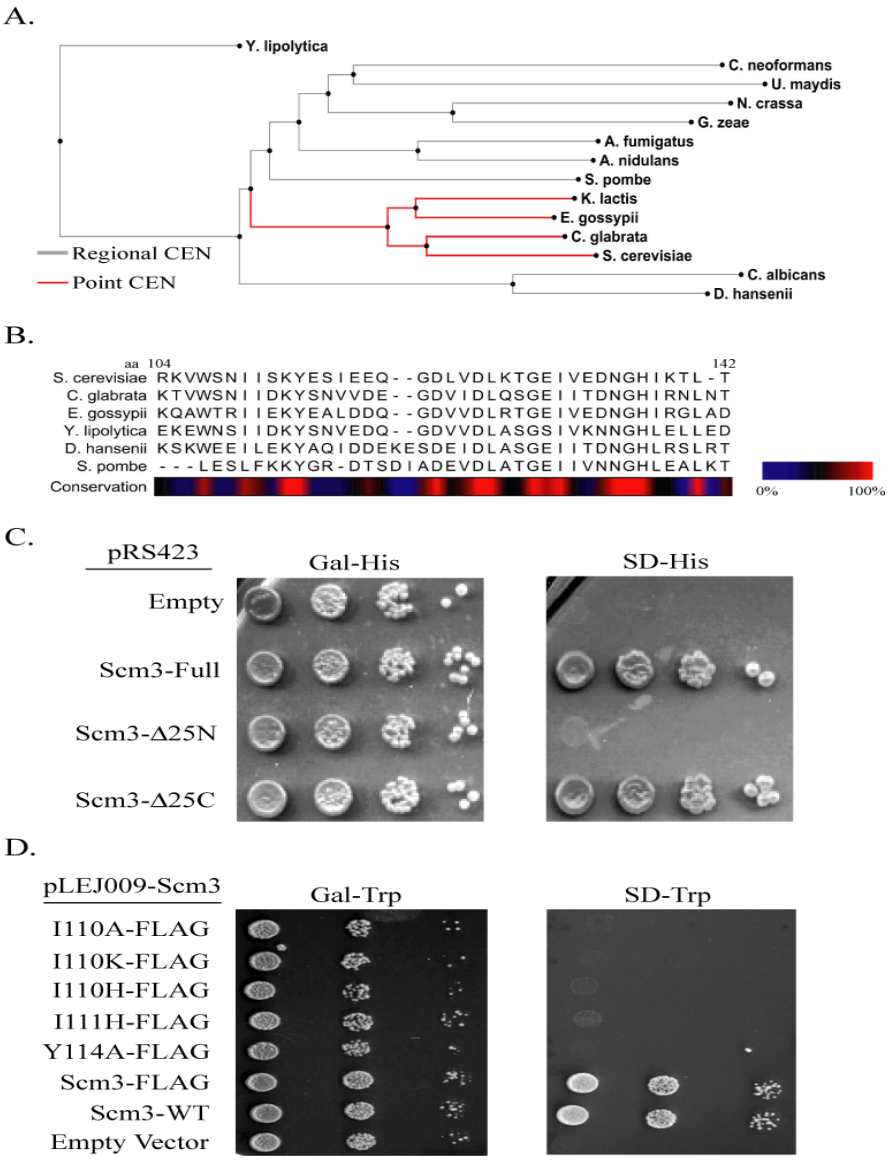

Figure 8. Phylogenic and functional analysis of Scm3.
A) Dendrogram of Scm3 in fourteen fungi which possess either point or regional centromeres. Grey branches represent fungi with regional centromeres and red branches those with point centromeres. B) Multiple protein sequence alignment of the conserved central domain (CCD) of Scm3 in various fungi. Scm3 exhibits conservation of numerous residues in this region, throughout all fungi. C) Deletion analysis reveals that deletion of the N-terminal 25 amino acids of Scm3 is lethal, while deletion of the C-terminal 25 amino acids of Scm3 is not. D) Site directed mutagenesis of conserved residues in the CCD. I110, I111, and Y114 are essential for Scm3 viability in Scm3^{off} conditions (SD-Trp).

terminal 25 amino acids of Scm3, the entire CCD sequence (39 amino acids), the first 25 amino acids of the CCD, the middle 25 amino acids of the CCD, or the last 25 amino acids of the CCD. Along with the pESC empty vector, these clones were transformed into a wild type yeast strain and a growth assay was performed to look at cell growth in either glucose (peptide not expressed) or galactose (peptide expressed). We find no discernable growth defect when the small Scm3 peptides are overexpressed in wild type cells (Figure 9A). To test for complementation of the Scm3 lethal mutants *scm3-Δ25N* and *scm3-I110H*, both mutants were cloned into both pRS423 and pRS425 expression vectors. Combinations of both plasmids were then transformed into a *scm3Δ* strain rescued by wild type *SCM3* on a plasmid (pRS314-Scm3). A plasmid-shuffle assay was then performed to look at viability. We find that no combination of the Scm3 lethal mutant proteins can rescue growth when co-expressed in the *scm3Δ* strain (Figure 9B).

4. Scm3 localizes specifically to centromeres in an Ndc10-dependent manner

Since Scm3 appears to be an inner kinetochore protein and is chromatin associated, we were interested in looking at its localization to DNA. A strain containing Scm3 tagged with 3 HA epitopes was grown to mid-log phase and arrested for two hours at metaphase with nocodazole. Cultures were harvested and genome-wide localization of Scm3-3HA was analyzed by chromatin immunoprecipitation followed by DNA microarray analysis (ChIP-chip). Scm3-3HA ChIP samples were hybridized against a total chromatin control to yeast whole genome microarrays.

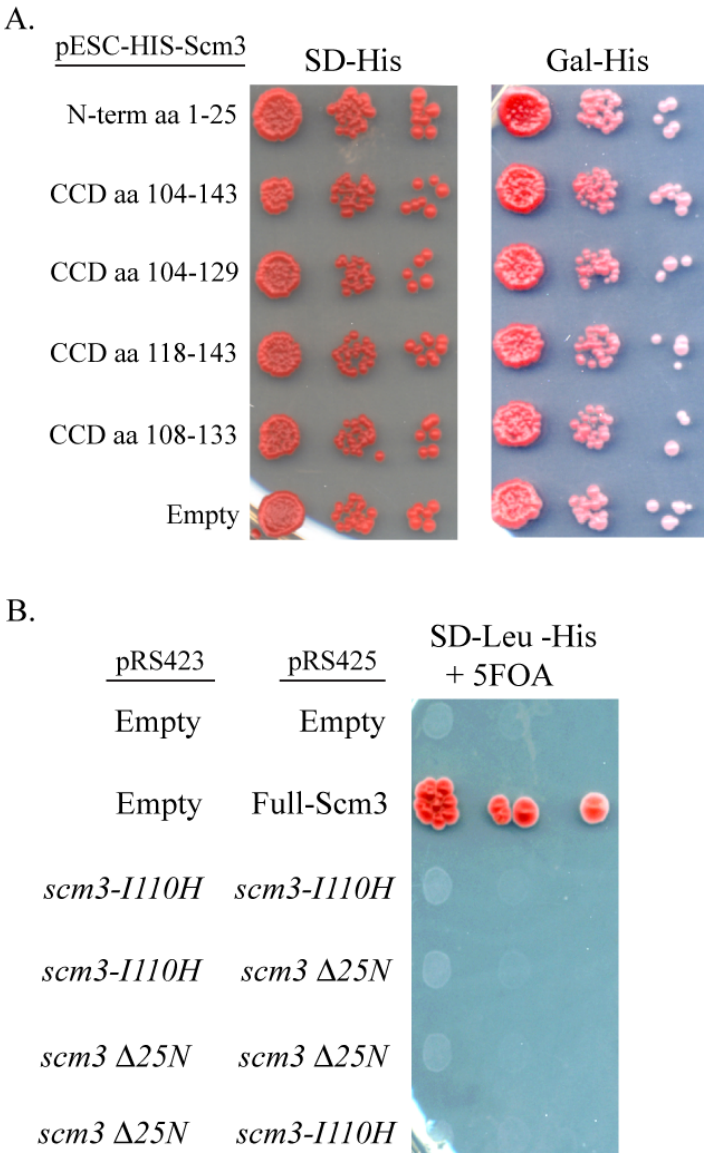

Figure 9. Scm3 peptide expression and mutant complementation.
A) Small peptide fragments of the Scm3 N-terminus and conserved central domain (CCD) amino acids (aa) were cloned into a galactose inducible expression plasmid (pESC-HIS) and transformed into wild type yeast. No difference in growth is observed when peptides are expressed (Gal-His) compared to growth when peptide are not expressed (SD-His). B) Plasmids pRS423 (HIS3) and pRS425 (LEU2) expressed wild type Scm3 and lethal mutants *scm3-Δ25N* and *scm3-I110H*. Plasmids were co-transformed into the *scm3Δ* strain covered by a wild type Scm3 expressed from pRS314. Cells were grown on media containing 5FOA to test for viability. No combination of Scm3 mutants can rescue growth on 5FOA.

Additionally, a negative (no antibody) control ChIP was performed. When we used αHA or no antibody precipitated samples as templates in semi-quantitative PCR reactions with primers that amplify sequence from CEN3, we observed a robust product with the αHA sample and no detectable product with the no antibody sample (data not shown). We were unable to amplify enough of the material precipitated in the absence of antibody for hybridization to a DNA microarray (data not shown). On microarrays Scm3 shows a strong enrichment exclusively to a region ~ 1.5 kb around all sixteen centromeres (Figure 10A). This result is consistent with a role for Scm3 in kinetochore function.

Several studies have shown Ndc10 to be the initial component of the kinetochore to localize to centromeres. This localization is necessary to establish centromeric chromatin and nucleate kinetochore formation, facilitating subsequent recruitment of downstream kinetochore proteins [79, 84, 88]. It has been previously shown that Cse4 fails to localize to centromeres in an *ndc10-1* [79] mutant at the non-permissive temperature [87, 92]. We tested whether the localization of Scm3 to centromeres requires Ndc10. We find that the centromeric localization of Scm3 is dependent on Ndc10 function. ChIP followed by quantitative PCR (qPCR) analysis reveals that centromeric localization of Scm3-3HA directly at CDE I-II-III is strongly reduced (~22 fold) in an *ndc10-1* mutant at non-permissive temperature (Figure 10B). The enhanced resolution of the qPCR relative to the DNA microarrays also reveals that at the permissive temperature Scm3 localizes strongly to ~300 bps, which encompass CDE I-II-III.

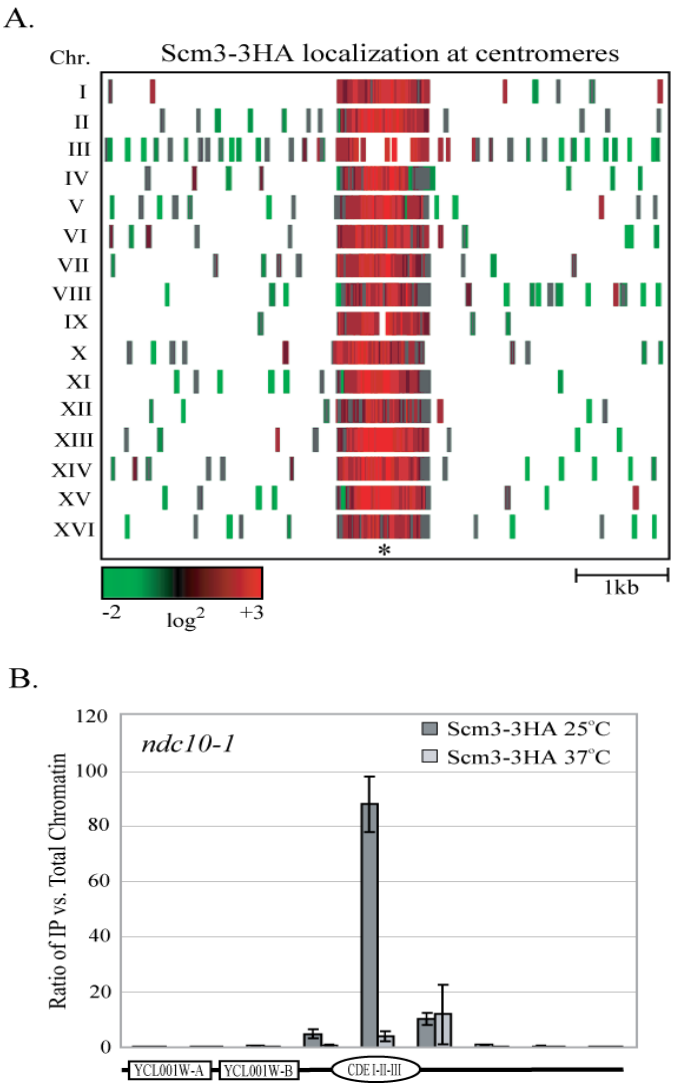

Figure 10. Scm3 localizes to the centromere and this requires Ndc10.
A) Genome-wide microarray analysis reveals Scm3 localizes specifically to centromeres. Cultures expressing Scm3-3HA were grown to mid-log phase and arrested in metaphase with nocodazole. ChIP-chip was performed on two independent biological samples and the results were averaged. The heatmap represents the $\log_2$ ratios of Scm3-3HA IP microarray signal divided by a total chromatin input control for each microarray feature. Centromeric regions were tiled at high resolution. A region corresponding to 4.5 kb surrounding the centromere is shown for all 16 chromosomes, with an asterisk indicating the region of CDE I-II-III. B) ChIP was performed for Scm3-3HA in the *ndc10-1* temperature sensitive background at permissive temperature (25°C) and after a 4 hour shift to non-permissive temperature (37°C), followed by qPCR. Scm3-3HA qPCR signal at CDE I-II-III (oval) is greatly reduced at 37°C as compared to 25°C. Error bars represent +/- average deviation of biological replicates.

5. Scm3 is essential for proper localization of inner kinetochore proteins to the centromere

The findings that Scm3 localizes to all sixteen centromeres, and depletion of Scm3 results in chromosome segregation defects strongly suggests a role for Scm3 in kinetochore function. Since Scm3 co-purified with Cse4 we decided to quantitatively analyze Cse4 localization to the centromere in the context of Scm3 depletion. Cse4 was tagged with 12 Myc epitopes in the $pGAL_{1\text{-}10}$-3HA-Scm3 background. Cultures were grown for ChIP, and qPCR was performed to measure Cse4-12Myc localization to a 2 kb region surrounding the centromere of chromosome 3 (CEN3) in the presence or absence of Scm3. When cells are grown in galactose, Cse4 exhibits a strong localization to CEN3. When cultures were switched to glucose-containing media for three hours, Cse4 levels at CEN3 are markedly decreased (4-fold) (Figure 11A). Interestingly, localization of histone H3 to this same site increases 8-fold in the absence of Scm3 (Figure 11B). This finding suggests that in the absence of Scm3, Cse4 is replaced with histone H3, effectively altering the specialized chromatin found at the centromere. We can also not rule out the possibility that in the absence of Scm3, the increased H3 signal at the centromere is simply due to an overall increase in ChIP antibody accessibility to H3-containing nucleosomes surrounding the centromere. Additionally, our ChIP results are consistent with the model that a single Cse4-containing nucleosome is positioned within the centromere sequence [77]. In addition to Cse4, we analyzed the localization of two other essential inner kinetochore proteins in the absence of Scm3. Utilizing the same ChIP/qPCR

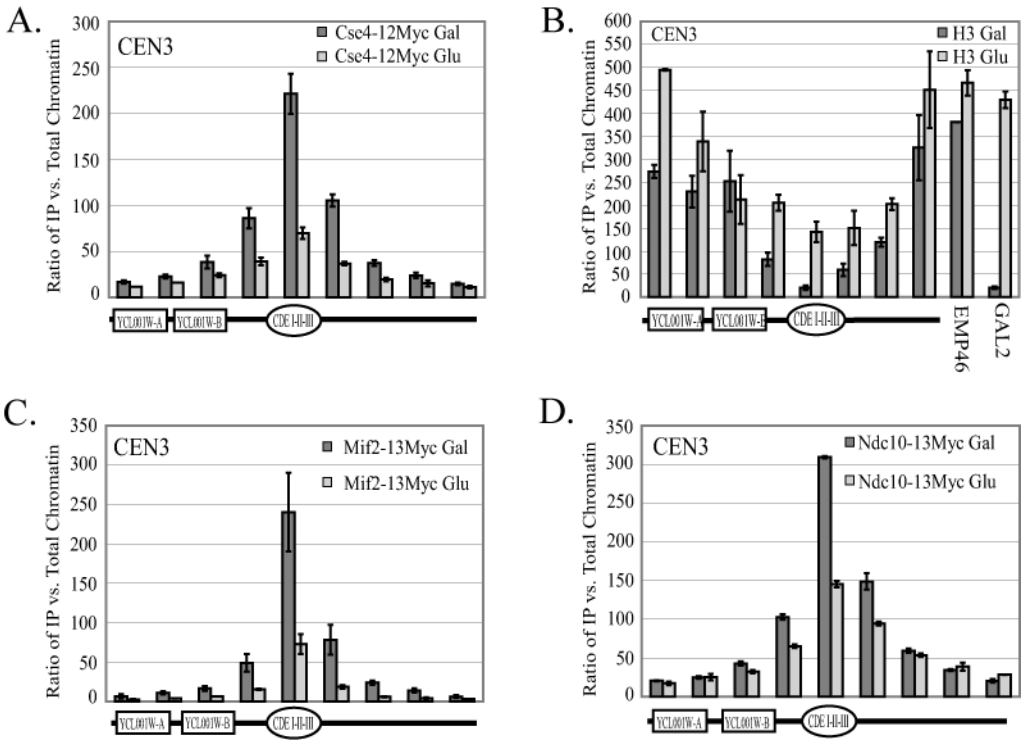

Figure 11. Centromeric localization of inner kinetochore proteins in Scm3$^{on/off}$. A-D. ChIP followed by qPCR was used to analyze the localization of inner kinetochore proteins to a 2 kb centromeric region on chromosome III in cultures grown with Scm3^{on} (galactose) or Scm3^{off} (glucose). A depiction of the features within the region is shown below each histogram. Error bar represent +/- the average deviation of biological replicates. A) Asynchronous Cse4-12Myc cultures switched to Scm3^{off} (glucose, 3hr.) exhibit a marked decrease (4-fold) in Cse4 signal at CDE I-II-III (oval). B) Conversely, histone H3 signal at CDE I-II-III increases 8-fold in Scm3^{off} (glucose). The *EMP46* gene in this case serves as a positive control region for histone H3. The signal at the *GAL2* gene serves as a positive region for histone H3 when transcription is off in glucose media and a negative region when transcription is on in galactose media. C) Asynchronous Mif2-13Myc cultures switched to Scm3^{off} (glucose) exhibit a decrease (3.5-fold) in Mif2 qPCR signal at CDE I-II-III. D) Ndc10 is depleted 2-fold in Scm3^{off} by qPCR.

technique from above, Mif2-13Myc shows a 3.5-fold decrease (Figure 11C) and Ndc10-13Myc shows a 2-fold decrease (Figure 11D) in CEN3 localization when Scm3 is depleted. Since Mif2 requires Cse4 to localize to the centromere [80], the loss of its localization to CEN3 can be attributed to loss of Cse4. The decrease in Ndc10 localization to the centromere is more surprising since Ndc10 is thought to be the first component of the kinetochore that localizes to the centromere, and no factors that contribute to its centromere-specific localization have been identified. Based on these findings, it appears that Scm3 is essential to initiate formation of a functional inner kinetochore.

Given the mutual dependence of Scm3 and Ndc10 for efficient localization to the centromere, and given the interaction between Scm3 and both Ndc10 and Cse4, we decided to examine the centromeric localization and physical interaction between Scm3 and Ndc10 in a *cse4-1* temperature sensitive mutant. It has previously been demonstrated that Ndc10 localization to CEN3 in a *cse4-1* mutant is unaffected at the non-permissive temperature [93]. We find that while both Ndc10 and Scm3 can localize to CEN3 in a *cse4-1* mutant at the non-permissive temperature, they do so with reduced efficiency (2-fold and 3.5-fold respectively) (Figure 12A-B). Ndc10 and Scm3 are still able to physically associate in a *cse4-1* mutant at the non-permissive temperature by co-immunoprecipitation (Figure 12C). We conclude that while Cse4 may help to stabilize an inner kinetochore complex composed of Cse4, Ndc10, and Scm3, it is not essential for Ndc10 and Scm3 interaction or localization to centromeres.

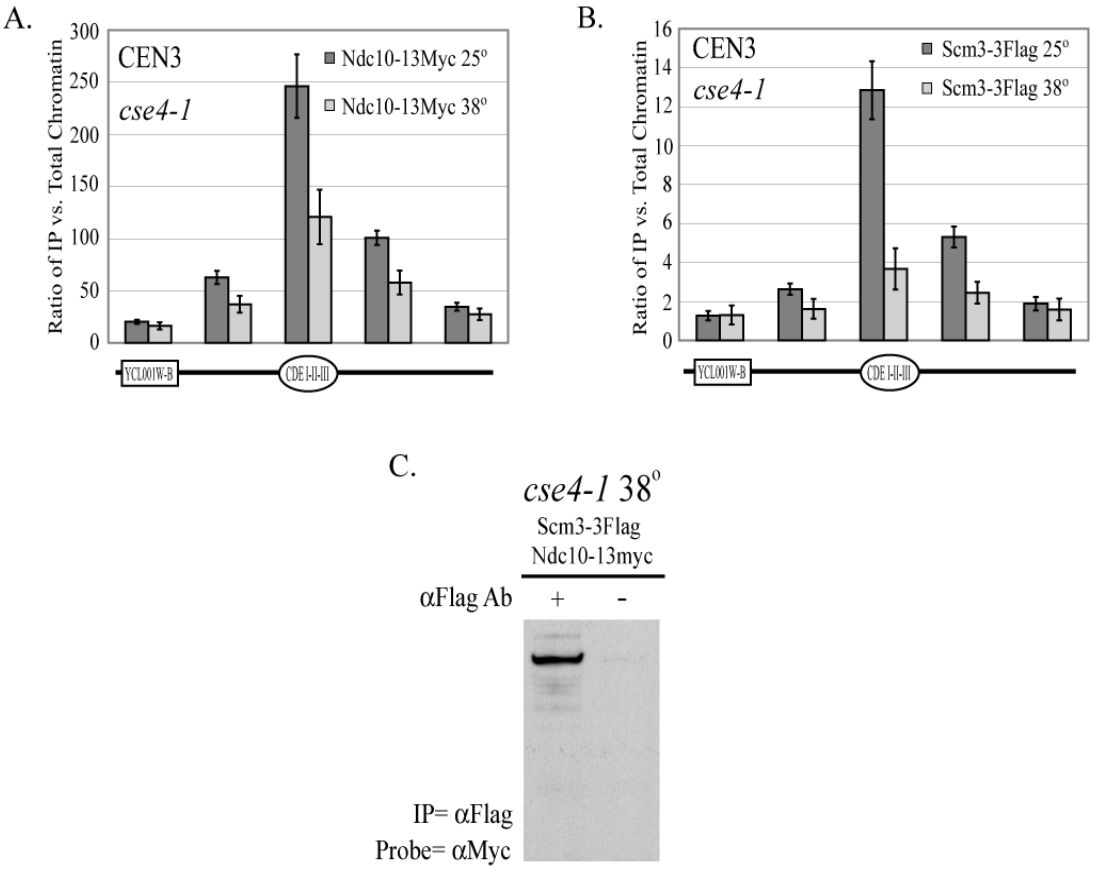

Figure 12. Centromeric localization of Scm3 and Ndc10 in the *cse4-1* mutant. A-B) ChIP at CEN3 was performed for both Ndc10-13Myc (A) and Scm3-3Flag (B) in the *cse4-1* background. Cultures were either maintained at permissive temperatures (25°C) or switched to non-permissive temperatures (38°C) in the presence of nocodozole for 4 hours. Error bar represents +/- the average deviation of biological replicates. C) Co-immunoprecipitation of Scm3-3Flag and Ndc10-13Myc in the *cse4-1* background at non-permissive temperature. Scm3 and Ndc10 still physically associate in the *cse4-1* mutant at non-permissive temperature.

In order to determine whether Scm3 was sufficient to target Ndc10 and Cse4 to non-centromeric sites in the genome, Scm3 was fused to a Gal4 DNA binding domain (Scm3-BD) and expressed from a high copy plasmid. Using this construct we were not able to obtain transformants, an indication that expression of Scm3-BD may be toxic to the cells (data not shown). Subsequently, we constructed a plasmid-based galactose inducible Scm3-BD fusion (pESC-Scm3-BD) with two Myc epitope tags, and transformed that into strains with either Cse4-3HA or Ndc10-3HA. When we maintained the cells in glucose they grow with no observable defects, but upon switch to galactose media, pESC-Scm3-BD-containing cells exhibit poor growth when compared to a strain harboring the pESC vector alone (Figure 13A). To test whether the Scm3-Gal4-BD fusion protein was functional, a plasmid shuffle assay was performed. We found that cells expressing pESC-Scm3-BD as the sole copy of Scm3 in the cell can indeed grow, although their growth is slower than cells expressing pESC-Scm3 without the Gal4 DNA binding domain (Figure 13B). When cultures are switched to inducing conditions (Gal-His), ChIP/qPCR analysis reveals the Gal4BD-Scm3 fusion protein efficiently targets both the endogenous *GAL2* promoter and a *GAL1* upstream activating sequence (UAS) integrated at YOL118c (Figure 13C). It also localizes, albeit to a lesser extent, to CEN3. Next we checked whether Cse4 localized to these sites. We found no significant Cse4-3HA enrichment at the *GAL2* UAS or *GAL1* UAS-YOL118c when pESC-Scm3BD was expressed (Figure 13D). Additionally, we checked whether Ndc10 could be targeted to these regions. We find, as with Cse4-3HA, Ndc10-3HA was not recruited to a non-centromeric region

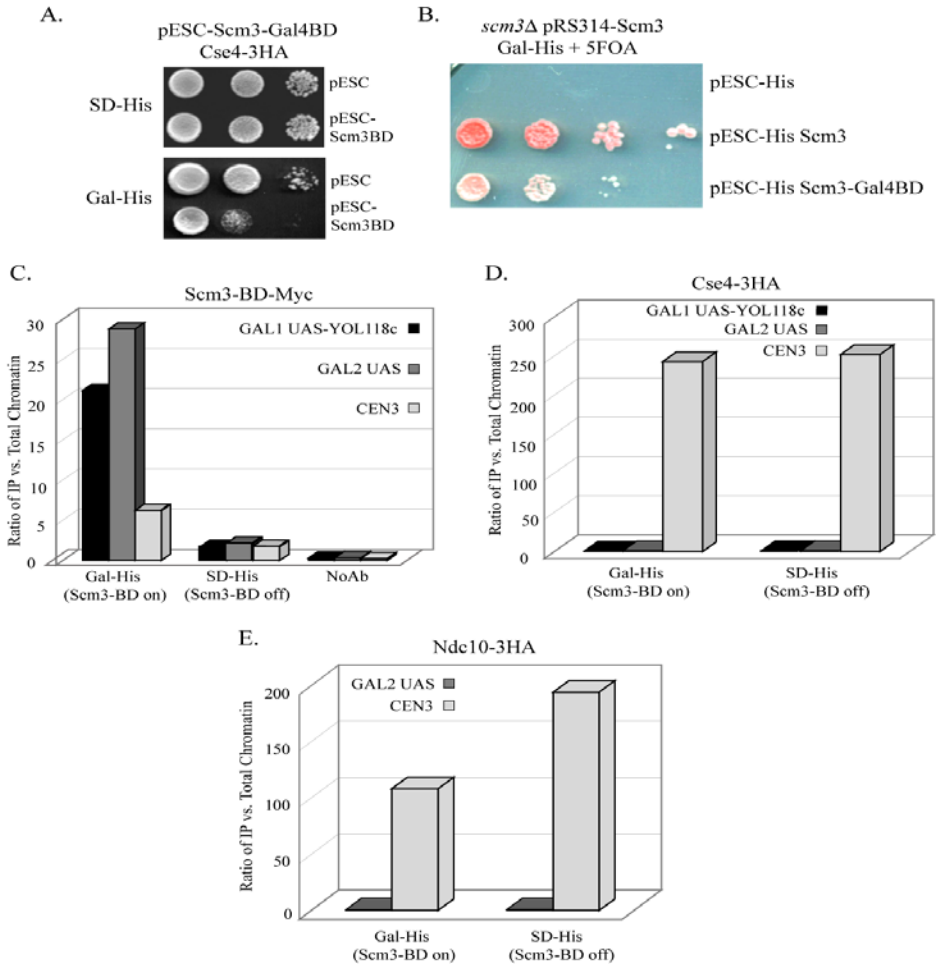

Figure 13. A Galactose-inducible Scm3 Gal4 DNA binding domain fusion is not able to recruit Cse4 or Ndc10 to the *GAL2* UAS.

A) A yeast strain harboring the empty plasmid vector pESC or the Scm3-Gal4 binding domain fusion protein (pESC-Scm3-BD) grows similarly on SD-His media. The strain with pESC-Scm3BD grows slower when the fusion protein is induced on Gal-His media. B) A plasmid shuffle assay was performed using pESC, pESC-Scm3 and pESC-Scm3-BD. On media containing 5FOA (Gal-His) we find both pESC-Scm3 and pESC-Scm3-BD can support growth. C) A strain containing pESC-Scm3-BD was grown under inducing (Gal-His) or non-inducing conditions (SD-His) and processed for ChIP/qPCR to monitor the localization of the fusion protein. Three different sites were monitored: CEN3 (light grey), the endogenous *GAL2* UAS (dark grey), and a *GAL1* UAS inserted at YOL118C (black). D) Experiment was performed as in (B) except that the localization of Cse4-3HA was monitored by ChIP/qPCR. Cse4-3HA localizes very strongly to CEN3 in both Gal-His and SD-His, but does not localize to either the *GAL2* UAS or *GAL1* UAS-YOL118c. E) Experiment was performed as in (B) except that the localization of Ndc10-3HA to the *GAL2* UAS and CEN3 was monitored via ChIP/qPCR.

(Figure 13E). Thus it appears that the Scm3-BD fusion protein is not sufficient to nucleate an inner kinetochore at non-centromeric sites.

6. Scm3 is required to establish and maintain a kinetochore that can activate the spindle checkpoint

In order to more closely examine the requirement for Scm3 in the assembly of the kinetochore, we arrested cells in G1 (with α-factor), depleted Scm3, and released them into the cell cycle to monitor DNA content as an indicator of checkpoint activation. In our previous experiments, depleting Scm3 in asynchronous cells activates the spindle checkpoint and arrests cells at metaphase. However, when cells are depleted for Scm3 prior to release from G1, they do not arrest with 2N DNA content (Figure 14A), an indication that they are not able to activate the spindle checkpoint. Additionally, three hours post-G1 release cells begin to exhibit broadening of the 2N peak, an indicator of ploidy problems. This cytometry profile closely resembles that of a *ndc10-1* temperature-sensitive mutant at non-permissive temperature [94]. Since activation of the mitotic spindle checkpoint requires functional Ndc10 at the kinetochore [95], the above phenotype may result from the failure of Ndc10 to associate with centromeres following their replication.

We hypothesized that the failure of cells to achieve metaphase arrest when Scm3 was depleted prior to S-phase was due to a failure in loading Ndc10. In order to test this hypothesis, we arrested cells in G1 and released cells into media containing hydroxyurea (HU) with either $Scm3^{on}$ or $Scm3^{off}$. HU depletes

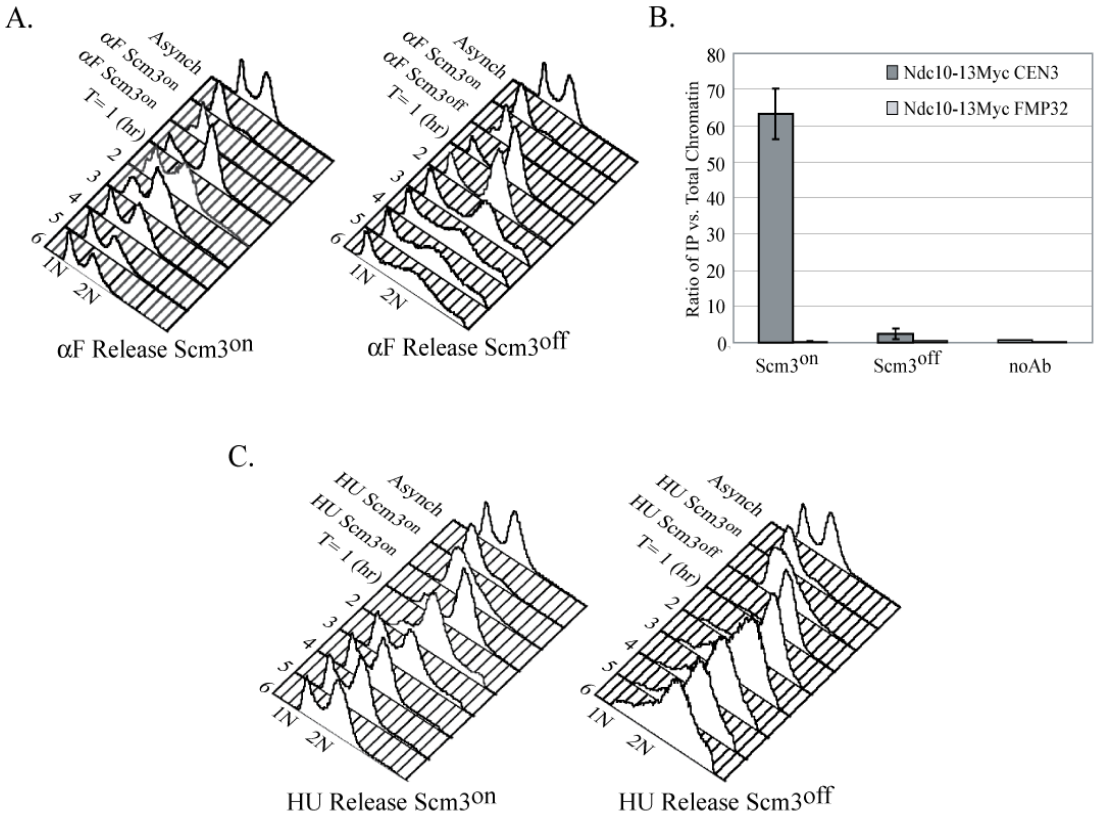

Figure 14. The effects of Scm3 depletion on checkpoint activity and Ndc10 association with the centromere. A) Cells were arrested in G1, maintained in galactose media (Scm3^{on}) or switched to glucose-containing media for 2 hours (Scm3^{off}) and released to follow cell cycle progression by FACS. When Scm3 is depleted during G1, cells fail to activate the spindle checkpoint and exhibit ploidy problems. B) ChIP/qPCR shows a significant decrease (7-fold) in Ndc10 association with the CDE I-II-III sequence at the centromere on chromosome III in HU-arrested cells when Scm3 is depleted during G1 arrest. *FMP32* is a gene on the arm of chromosome VI that serves as a negative control sequence for Ndc10 association. Error bars represent +/- the average deviation of biological replicates. C) When Scm3 is depleted during HU arrest, and the cells are released with Scm3^{off}, cells do not regain asynchronous DNA content, an indication that cells do not proceed past metaphase and the spindle checkpoint is activated.

deoxyribonucleotide pools, causing cell cycle arrest prior to the completion of DNA replication, with replication of most centromeres completed due to nearby replication origins [96]. Since inner kinetochore proteins are thought to re-load very early in S-phase, Ndc10 should localize to the centromere in a HU arrest. We found that when centromeres are replicated in the presence of Scm3, the level of Ndc10 at CEN3 is significantly higher than in the absence of Scm3. In the absence of Scm3, Ndc10 levels fall to levels near those of the negative controls (Figure 14B). Thus, it appears that Scm3 is required to load Ndc10 at centromeres following their replication.

To further test the contribution of Scm3 to the assembly of a functional kinetochore, we depleted Scm3 in cells arrested in HU. If Scm3 is not required following early S phase for kinetochore function, the Scm3^{off} culture should proceed through metaphase following release from HU. Instead, cells released from HU in the absence of Scm3 fully arrest with 2N DNA content in the same cell cycle (Figure 14C) and remain large-budded. The checkpoint appears to be activated, suggesting that Ndc10 is located at centromeres, but the kinetochore is still defective.

To test for the requirement of Scm3 at G2/M, we arrested cells in G2/M with NZ, depleted Scm3, and then released them and analyzed DNA content (Figure 15A). We found that following depletion of Scm3, cells were unable to recover from a metaphase arrest. The cytometry profiles reveal that chromosome segregation does not resume normally after release with Scm3^{off}, an indication that Scm3 function is required during metaphase to maintain a segregation-competent kinetochore.

In order for cells enter anaphase, sister chromatid cohesin must be removed

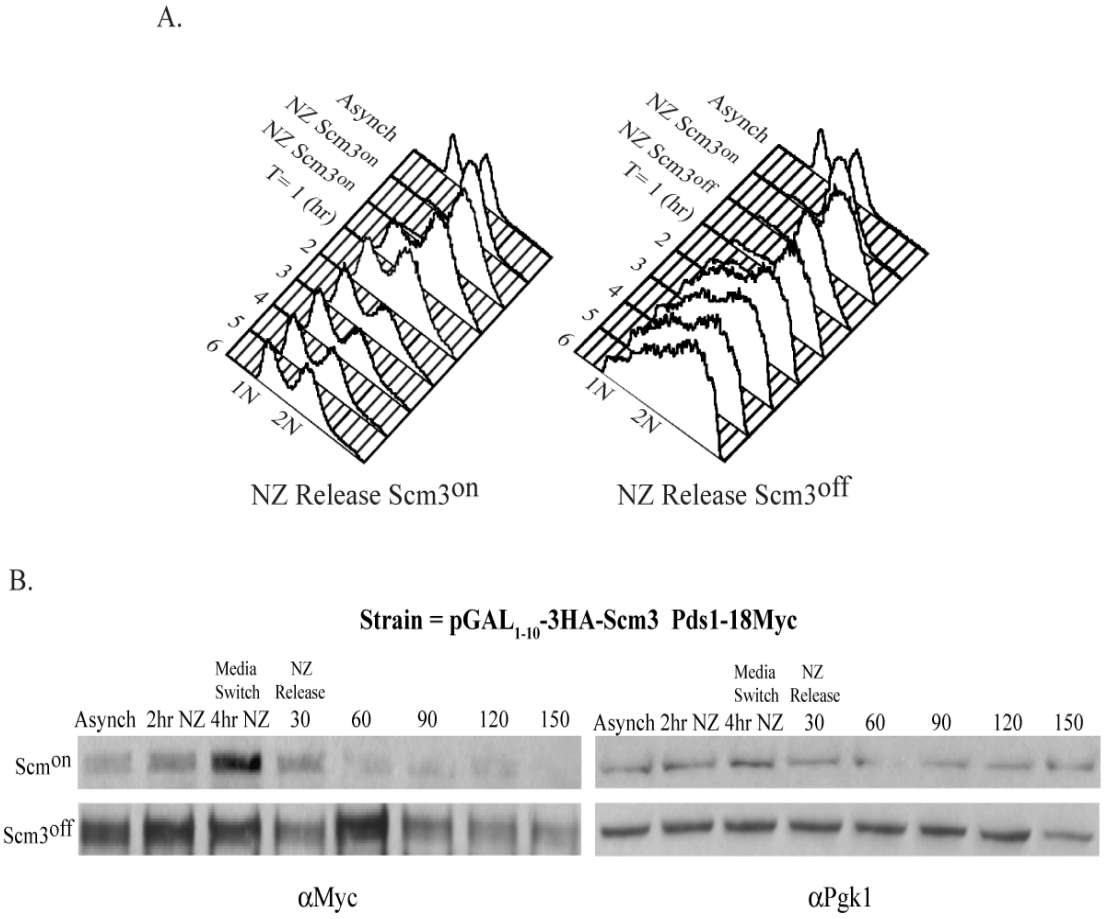

Figure 15. Scm3 depletion in metaphase arrested cells causes sustained checkpoint activity following release.

A) Cells were arrested in nocodazole (NZ), maintained in galactose media (Scm3^{on}) or switched to glucose-containing media for 2 hours (Scm3^{off}) and released to follow cell cycle progression by cytometric analysis. When Scm3 is depleted during a nocodazole arrest (metaphase) cells cannot recover, remaining arrested with 2N DNA content. B) Stability of Pds1-18Myc was monitored by Western blot analysis. The last 5 timepoints on each blot represent minutes after release from nocodazole arrest. When cells were released from the nocodazole arrest with Scm3^{on}, Pds1-18Myc was degraded in a time dependent manner. This indicates that the checkpoint arrest was removed and cells were entering anaphase. Conversely, when cells were released with Scm3^{off}, levels of Pds1-18myc remained unchanged, an indication that Pds1 was not degraded and the chromosomes were held together in a checkpoint arrest. A Pgk1 blot serves as a loading control.

during metaphase. The protein Esp1 (Separase) effectively cleaves the cohesin holding the sister chromatids together, allowing chromosomes to segregate during anaphase. Esp1 is sequestered in a non-active form by a protein called Pds1 (Securin) until it is needed. Once the signal has been received to enter anaphase Pds1 is degraded and Esp1 is released to relieve sister chromatin cohesion. If the spindle checkpoint is activated, Pds1 is not cleaved, Esp1 remains sequestered, and cells to not enter anaphase. To test if the spindle checkpoint remains active after NZ release in Scm3$^{on/off}$, stability of Pds1-18Myc was monitored by Western blot analysis. When cells were released from the NZ arrest with Scm3^{on}, Pds1-18Myc was degraded in a time dependent manner. This degradation of Pds1 indicates that the checkpoint arrest was removed and cells were entering anaphase. Conversely, when cells were released with Scm3^{off}, levels of Pds1-18Myc remained unchanged, an indication that Pds1 was not degraded and the cells maintained the checkpoint arrest (Figure 15B).

Based on these results we hypothesize that when Scm3 is shut-off during a metaphase arrest, the cells can not re-enter the cell cycle due to the persistence of spindle checkpoint activation. To test if either of the Scm3 lethal mutants were capable of undergoing mitosis after a metaphase arrest, we transformed both pRS423-*scm3Δ*25N and pRS423-Scm3-I110H into the Scm3 shut-off strain. Cells were arrested in metaphase with nocodazole, Scm3 was depleted by addition of glucose-containing media, and after Scm3 was depleted, cells were released from the NZ arrest with the Scm3 mutant as the only functional copy of the protein in the cell. We find that upon release from the NZ arrest, cells that contain empty vector (pRS423),

pRS423-*scm3Δ*25N or pRS423-Scm3-I110 cannot proceed through metaphase (Figure 16). This result indicates that neither of the Scm3 mutants is functional to alleviate the spindle checkpoint arrest.

7. Ipl1 is required to activate the spindle checkpoint when Scm3 is depleted

Ipl1, a homolog of human Aurora kinase B, has been shown to destabilize improperly attached kinetochore microtubules, which in turn activates the spindle assembly checkpoint [97]. To determine whether the spindle checkpoint activation following Scm3 depletion post-G1 is due to Ipl1 detaching improper kinetochore-microtubule attachments, or due to a failure to attach microtubules altogether, we depleted Scm3 in the *ipl1-321* background. Cells were synchronized in HU and released with Scm3^{off} at both permissive (25°C) and non-permissive temperatures (37°C). We find that Scm3^{off} cultures released at the permissive temperature arrest with 2N DNA content in the same cell cycle as expected, whereas cultures released into non-permissive temperatures fail to arrest and exhibit significant segregation defects (Figure 17A). This result indicates the Mad1-mediated metaphase arrest observed in Scm3^{off} is due to Ipl1 detaching improper kinetochore-microtubule attachments.

Direct-immunofluorescence of GFP-marked centromere IV [98] was performed to study the behavior of centromeric foci. Cells released from HU arrest with Scm3^{off} at permissive temperatures contain a single centromeric focus near the bud neck, indicative of a metaphase arrest, and a lack of kinetochore-microtubule

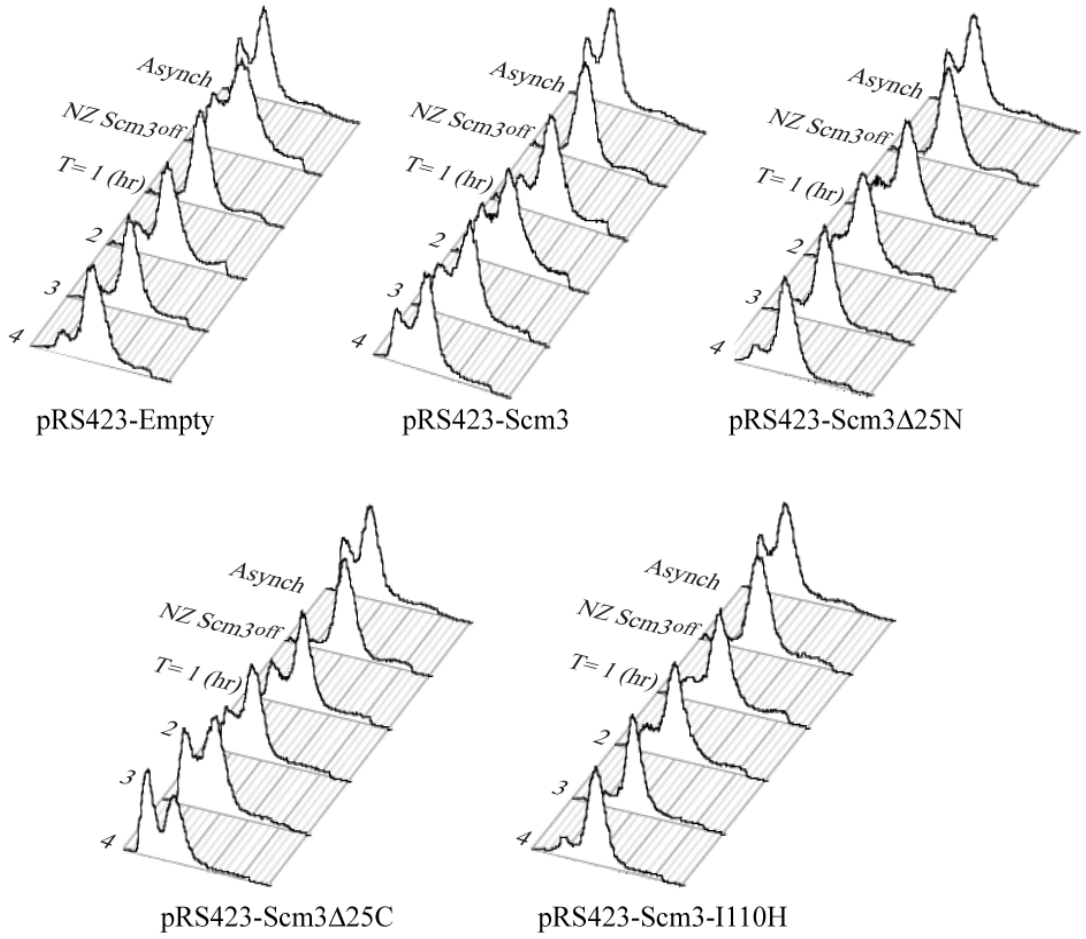

Figure 16. Scm3 mutants cannot re-enter the cell cycle after a metaphase arrest. Yeast containing the Scm3 shut-off allele were transformed with pRS423, pRS423-Scm3(WT), pRS423-*scm3Δ*25N, pRS423-*Scm3Δ*25C, and pRS423-Scm3I110H. Cells were arrested in nocodazole (NZ), switched to glucose-containing media for 2 hours ($Scm3^{off}$), and subsequently released to follow cell cycle progression by cytometric analysis. When Scm3 is depleted during a nocodazole arrest (metaphase) cells containing empty vector, pRS423-*scm3Δ*25N, or pRS423-Scm3I110H cannot recover, remaining arrested with 2N DNA content.

mediated chromosome movement (Figure 17B). In the cultures with Scm3^{on} at the non-permissive temperature for Ipl1, we find that the Ipl1 mutation alone results in 59% of chromosome IV centromeres migrating to a single pole, consistent with previous work demonstrating that mutation of Ipl1 results in increased microtubule attachments to a single pole (monopolar attachments) and chromosome segregation defects [99]. Under double mutant conditions, 93% of chromosome IV centromeres move towards a single spindle pole (Figure 17B), suggesting the spindle checkpoint is bypassed, spindle microtubules are attached to chromosomes, albeit improperly, and chromosome movement does occur. This movement of the two centromeres to a single cell body is suggestive of monopolar kinetochore-microtubules attachments, and has been observed in other kinetochore mutants [81, 84]. However, the *scm3 ipl1-321* double mutant phenotype is more severe than the *ipl1-321* single mutant phenotype. This result contrasts to what has been observed for a *mtw1-1 ipl1-321* double mutant strain in which the double mutant and single mutants have similar phenotypes [97], suggesting that Scm3 plays an additional role in biorientation (see Discussion). Our results suggest Scm3 is not essential for attachment of kinetochores to microtubules after the early kinetochore has formed, but is required to achieve sister kinetochore biorientation thereafter.

The inner kinetochore has been shown to enhance pericentric cohesin association and promote high-fidelity chromosome segregation under some conditions [100, 101]. One possible explanation for the biorientation defect is that Scm3 is needed for maximal pericentric cohesin association following release from

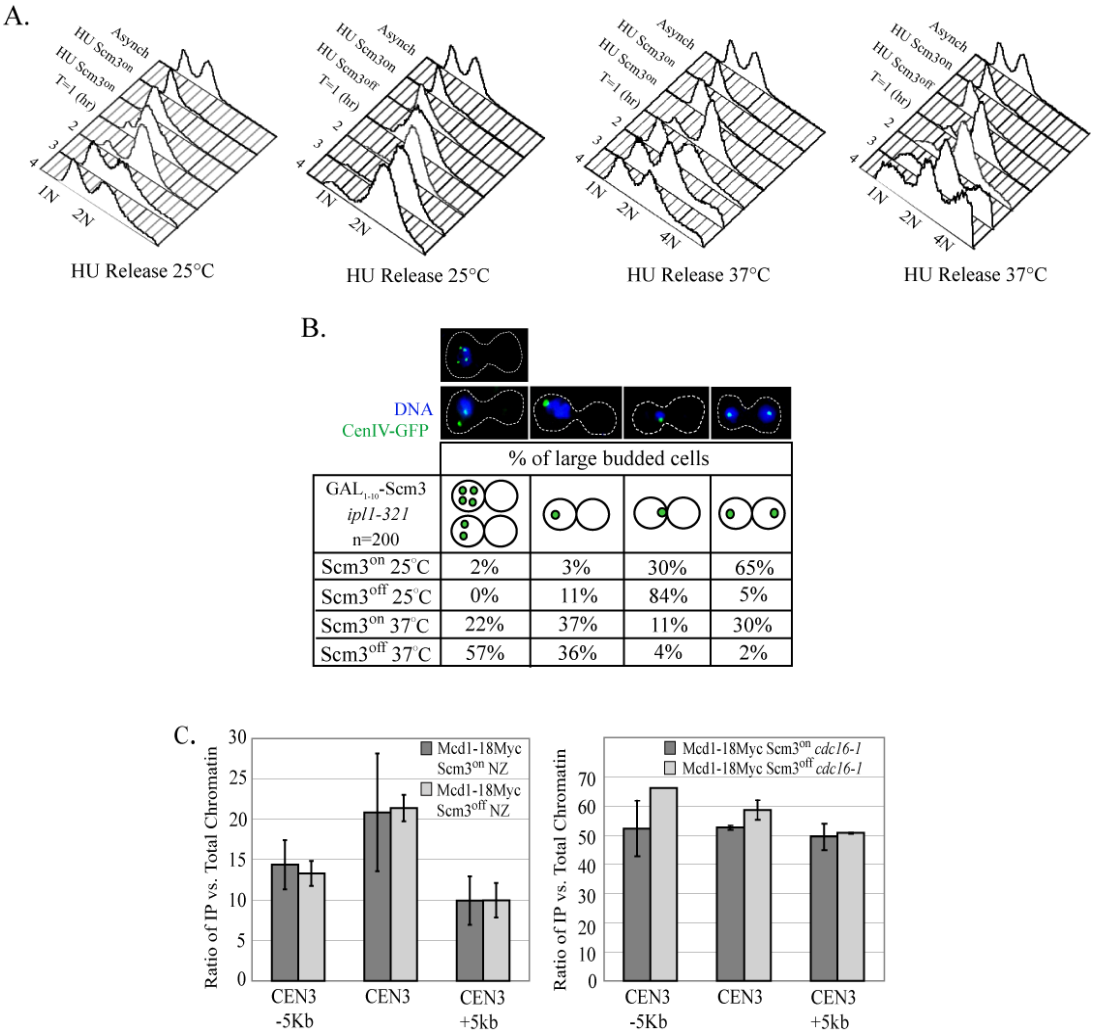

Figure 17. Ipl1 is required to activate the spindle checkpoint in Scm3^{off}.
A) FACS analysis was performed on cells synchronized with HU, and then released into either *ipl1-321* permissive (25°C) or non-permissive (37°C) temperatures with either Scm3^{on} or Scm3^{off}. B) Direct fluorescence of CenIV-GFP loci at 3 hours after release from HU in the 4 above mentioned conditions. CenIV-GFP loci were assessed in 200 large budded cells for each condition. Compared to *ipl-321* at 37°C, a larger percentage of CenIV foci in Scm3 ^{off} *ipl1-321* at 37°C migrate to a single pole. C. Pericentric cohesin association was monitored by ChIP for Mcd1-18Myc followed by qPCR at CEN3. Cultures were arrested with HU and Scm3 was depleted from half of the culture by transfer to glucose. Cultures were released to a G2/M arrest mediated either by addition of nocodazole or by temperature sensitive *cdc16-1*. In neither case did we detect a difference in the amount of Mcd1-18Myc following depletion of Scm3. Error bars represent +/- average deviation of biological replicates. defects observed in Scm3^{off} (bent and broken microtubules) resemble those of *dam1*

HU arrest. We tested this by arresting cells in S phase with HU, depleting half of the culture for Scm3, and then releasing the culture to a G2/M arrest, mediated either by *cdc16-1* or nocodazole. We used ChIP/qPCR to monitor the levels of Mcd1-18Myc. We found no difference in the levels of pericentric cohesin association in the presence or absence of Scm3, arguing that a lack of cohesin does not explain the biorientation defect observed (Figure 17C).

8. The role of Scm3 localization and regulation of the outer kinetochore

As mentioned earlier, when cells are depleted for Scm3 after the kinetochore has presumably formed (HU and NZ arrest), they are not able to continue through the cell cycle and activate the spindle checkpoint. This is an indication that Scm3 has a function outside of formation of the inner kinetochore. . Additionally, some of the microtubules defects observed in $Scm3^{off}$ (bent and broken microtubules) resemble those of *dam1* temperature sensitive mutants at non-permissive temperatures [83]. Based on these observations**,** it is hypothesized that Scm3 may be required for the proper localization of the outer kinetochore. To test this, we fused the endogenous copy of Dam1 to a green fluorescent protein tag (Dam1-GFP) in the $pGAL_{1\text{-}10}$-HA-Scm3 background. Cells were then arrested using HU and subsequently released from the HU arrest with either $Scm3^{on}$ or $Scm3^{off}$. Samples were collected every hour, for three hours and localization of Dam1-GFP was monitored by fluorescence microscopy. At 2 hours post HU release with $Scm3^{on}$ we observe localization of Dam1-GFP to kinetochores, with some cells in anaphase and some cells that had

not yet begun chromosome segregation (Figure 18A). With Scm3^{off}, we observed only cells which had not entered anaphase, although discrete localization of Dam1-GFP was still observed (Figure 18A). This result suggests that depletion of Scm3 after the inner kinetochore has formed does not preclude the recruitment of Dam1 to the kinetochore.

Although it appears that the outer kinetochore protein Dam1 properly localizes in Scm3^{off}, the spindle checkpoint is still activated, suggesting the kinetochore is not functional. This finding suggests that Scm3 may play a role in the checkpoint signaling pathway. It has previously been shown that di-methylation of lysine 233 (K233me^2) of Dam1 antagonizes phosphorylation of the 2 serine residues flanking K233, and this is required to signal that the kinetochore is attached to microtubules and the chromosomes are ready for segregation [102]. To monitor whether Dam1 was properly modified in the absence of Scm3, we performed immunoprecipitation of Dam1-13Myc in both Scm3^{on} and Scm3^{off}. Immunoprecipitates were then subjected to Western blot analysis and probed using an antibody that recognizes Dam1 K233me^2. It was observed that Dam1 di-methylation of K233 does incur even in the absence of Scm3 (Figure 18B). Taken together these results suggest that the outer kinetochore protein Dam1 does indeed localize to kinetochores in the absence of Scm3 and is properly modified.

IV. Discussion

Although many *S. cerevisiae* kinetochore proteins have been characterized, it

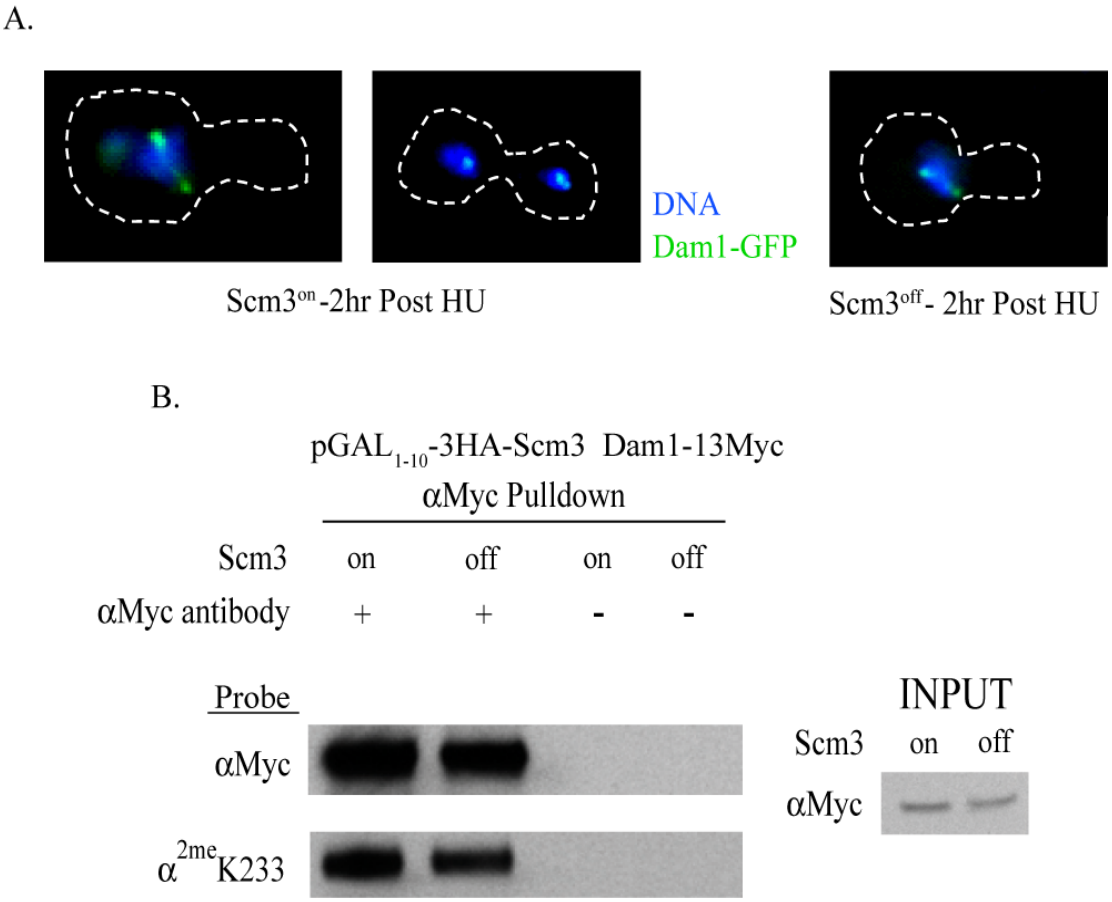

Figure 18. Localization and post-translational modification of Dam1 in cells depleted for Scm3.
A) Dam1 was fused to a green fluorescent protein tag (Dam1-GFP) in the pGAL$_{1-10}$-3HA-Scm3 background. Cells were then arrested using HU and subsequently released from the HU arrest with either Scm3^{on} or Scm3^{off}. Samples were collected every hour, for three hours and localization of Dam1-GFP was monitored by fluorescence microscopy. The 2hr post-release timepoints are shown. B) Dam1-13Myc cultures were arrested with HU and cultures were either maintained with Scm3^{on} or switched to Scm3^{off}. Cells were released from the HU arrest and grown for 2 hours before they were harvested for anti-Myc immunoprecipitation. Immunoprecipitates were subjected to Western blot analysis, and probed with antibodies against either the Myc epitope or dimethyl lysine 233 of Dam1. Dam1 K233me^2 is detected in both Scm3^{on} and Scm3^{off}.

remains unclear how kinetochore formation is initiated, and how the essential Cse4-containing chromatin is established specifically at the centromere. We have identified Scm3, a previously uncharacterized protein essential for viability in budding yeast. We find that Scm3 has homologs in yeast that contain both point and regional centromeres. Functional analysis of Scm3 reveals that both the N-terminus and the evolutionarily conserved central domain are essential for Scm3 protein function. Scm3 is the first protein shown to physically interact with both inner kinetochore proteins Cse4 and Ndc10. By exploiting a galactose-regulated promoter, the phenotype of cells depleted for Scm3 has been characterized. Experimental evidence demonstrates that Scm3 plays an essential role in formation and maintenance of a segregation-competent kinetochore. Specifically, it has been shown that Scm3 is necessary for localization of inner kinetochore proteins to the centromere, including Ndc10, which has previously been proposed to be the initial component of the kinetochore to associate with the centromere. Without Scm3, Cse4-containing centromeric chromatin is not efficiently established at the centromere. Additionally it has been shown that Scm3 is required for the maintenance of kinetochores that are competent to signal the spindle assembly checkpoint, and biorient with respect to spindle poles.

1. The role of Scm3 in establishing the inner kinetochore

Due to the lack of Cse4 localization to the centromere in an *ndc10-1* mutant [87, 92], functional Ndc10 appears to be necessary for recruitment of Cse4. One of

the key questions remaining regarding budding yeast inner kinetochore formation is which factor, if any, is responsible for facilitating the recruitment of Cse4 to centromeres after Ndc10 has found its target. We have shown that *in vivo* the inner kinetochore protein Scm3 interacts with both Ndc10 and Cse4, and is required for proper localization of both proteins to the CEN. Based on these findings we propose that Scm3 links kinetochore nucleation by Ndc10 to recruitment of Cse4. Since Scm3 and Ndc10 require each other to localize to the CEN, and furthermore Cse4 is required to stabilize their association at the CEN, this early step in kinetochore formation is not hierarchical, but instead, cooperative. We have observed that purified Scm3 displays non-specific DNA binding *in vitro* (Li and Workman, unpublished results), consistent with Ndc10 imparting centromeric sequence specificity to the Scm3/Ndc10 complex. We propose that Scm3 bound to Ndc10 interacts with the CEN DNA sequence, and the interaction between Scm3 and Cse4 helps bring Cse4 to this site, with all three proteins required for stable complex formation. This role in Cse4 recruitment is consistent with the previous finding that Scm3 is a high copy suppressor of a Cse4 histone fold domain mutant. Since the histone fold domain of Cse4 is essential to target Cse4 to the CEN [103], overexpression of Scm3 may help this mutant protein locate the centromere.

We have identified putative orthologs of Scm3 in fungi that do not contain identifiable Ndc10 homologs, whereas all fungi in which we have identified Scm3 also contain Cse4/CENP-A. This is consistent with an Ndc10-independent role for Scm3 in recruiting Cse4 to the centromere. Although we have been unable to identify

putative orthologs of Scm3 in higher eukaryotes, it seems likely that higher eukaryotes will also contain proteins that specifically function in establishing centromeric chromatin.

2. Scm3 is required to maintain kinetochore function throughout the cell cycle

When we deplete Scm3 in G1, Ndc10 does not localize to the centromere, and the spindle checkpoint is not activated. This suggests that the kinetochore fails to form, precluding spindle microtubule-centromere interaction. However, even if Ndc10 is allowed to load at centromeres and then Scm3 is depleted, the spindle checkpoint is activated, indicating at least a partial kinetochore forms, but is defective. This demonstrates that Scm3 continues to function in kinetochore maintenance even after the initial loading of Ndc10 and formation of the inner kinetochore. We can imagine three possible functions for Scm3 in the maintenance of a segregation-competent kinetochore: 1) recruitment of central or outer kinetochore components, 2) loading of additional Ndc10, and 3) signaling the spindle checkpoint that the kinetochore is properly formed. These functions would not necessarily be mutually exclusive and are likely interrelated. Based on the result that Dam1 can still localize to kinetochores when Scm3 is depleted, it seems likely that the outer kinetochore is able to form properly without Scm3. Additionally, di-methylation of Dam1 K233 occurs in cells that are depleted for Scm3, an indication that Scm3 is not required for the PTMs of outer kinetochore proteins.

When we deplete Scm3 after initial kinetochore formation (HU arrest) we suggest that the kinetochore is competent to make microtubule attachments to the newly formed kinetochore, as evidenced by the movement of both sister chromatids in a single cell body (Figure 16B). We hypothesize that these chromatids may move via monopolar lateral attachments. One possibility is that without Scm3, there is a failure to convert lateral attachments to end-on attachments [104], a necessary step which imparts tension and facilitates biorientation. This defect could be due to a failure to load components of the central or outer kinetochore, or due to incomplete loading of Ndc10.

Ndc10 continually loads at centromeres during the entire cell cycle, both by itself, and in the context of the CBF3 complex [65, 105]. This continual loading is required to maintain kinetochore function. Since Scm3 is essential for loading of Ndc10 at centromeres following their replication, and levels of Ndc10 at the centromere in asynchronous cultures switched to $Scm3^{off}$ are decreased, it seems likely that Scm3 contributes to the loading of additional Ndc10 later in the cell cycle (post S-phase). Since Ndc10/CBF3 complex may be involved in the attachment of microtubules to kinetochores [105], a defect in loading might lead to defective microtubule-kinetochore attachments.

Functional Ndc10 is required to establish a large domain of pericentric cohesin on each chromosome, which is necessary for accurate sister chromatid segregation [101]. Thus, when Scm3 is depleted in G1 and Ndc10 loading is diminished, pericentric cohesion may be reduced. However, reduced cohesin does

not appear to explain the chromosome segregation defect when Scm3 is depleted following early S phase. Thus, a defect in pericentric cohesin is an unlikely explanation for the increase in chromosome mis-segregation in the Scm3^{off}/*ipl1-321* background as compared to the *ipl1-321* background. It has been observed that central (Mtw1 complex) and outer kinetochore (Dam/Duo Complex) mutants fail to establish bipolarity and form monopolar attachments to sister chromatids [81, 84]. However, the frequency of sisters segregating to a single pole in an *mtw1-1 ipl1-321* double mutant is similar to that of either a *mtw-1* or *ipl1-321* single mutant alone, an indication that Mtw1 operates in the same pathway as Ipl1 in establishing chromosome biorientation or tension [97]. In contrast, the Scm3^{off} *ipl1-321* double mutant exacerbates the *ipl1-321* biorientation defect, suggesting Scm3 operates in an additional (non-Ipl1) pathway to establish sister kinetochore biorientation. At this time we have not yet characterized the molecular role Scm3 plays in establishing sister chromatid biorientation.

Chapter 3.

Analysis of the Composition of the Yeast Centromeric Nucleosome

I. Abstract

The budding yeast CenH3 histone variant Cse4 localizes to centromeric nucleosomes and is required for kinetochore assembly and chromosome segregation. The exact composition of centromeric Cse4–containing nucleosomes is a subject of debate. ChIP-chip experiments and high resolution quantitative PCR confirm that there is a single Cse4 nucleosome at each centromere, and additional regions of the genome contain Cse4 at low levels. Using biochemical, cell biological, and genetic experiments we have tested the composition of Cse4-containing nucleosomes. Using micrococcal nuclease-treated chromatin from yeast cells, we find that Cse4 is associated with the histones H2A, H2B, and H4, but not H3 or the non-histone protein Scm3. Scm3 is an essential protein that has previously been shown to be important for centromere specification and has been proposed to be a component of Cse4-containing nucleosomes. Overexpression of Cse4 in budding yeast rescues the lethality of a *scm3* deletion, indicating Scm3 is not essential for the formation of functional centromeric chromatin. Alanine scanning mutagenesis of Cse4 indicates that the Cse4-Cse4 interaction domain is essential for function. Taken together, our experimental evidence supports the model that the Cse4-nucleosome is an octamer, containing two copies each of Cse4, H2A, H2B, and H4.

II. Introduction

One of the most critical tasks for a dividing cell is to make sure that the two new cells each have an accurate and complete copy of the genome. In all eukaryotes, each chromosome contains a specialized DNA sequence that helps to ensure proper segregation, known as the centromere. At each centromere a large proteinaceous structure called the kinetochore is formed. Microtubules attach to the kinetochore and pull sister chromatids to opposite spindle poles. Two types of centromeres have been identified; point centromeres and regional centromeres. Regional centromeres are typically found in higher eukaryotes, and are composed of numerous copies of repetitive DNA sequences [106]. In humans, some centromeres can be as long as a megabase [107]. *S. cerevisiae* and other hemiascomycetous fungi contain point centromeres. In these organisms the centromere sequence is ~125 base pairs (bp) and is comprised of three DNA elements: CDE I, CDE II, and CDE III [52, 108].

Although their DNA sequences are highly variable between species, all eukaryotic centromeres are thought to be epigenetically marked by the presence of a centromere specific histone variant (CenH3). This variant, known as Cse4 in budding yeast and more generally as CENP-A, is essential for the formation of a kinetochore and for proper chromosome segregation [77, 109]. Structurally, CENP-A homologs have two major domains: an evolutionarily conserved histone fold domain (HFD) and a divergent amino-terminal domain (see Figure 2). The HFD of CENP-A homologs has a high degree of amino acid identity to histone H3, while the amino-terminal portion of the protein can vary greatly between species. The function of the CenH3

nucleosome is highly conserved, as demonstrated by the functional complementation of RNAi-depleted CENP-A in human cells by yeast Cse4 [41]. In *S. cerevisiae*, Cse4 localizes *in vivo* to a single nucleosome directly at CDE I-II-III, and is thought to replace histone H3 at this site [64, 110]. In organisms with regional centromeres, CenH3 is found in multiple nucleosomes at or near the centromeric repeats. In human cells, CENP-A localizes to the large arrays of α-satellite DNA, interspersed among canonical histone H3-containing nucleosomes [111]. In the case of human (CENP-A) or *Drosophila melanogaster* (CID) CenH3 octamers assembled *in vitro*, it has been shown that CENP-A and CID can substitute for histone H3 [112, 113].

Although it is generally accepted that Cse4 is assembled into nucleosomes at the budding yeast centromere, the overall composition of this nucleosome is a topic of debate. The most conservative model for the centromeric nucleosome is that CENP-A simply replaces H3 in an octameric nucleosome which contains Cse4, H2A, H2B, and H4 (Figure 19A). Given the crystal structure of a canonical nucleosome [4], this model is based in part on the strong sequence identity between the HFD of the CENP-A homologues and that of H3. In addition, octameric nucleosomes containing human or *Drosophila* CenH3 can be reconstituted *in vitro* [112, 113]. Another more provocative model suggested for centromeric nucleosomes is that they contain a single molecule of each CenH3, H2A, H2B, and H4, which forms a tetrameric structure called a "hemisome" (Figure 19B) [114]. This hemisomal complex was purified from interphase *Drosophila* S2 cells by crosslinking and immunoprecipitation of CID. Hemisomes are predicted to wrap <120bp of DNA, and

when analyzed by atomic force microscopy appear to be half the height of canonical bulk nucleosomes [115].

The final model for centromeric nucleosome composition involves the newly identified budding yeast kinetochore protein Scm3. Scm3 was initially identified as a high copy suppressor of a Cse4-HFD mutant [40], and has since been shown to be an essential kinetochore protein required for Cse4 localization to the centromere and for proper chromosome segregation [116-118]. *SCM3* homologs are found in fungi with both point and regional centromeres. Scm3 has been shown to facilitate the exclusion of histones H2A and H2B from preassembled Cse4-containing octamers *in vitro*. Additionally, chromatin immunoprecipitation studies (ChIP) suggest that histones H2A and H2B are absent from the centromeric nucleosome *in vivo* in budding yeast [117]. Based on these findings it has been proposed that along with Cse4 and H4, Scm3 forms a unique hexameric nucleosome specifically at centromeres (Figure 19C). Unlike canonical nucleosomes which contain two heterodimers of the histones H2A/H2B complexed with a tetramer of the histones H3/H4 [4], this specialized centromeric nucleosome is predicted to contain a tetramer of Cse4-H4 and two copies of Scm3 [117].

To gain a better understanding of the content and structure of Cse4-containing chromatin, we mapped the genomic locations of Cse4 in budding yeast using chromatin immunoprecipitation followed by hybridization to DNA microarrays (ChIP-chip) and high resolution quantitative PCR (qPCR). As expected, we find evidence for localization of Cse4 to a single centromeric nucleosome at every

centromere, and also at low-levels at select non-centromeric sites. Solubilization and immunoprecipitation of Cse4-containing mononucleosomes indicate that the Cse4 nucleosome contains histones H2A and H2B but not Scm3 or H3. Additionally, we find that overexpression of Cse4 can rescue a *scm3Δ* strain, indicating that a specialized Scm3-containing nucleosome is not essential for centromere function. Cse4-containing octamers can be assembled *in vitro* that contain histones H2A, H2B, and H4. These octamers can wrap DNA to form nucleosomes. Moreover, comprehensive mutagenesis of Cse4 indicates that Cse4-Cse4 interactions are essential for its function. Taken together these data support the model that Cse4-containing nucleosomes have a structure similar to canonical octameric nucleosomes.

III. Results

1. Cse4 localization at centromeres and non-centromeric locations

Cse4 has been shown to localize to centromeres in budding yeast by both ChIP and microscopy [40, 119, 120]. In the case of Cse4 fused to GFP, the only signal reported corresponds to centromeres [121]. In the ChIP studies, the presence of Cse4 was only tested at a centromere or a select few other non-centromeric loci [119, 120]. In order to take an unbiased approach and discover all the locations of Cse4 in the genome, we utilized DNA microarrays. The microarrays we used contain approximately 13,000 PCR fragments corresponding to each open reading frame and each intergenic region in the yeast genome.

We analyzed the location of 1) Cse4 tagged with 12Myc epitopes (Cse4-

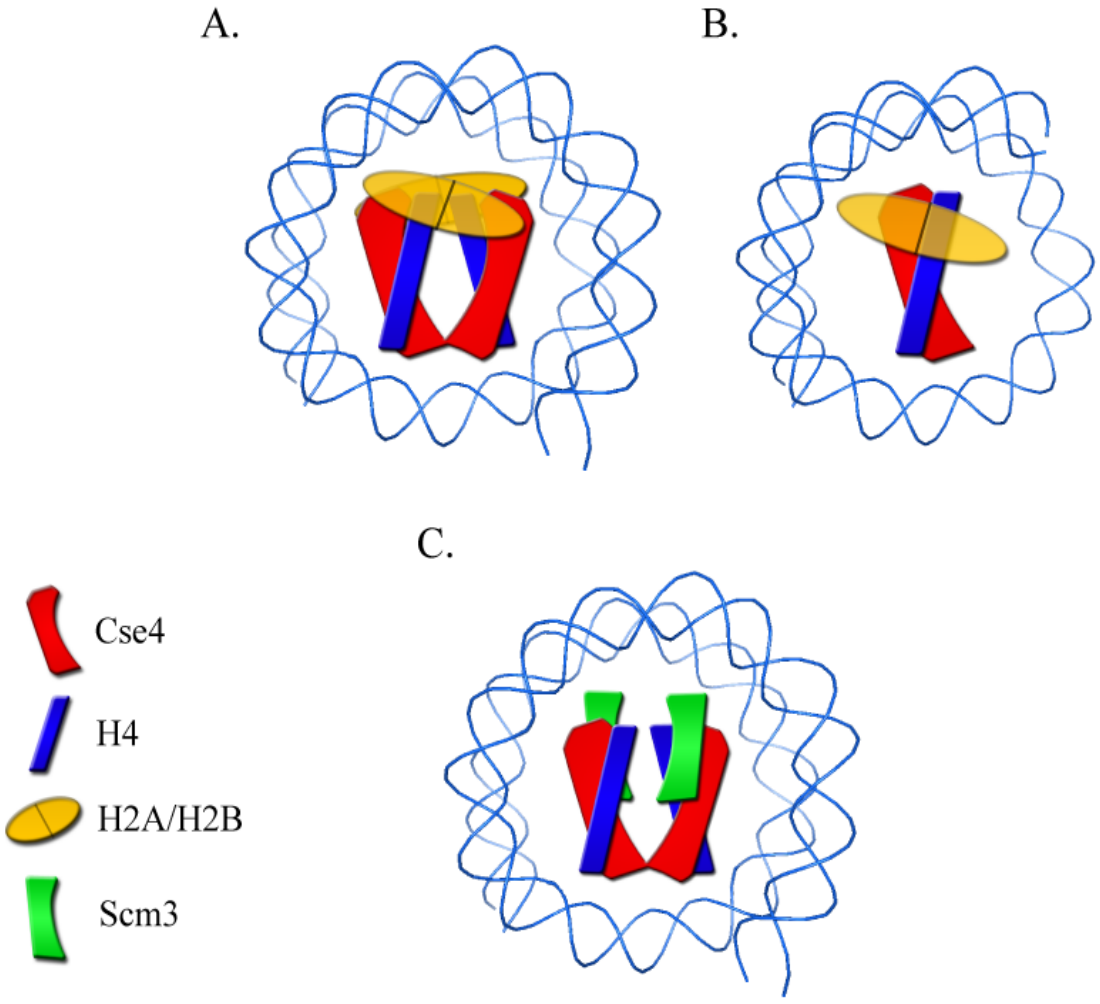

Figure 19. Three models of the budding yeast centromeric nucleosome. The cartoon schematic represents each of the proposed centromeric nucleosomes wrapped by DNA. The DNA is represented by the blue lines. Actual nucleosome/DNA contact points are unknown for all three models. A) The octamer model proposes that Cse4 is found in a canonical-like octameric configuration. B) The hemisome model predicts that the centromeric nucleosomes consist of a monomer of each Cse4, H2A, H2B, and H4. The hemisome is predicted to wrap less DNA than an octameric or hexameric nucleosome (~120bp). C) The hexamer model proposes that the centromeric nucleosome is comprised of a tetramer of Cse4-H4 and two molecules of Scm3.

12Myc), 2) an ectopic copy of Cse4-12Myc overexpressed from the *GAL$_{1-10}$* promoter (pGAL$_{1-10}$-Cse4-12Myc), and 3) the *cse4-351* dominant lethal mutant (pGAL$_{1-10}$-*cse4-351*-12Myc). *cse4-351* is an allele of *CSE4* that was generated by random mutagenesis that contains 14 amino acid changes distributed throughout the protein [122]. It is a stable dominant lethal mutant that localizes to euchromatin as shown by chromosome spreads and ChIP/PCR to three genomic locations [120]. The lethality was attributed to a lack of proteolysis from non-centromeric locations.

DNA recovered from ChIPs and "no antibody" controls was tested for enrichment of CEN3 sequence by semi-quantitative PCR prior to hybridization to microarrays. For both Cse4-12Myc and pGAL$_{1-10}$-Cse4-12Myc, the strongest signal detected by microarray on each chromosome was at the centromere (Figure 20A) (Appendix 3). As expected from previous published reports that *cse4-351* localizes to non-centromeric loci [122], we found that pGAL$_{1-10}$-*cse4-351*-12Myc localized randomly across the entire chromosome, but interestingly, no localization to the centromere was observed (Figure 20A) (Appendix 3). We also observed that a few repetitive regions consistently showed a low level of Cse4 enrichment in all three samples when compared to background. These sites include the Ty transposable elements, telomeres, and the rDNA repeats. Stringent statistical analysis of the microarray data was performed to confirm the data was statistically significant (see Chapter 2-section 7) (Figure 20B-D). Notably, overexpression of Cse4 does not appear to cause a large increase in non-centromeric localization, as has been shown for overexpression of CENP-A and CID [123, 124].

In order to verify the low levels of Cse4 at non-centromeric locations, we performed qPCR utilizing primer pairs representing *NTS2* (rDNA), and two different Ty-1 transposable elements. As a negative control, we used primers which amplified regions of two genes where no detectable Cse4 signal was observed by DNA microarray analysis (*GAL2*, *SRL2*). All ChIP intensities are shown relative to the signal from total chromatin, so we have controlled for the fact that these sequences may be repeated in the genome. We found that sequences from *NTS2* and Ty elements were significantly enriched relative
to a control ChIP performed without antibody, and relative to the negative control regions (*GAL2*, *SRL2*) (Figure 20E). We were unable to verify the low level of Cse4 enrichment observed at telomeres by qPCR.

2. High resolution mapping of centromeric chromatin

In order to define centromeric chromatin, we utilized a high resolution ChIP/qPCR approach. To do this we isolated chromatin from a yeast strain expressing Cse4-12Myc. The culture was arrested with nocodazole, crosslinked with formaldehyde, and treated with micrococcal nuclease (MNase) to generate mononucleosomes. We then performed ChIP with an antibody against the Myc epitope. The immunoprecipitated DNA was used as a template for qPCR. To achieve the highest resolution possible we designed tiled qPCR primers for ~0.4 kb flanking CDE I-II-III of CEN3. This primer set generated products that averaged ~95 bp and overlapped by ~50-60 bp. Of the 16 primer sets utilized, we found that the

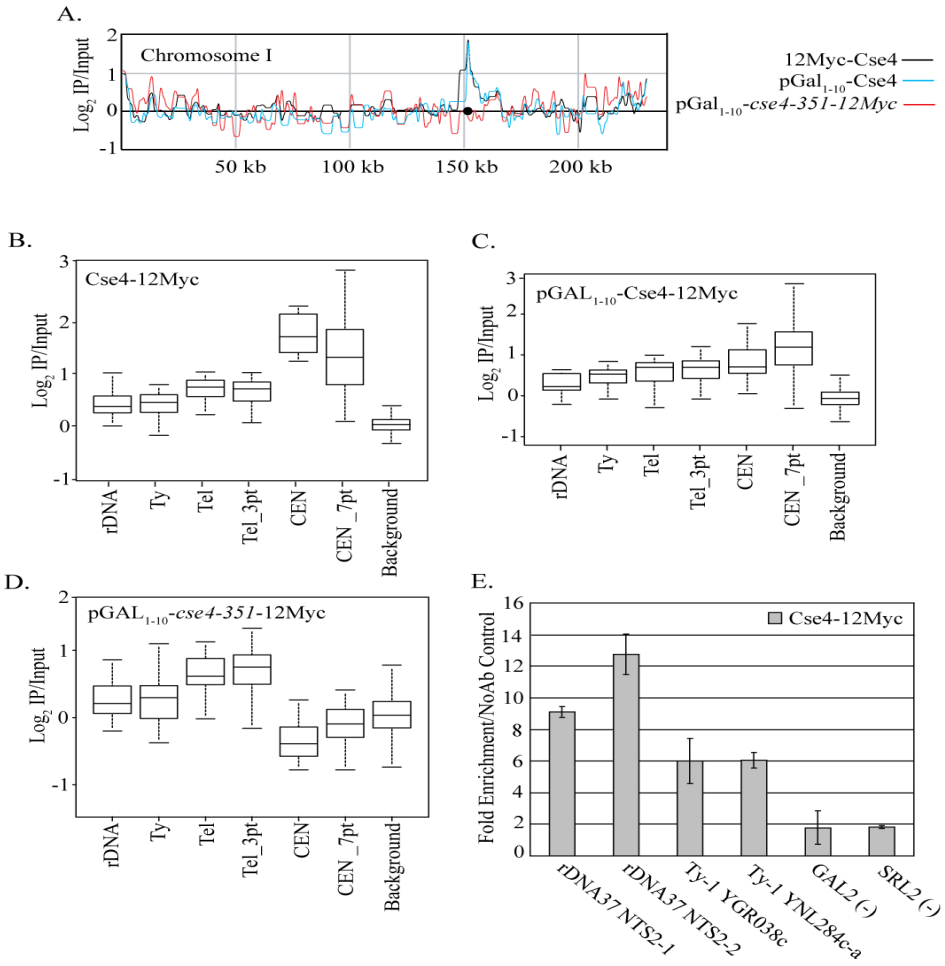

Figure 20. Genome-wide localization of Cse4. Cultures expressing Cse4-12Myc, pGAL$_{1-10}$-Cse4-12Myc, pGAL$_{1-10}$-*cse4-351*-12Myc were grown to mid-log phase and arrested in metaphase with nocodazole. ChIP-chip and qPCR were performed using two independent biological samples and the results were averaged. A) PeakFinder display [125] of the pattern of Cse4-12Myc and pGAL$_{1-10}$-Cse4-12Myc, and pGAL$_{1-10}$-*cse4-351*-12Myc on Chromosome 1 (for all chromosomes see appendix 3). The centromere is indicated by the circle B-D) Box plots representing Cse4-12Myc, pGAL$_{1-10}$-Cse4-12Myc, and pGAL$_{1-10}$-*cse4-351*-12Myc localization at all centromeres (CEN), centromeres along with 3 array spots on both sides (CEN_7pt), the sequence at the rDNA locus, Ty elements, the telomeres, 3 array spots proximal to all telomeres (Tel_3Pt) and all other array spots (Background). The span of each box represents a range where 95% of the array spots fall. The line in the box represents the median of each sample. The whiskers represent the 1.5 interquartile range. E) ChIP/qPCR was carried out for several non-centromeric regions. Cse4-12Myc ChIP/total chromatin signal was divided by the no antibody/total chromatin control for each region to obtain the fold-enrichment. Error bars represent +/- the average deviation of biological replicates.

three PCR primer pairs which directly included sequences of CDE I-II-III had the highest signal for Cse4 (Figure 21). Similar results were observed for CEN1 (Figure 22). Based on the observed DNA fragments amplified by these primers and the absence of signal directly adjacent, we narrowed down the possible location of Cse4 to <200bp of DNA, which includes the centromeric DNA elements. Assuming that a Cse4-containing nucleosome is wrapped around a similar amount of DNA as a canonical H3-containing nucleosome (~146 bp), this finding is consistent with the observation that Cse4 is confined to a single centromeric nucleosome [110].

Next, using antibodies against histones H2B, H3, and H4, and epitope-tagged 3FLAG-H2A we attempted the same high resolution ChIP/qPCR. We found that we could not reproducibly ChIP any core histones to the centromere in MNase-treated chromatin (data not shown). Interestingly, the high resolution Scm3-3HA qPCR revealed that the localization pattern of Scm3-3HA differs from that of Cse4-12Myc. Scm3-3HA localizes to the centromere with a bias towards the CDE III end of the centromeric sequence. This result is similar to what has been observed for the inner kinetochore proteins Ndc10 and Mif2 [126, 127] (Figure 23). Using sheared chromatin as a substrate for ChIP, we also failed to detect any of the core histones at the centromere (data not shown). Based on our inability to ChIP any of the core histones to the centromere, including H4, we have concluded that ChIP is not a useful tool to elucidate the complete composition of the centromeric nucleosome. We suspect that the formaldehyde may crosslink other kinetochore proteins to the centromeric

nucleosome, and physically block the histone epitopes located in the underlying chromatin.

3. Cse4 co-immunoprecipitates with H2A, H2B, and H4 in MNase solubilized chromatin

Using sub-cellular fractionation and salt challenge experiments, we have previously shown that Scm3 and Cse4 strongly associate with chromatin [116]. However, these experiments did not directly address whether these proteins are actually components of nucleosomes or just intimately associated with them. To test this, we decided to perform chromatin fractionation followed by co-immunoprecipitation (co-IP) and Western blot analysis. Yeast nuclei were isolated and the soluble nuclear proteins were separated from the chromatin fraction. The chromatin fraction was then treated with MNase and the solubilized chromatin was recovered. We refer to this fraction as MNase-solubilized chromatin. Western blotting was performed to detect proteins in the nuclear lysate, the MNase solubilized chromatin and the insoluble chromatin fraction. Using antibodies against epitope-tagged 3FLAG-H2A and Cse4-12Myc, and endogenous H2B, H3, H4, and Scm3 we could detect all of the above proteins in the total nuclear lysate (Figure 24A). Interestingly, Cse4, H2A, H2B, H3, and H4 were all detected in the MNase-solubilized fraction but Scm3 was not (Figure 24A). Scm3 remained insoluble following MNase treatment. The simplest interpretation of this result is that Scm3 is not a component of a nucleosome, although we cannot rule out the possibility a Scm3-containing nucleosome species exists that cannot be solubilized by MNase.

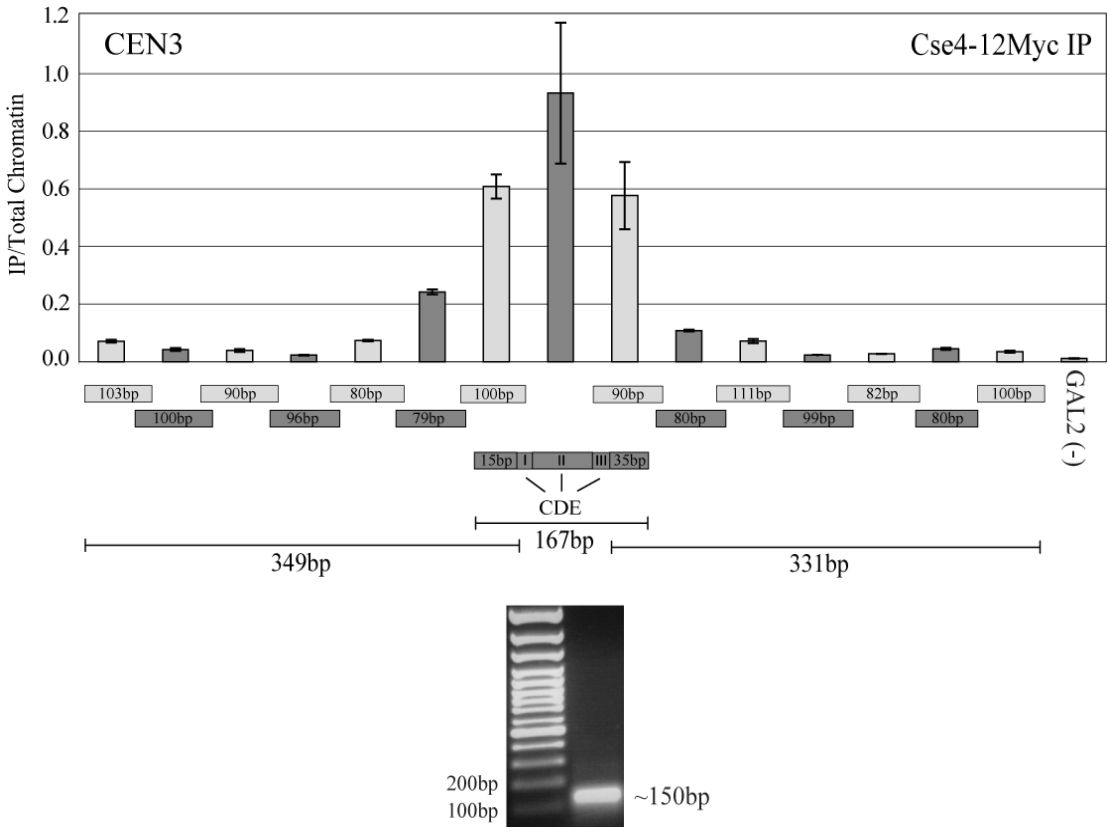

Figure 21. Cse4 location at high resolution *in vivo* at CEN3.
ChIP/qPCR analysis was performed on MNase treated chromatin from a Cse4-12Myc strain using overlapping primers that span ~ 700 bp across the centromere on Chromosome 3. *GAL2* is a gene located on the arm of Chromosome 12 and is a negative control for Cse4 localization. MNase-treated input chromatin was visualized with ethidium bromide on an agarose gel and is shown below the histogram. Only three primer pairs contained sequences from CDE I-II-III, as indicated. The size of each primer pair product is indicated below its respective bar on the histogram. Without antibody, the ChIP/qPCR signal was <10% of the total signal; this has been subtracted from the values presented. The signal from each ChIP has been divided by the signal obtained with total chromatin. Error bars represent +/- the average deviation of biological replicates.

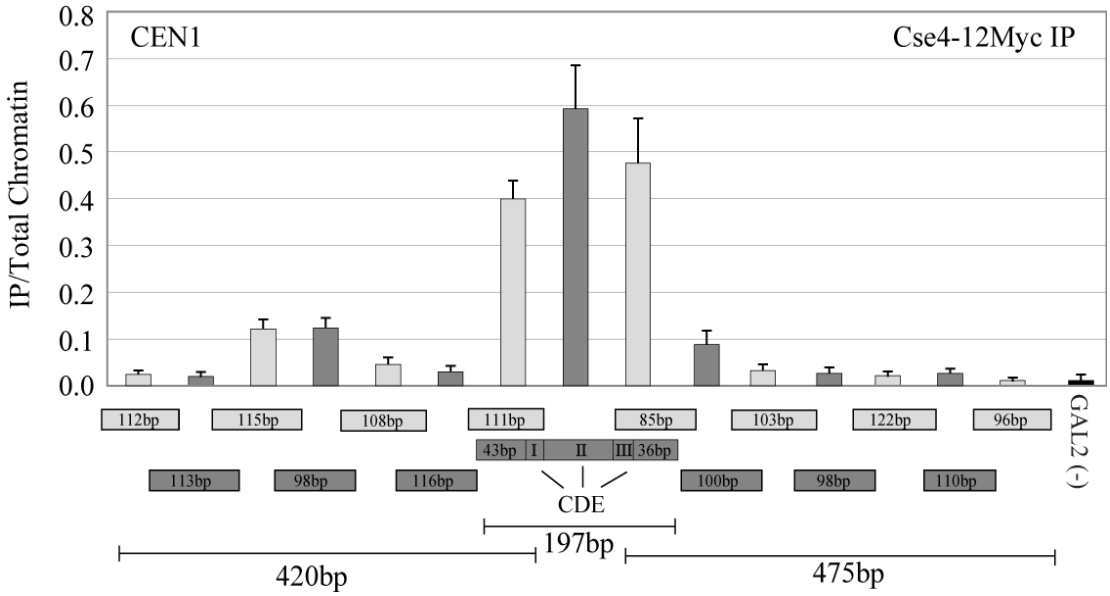

Figure 22. Cse4 location at high resolution *in vivo* at CEN1.
ChIP/qPCR analysis was performed on MNase treated chromatin from a Cse4-12Myc strain using overlapping primers that span ~ 900 bp across the centromere on Chromosome 1. *GAL2* is a gene located on the arm of Chromosome 12 and is a negative control for Cse4 localization. Only three primer pairs contained sequences from CDE I-II-III, as indicated. The size of each primer pair product is indicated below its respective bar on the histogram. Without antibody, the ChIP/qPCR signal was <10% of the total signal; this has been subtracted from the values presented. The signal from each ChIP has been divided by the signal obtained with total chromatin. Error bars represent +/- the average deviation of biological replicates.

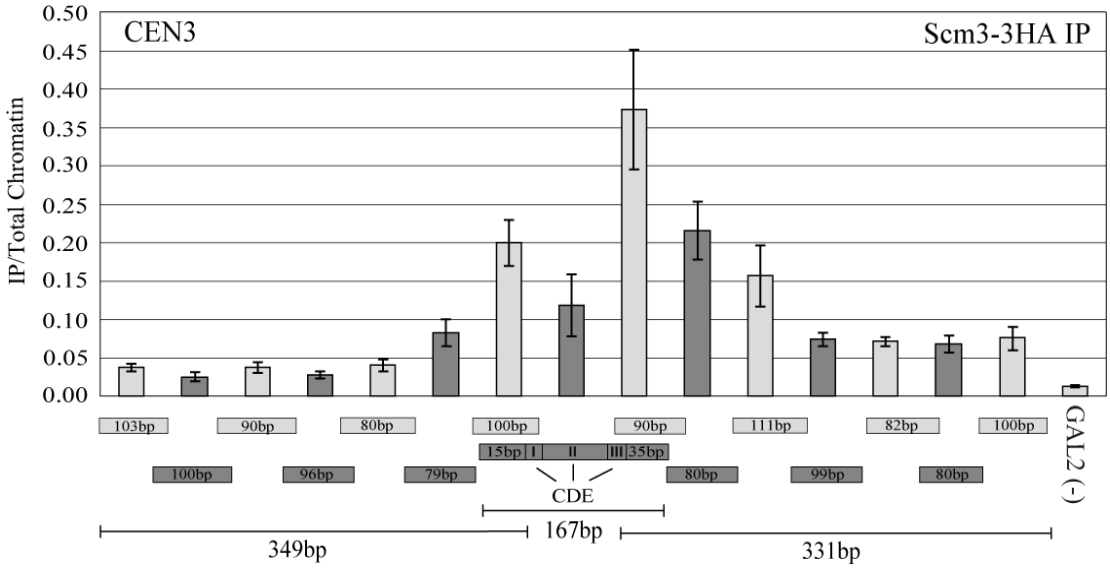

Figure 23. Scm3 location at high resolution *in vivo* at CEN3.
ChIP/qPCR analysis was performed on MNase treated chromatin from a Scm3-3HA strain using overlapping primers that span ~ 700 bp across the centromere on Chromosome 3. *GAL2* is a gene located on the arm of Chromosome 12 and is a negative control for Cse4 localization. Only three primer pairs contained sequences from CDE I-II-III, as indicated. The size of each primer pair product is indicated below its respective bar on the histogram. Without antibody, the ChIP/qPCR signal was <10% of the total signal; this has been subtracted from the values presented. The signal from each ChIP has been divided by the signal obtained with total chromatin. Error bars represent +/- the average deviation of biological replicates.

Next we performed co-IP using the MNase-solubilized chromatin. Pulldowns were performed using beads conjugated to αFLAG or αMyc antibodies. The immunoprecipitations were probed for all other core histones. Immunoprecipitation of 3FLAG-H2A pulled down Cse4-12Myc, H3, H2B, and H4 (Figure 23B). When we immunoprecipitated Cse4-12Myc, we were able to detect an interaction with H2A, H3, and H4, but not H3 by Western blot (Figure 24C). In addition, silver-stained polyacrylamide gels and mass spectrometric analysis confirmed these results (data not shown).

To alleviate the concern that the MNase-solubilized chromatin fraction did not contain centromeric nucleosomes, we performed qPCR using DNA prepared from both the 3FLAG-H2A and the Cse4-12Myc immunoprecipitated samples. Using primers that amplify either CEN3, or the region of a positioned canonical nucleosome at the *PHO5* promoter [128], we observed that the 3FLAG-H2A immunoprecipitation was enriched for sequences from both sites, while the Cse4-12Myc immunoprecipitation was significantly enriched only for CEN3 DNA (Figure 24D). We also performed qPCR to look for enrichment of DNA from either the rDNA or Ty elements. We found only a slight enrichment for rDNA (2-fold over control) and no enrichment for Ty elements in the DNA that immunoprecipitated with Cse4-12Myc, an indication that the majority of nucleosomes in the Western blot analysis were centromeric in origin (Figure 24E). The differences in the levels of rDNA and Ty sequences between Figure 20E and Figure 24E are likely due to the different methods used to isolate DNA. In Figure 20E the samples were crosslinked prior to the

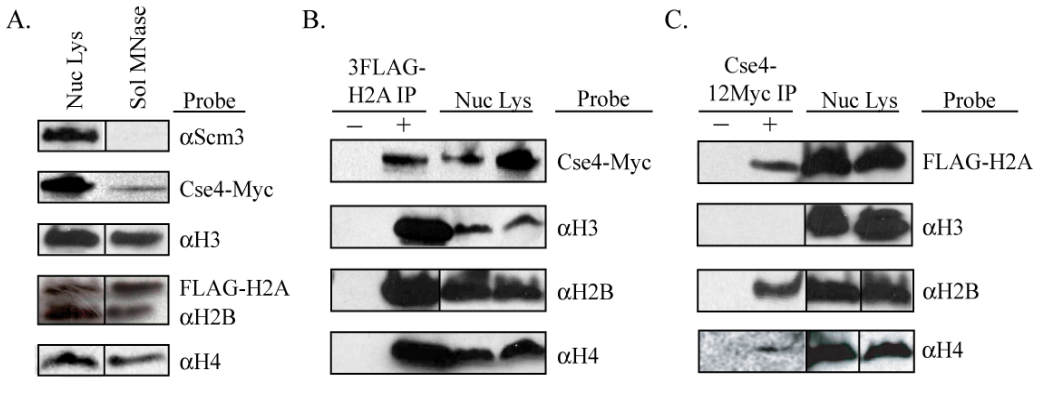

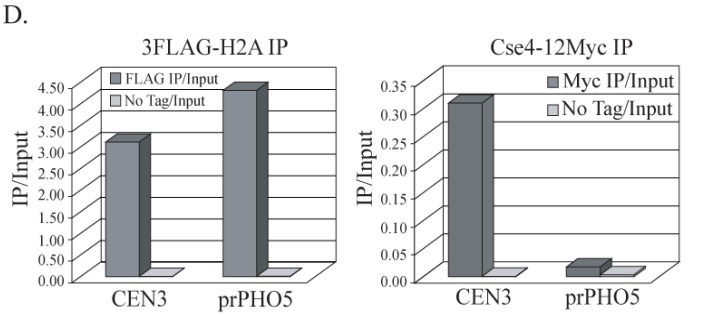

E.

	Genomic location	Fold enrichment over untagged control
Cse4-12Myc	CEN3	375.76
	rDNA (NTS2)	12.65
	YGR038 (Ty-1)	5.88
	YNL284 (Ty-1)	6.12
	prPHO5	5.17
3FLAG-H2A	CEN3	600.67
	rDNA (NTS2)	1074.47
	YGR038 (Ty-1)	1093.25
	YNL284 (Ty-1)	1266.67
	prPHO5	530.22

Figure 24. Co-Immunoprecipitation of histones from MNase-solubilized chromatin. Nuclear lysates were made from a strain expressing both 3FLAG-H2A and Cse4-12Myc. The chromatin fraction was pelleted and treated with MNase. Western blots were probed with each antibody listed. For each antibody, the lanes are from a single exposure of the same gel. Vertical lines indicate that intervening lanes were cropped. A) Both the MNase-solubilized chromatin fraction and the total nuclear lysate were loaded for Western blot. B) Co-immunoprecipitation was performed using the MNase-solubilized chromatin. αFLAG-conjugated beads were used to pulldown 3FLAG-H2A, and the pulldown was probed using the antibodies listed. The control pulldown was performed using chromatin from a strain lacking 3FLAG-H2A. C) αMyc-conjugated beads were used to pulldown Cse4-12Myc from chromatin made from, and the pulldown was probed using the antibodies listed. The control pulldown was performed using chromatin from a strain lacking Cse4-12Myc. D) DNA was isolated from both the αFLAG and αMyc pulldowns. qPCR was then performed to look for enrichment of DNA at either CEN3 or at the site of a well-positioned canonical nucleosome at the *PHO5* promoter (prPHO5). Cse4 is significantly enriched at CEN3 when compared to the *PHO5* promoter. Levels of 3FLAG-H2A are similar at both sites. E) qPCR signal from immunoprecipitated Cse-12Myc and 3FLAG-H2A compared to an untagged control strain at CEN3, the rDNA, Ty elements and the *PHO5* promoter. Fold enrichment was calculated by dividing IP/input ratios from the untagged control by the IP/input ratios of the epitope-tagged samples.

immunoprecipitation, while those in Figure 24E were not. Taken together, these results strongly suggest that *in vivo*, the centromeric Cse4 nucleosome contains histones H2A, H2B, and H4, and excludes H3 and Scm3.

4. Overexpression of Cse4 can rescue a Scm3 deletion

Deletion of *SCM3* in budding yeast is lethal [91]. We tested whether overexpression of other proteins could rescue the viability of a *scm3Δ* strain. A *CSE4*/*cse4Δ* and *SCM3*/*scm3Δ* heterozygous diploid knockout strain ("Magic Marker") were transformed with plasmids from the yeast Harvard Institute of Proteomics ORF collection (pHIP), sporulated, and then pinned in quadruplicate to medium that allows the recovery of haploid yeast that contain both the $GAL_{1\text{-}10}$ overexpression plasmid and the *scm3* or *cse4* deletion. As expected, overexpression of either Cse4 (pHIP-Cse4) or Scm3 (pHIP-Scm3) allows growth in each of their respective knock-out strains (Figure 25A). Surprisingly, we found that overexpression of Cse4 could rescue a *scm3Δ* strain. The *scm3Δ* strain covered by the Cse4 overexpression plasmid grows slightly slower than *scm3Δ* covered by a plasmid overexpressing Scm3 (Figure 25B). To confirm this finding we also transformed the galactose/glucose regulatable $Scm3^{on/off}$ strain [116] with a plasmid containing Cse4 expressed under the control of the *CUP1* (copper-inducible, pCUP1-Cse4) promoter. We found that with the addition of copper (Cu^{++}) to the growth medium, pCUP1-Cse4 can rescue growth on medium containing glucose ($Scm3^{off}$) (Figure 25D).

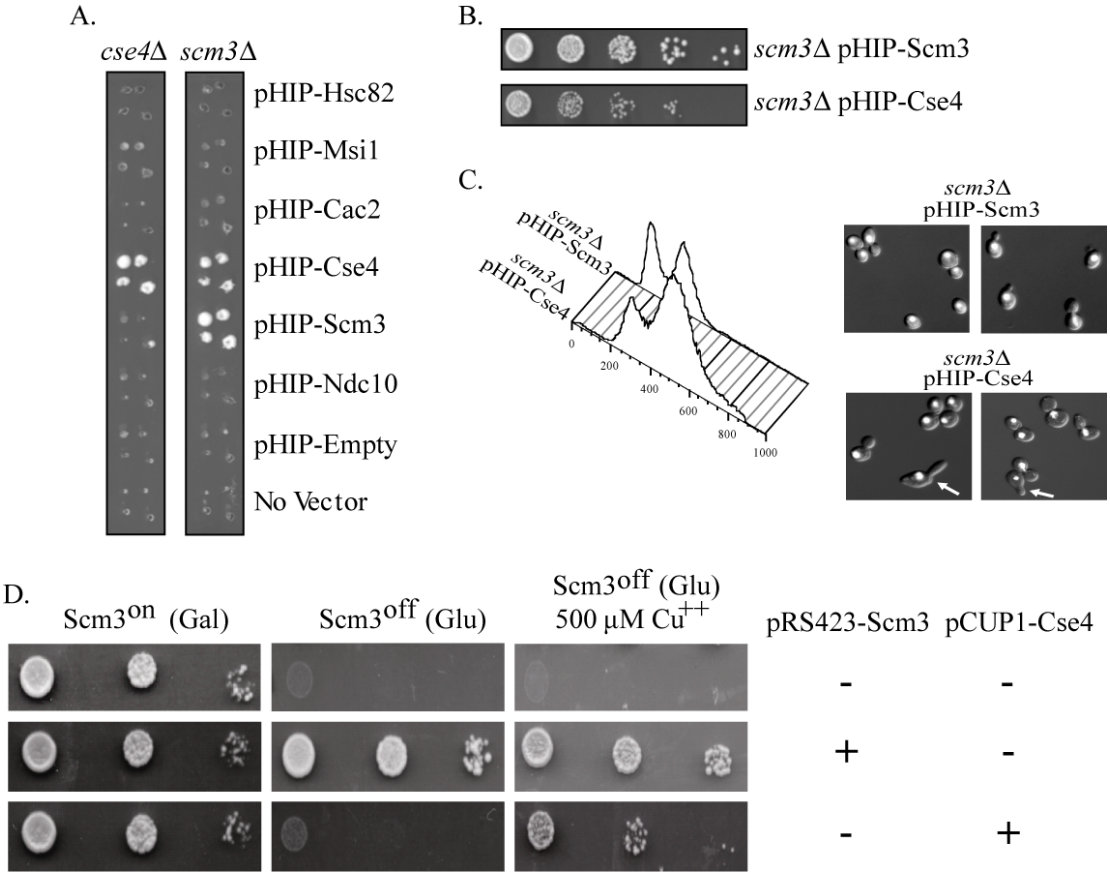

Figure 25. Suppression of the *scm3Δ* lethal phenotype.
The *SCM3*/*scm3Δ* or *CSE4*/*cse4Δ* heterozygous diploid knockout strain was transformed with plasmids from the HIP overexpression library. A) Sporulated cultures were pinned in quadruplicate onto medium which allowed the recovery of haploid yeast containing either *scm3Δ* or *cse4Δ* and the plasmid indicated. B) Dilution assay comparing the growth of *scm3Δ* covered by either pHIP-Scm3 or pHIP-Cse4 on Gal-Ura medium. C) FACscan analysis and DAPI staining of the *scm3Δ* strain covered by pHIP-Scm3 and *scm3Δ* covered by pHIP-Cse4. DAPI stained DNA is shown in white. Arrows indicate cells with abnormal morphology (elongated buds). D) Overexpression of Cse4 can rescue the $Scm3^{on/off}$ phenotype. The Scm3on/off strain was grown with no plasmid, or transformed with the copper inducible pCUP1-Cse4 plasmid or pRS423-Scm3. Yeast were tested for growth on galactose, glucose, and glucose plus Cu^{++}. $Scm3^{on/off}$ can only grow on glucose with the addition of Cu^{++} to the growth medium.

To test for mitotic defects, we performed FACscan analyses (FACs) to look at DNA content in *scm3Δ* cells that are rescued by pHIP-Cse4 (Figure 25C). We find that when we analyze DNA content by FACs, *scm3Δ* cells covered by pHIP-Cse4 have a mitotic delay, with a larger proportion of the cells exhibiting 2N DNA content, as compared to *scm3Δ* cells covered by pHIP-SCM3. Additionally, we have also performed DAPI staining to visualize the DNA (Figure 25C). The DAPI staining shows that chromosome segregation is occurring, although the preponderance of the cells are large budded, with some exhibiting morphology defects (elongated buds). We therefore conclude that the kinetochore is functional for chromosome segregation in the absence of Scm3, but there are probable kinetochore defects. To confirm that Cse4 still localized properly to the centromere in the absence of Scm3, we performed ChIP using a Myc epitope tagged pHIP-Cse4 (pHIP-Myc-Cse4) in the *scm3Δ* strain. Using ChIP/qPCR and sheared chromatin we find that in the absence of Scm3, Cse4 localizes to the centromere in a pattern consistent with single nucleosome (Figure 26). We also observed that in the absence of Scm3, we still cannot detect histones H2A, H2B, or H4 at the centromere by ChIP (data not shown). Based on these findings, we conclude that functional Cse4-containing centromeric chromatin can be formed in the absence of Scm3, and when we overexpress Cse4, a specialized Scm3-containing nucleosome is not essential for kinetochore function or chromosome segregation in budding yeast.

5. Cse4-containing octameric nucleosomes can be assembled in vitro

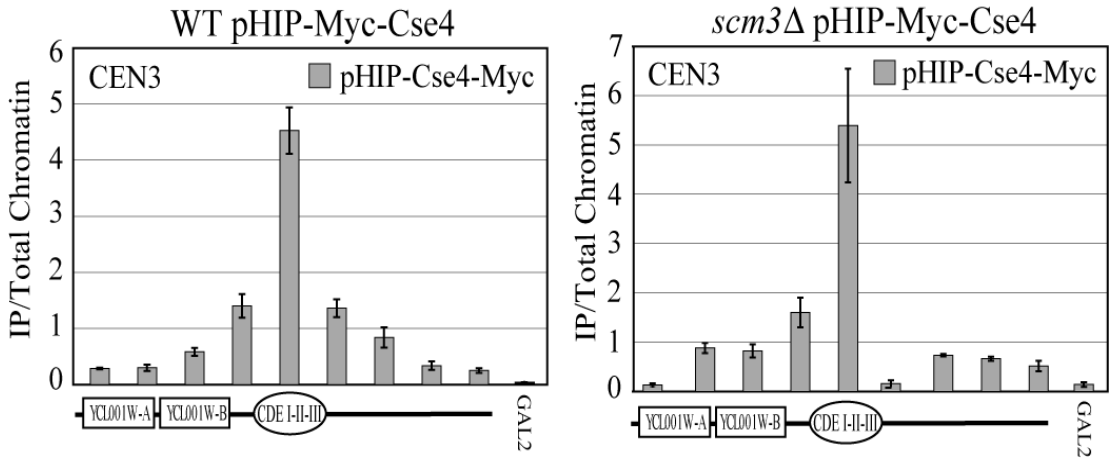

Figure 26. Cse4 localization in the *scm3Δ* strain.
A wild type strain containing the pHIP-Myc-Cse4 plasmid and a *scm3Δ* strain containing the pHIP-Myc-Cse4 plasmid were grown on SGal-Ura to mid-log phase and then arrested with nocodazole. qPCR analysis of pHIP-Myc-Cse4 localization was performed in both strains. The primers used amplify a +/- 2kb region around CEN3. A depiction of the features within the region is shown below each histogram. *GAL2* serves as a negative control for Cse4 localization. Error bars represent +/- the average deviation of biological replicates

Our *in vivo* data suggested that we should be able to reconstitute octameric Cse4-containing nucleosomes *in vitro*. To this end, we purified recombinant Cse4 and canonical histones (H2A, H2B, H3, and H4), and reconstituted Cse4-containing octamers and canonical octamers (Figure 27A). Recombinant yeast canonical histones were reconstituted into octamers (10% octamer, 20% tetramer; 40% dimer with the remainder being aggregates, Figure 27B). The reconstituted Cse4 octamers contained two copies of Cse4, H2A, H2B, H4 and no H3. By comparison to canonical octamers, reconstitution of Cse4-containing octamers is very efficient. There is little protein aggregation and >95% of histones are in octamer form (Figure 27C). Additionally, we observed that Cse4-H4 tetramer reconstitution is dramatically inefficient, with ~.05% of the total input protein actually forming a tetramer (data not shown).

Using purified Cse4-containing octamers and canonical octamers we reconstituted nucleosomes. We find that Cse4-containing octamers can be reconstituted with both a "601" nucleosome positioning sequence [129] as well as a random sequence from the arm of chromosome 6 (Figure 28A). At the higher ratios of octamer to DNA, the Cse4 octamers assemble with DNA much more efficiently than their canonical counterpart, exhibiting a strong positioning effect on the DNA. All attempts to reconstitute Cse4 nucleosomes using a centromeric DNA sequence failed (data not shown). This will be an important goal for future studies. To examine the integrity of Cse4-containing nucleosomes, we performed DNaseI accessibility analysis using the mononucleosome bands excised from Figure 28A.

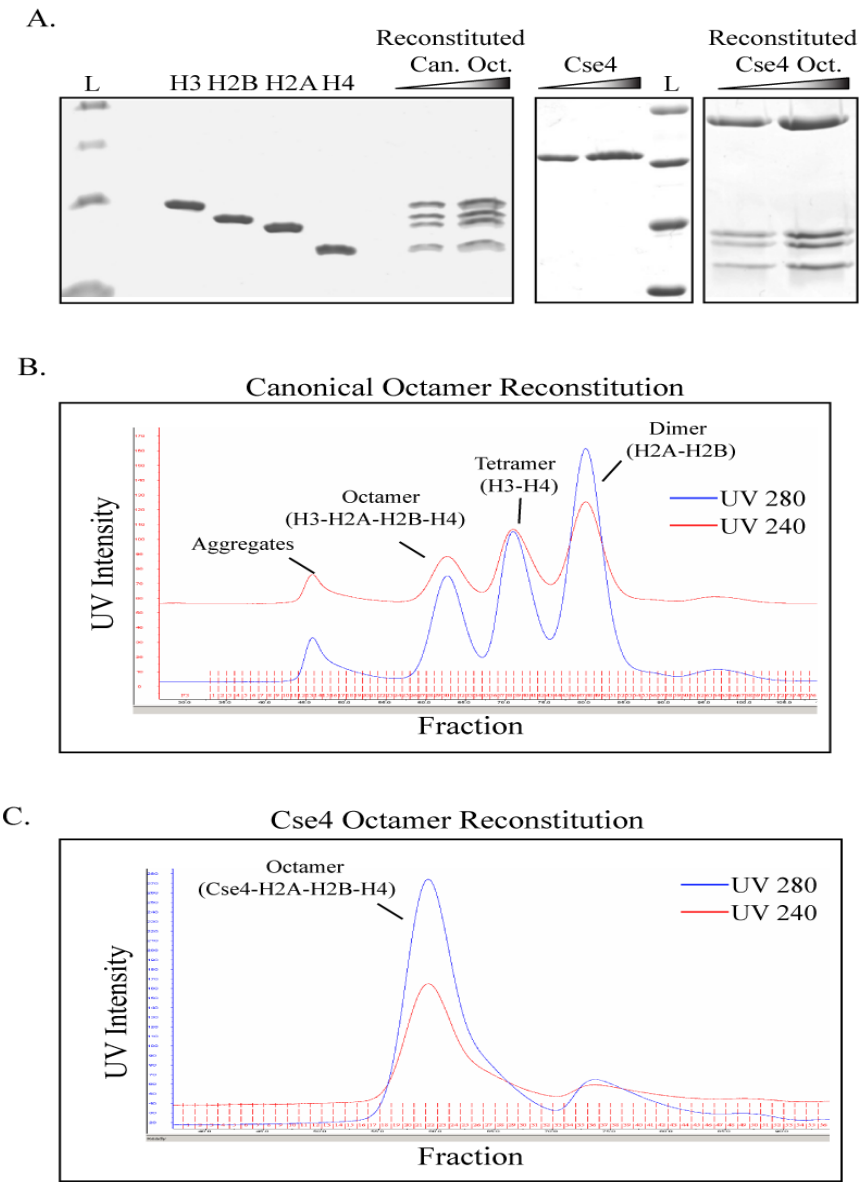

Figure 27. Reconstitution of Cse4 and canonical octamers.
A) Individual histones were purified from *E. coli* inclusion bodies and Cse4 and canonical octamers were reconstituted using salt dilution [130]. B) Canonical octamers were assembled by salt dialysis and purified by FPLC. When gel filtration chromatography fractions are collected for canonical octamers, four distinct populations are present: octamers, tetramers, dimers, and aggregates. C) When Cse4 octamers are reconstituted, only the octamer population is detected in the gel filtration fractions. The protein composition of all above peaks was verified on a Coomasie-stained poly-acrylamide gel (data not shown).

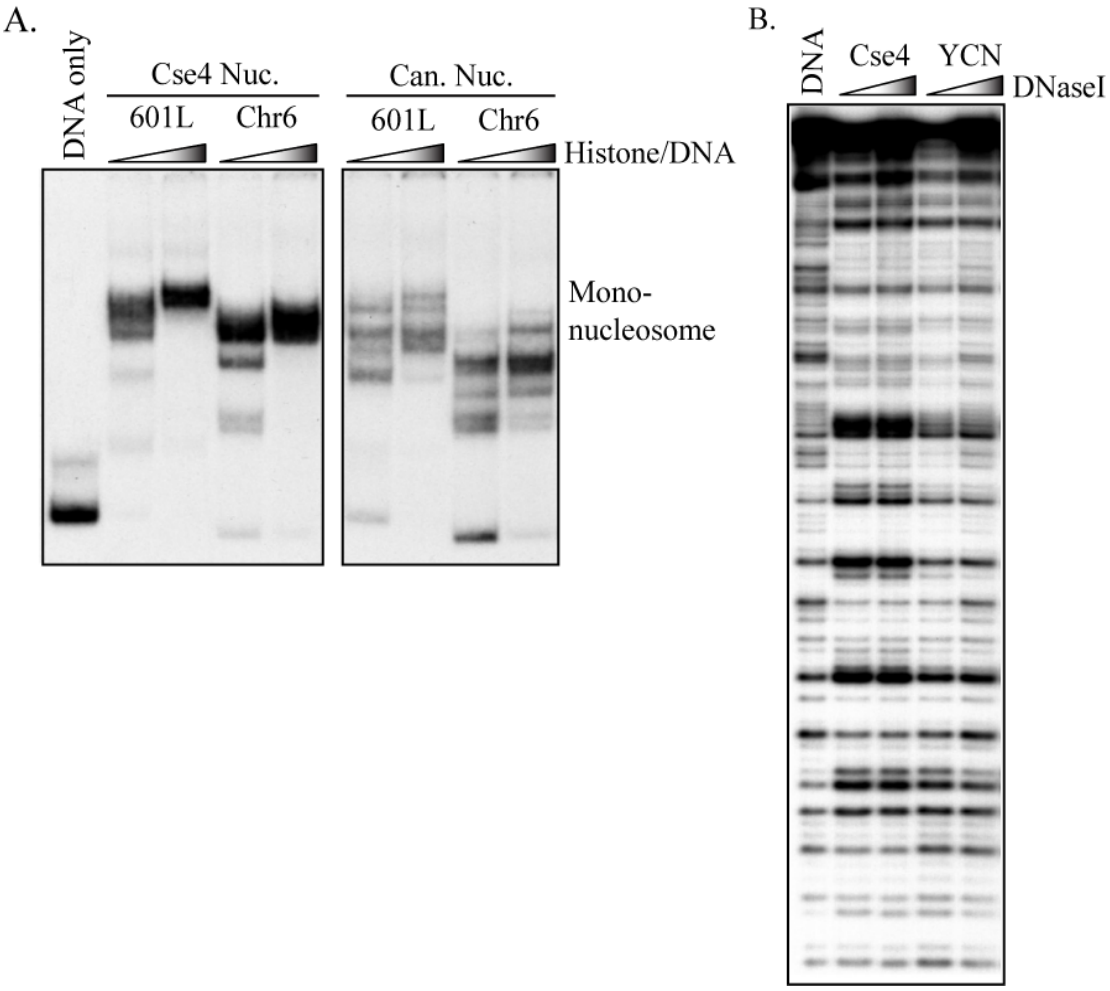

Figure 28. Assembly of Cse4 nucleosomes *in vitro*.
A) Cse4 and canonical histone octamers were assembled with either the 601L nucleosome positioning sequence or a sequence from the arm of yeast chromosome 6 (Chr6). The resulting nucleosomes were resolved on a 5% native poly-acrylamide gel. B) Mononucleosome species were gel purified, treated with DNaseI, and the products were separated on an 8% denaturing poly-acrylamide gel. DNaseI accessibility was mapped for Cse4 and yeast canonical nucleosomes (YCN) assembled from recombinant histones and ^{32}P 5'-labelled Chr6 DNA.

The DNaseI digestion pattern of Cse4 nucleosomes closely resembles that of canonical nucleosomes, an indication that the DNA configuration of a Cse4 nucleosome *in vitro* is similar to its canonical counterpart (Figure 28B). Coupled with the *in vivo* precipitation data, our *in vitro* data supports the model that Cse4 forms an octameric nucleosome, whose overall structure resembles that of a canonical nucleosome.

6. Reconstitution of Scm3 hexamers in vitro

It was previously reported that when recombinant Scm3 was added to Cse4-containing octamers, H2A-H2B dimers were evicted, and a hexameric Scm3-Cse4-H4 complex was formed [117]. To study the properties of this Scm3 hexamer we have purified recombinant histidine-tagged Scm3 (6HIS-Scm3) from *E. coli* (Figure 29A). Using 6HIS-Scm3 and pre-assembled Cse4 octamers we have confirmed the finding that 6HIS-Scm3 evicts histones H2A and H2B from preassemble Cse4 octamers (Figure 29B), and we have isolated the 6HIS-Scm3-Cse4-H4 hexamer (Figure 29C). Surprisingly, we also found that when recombinant 6HIS-Scm3 was added to canonical octamers, H2A-H2B dimers were evicted and a complex consistent with a Scm3-H3-H4 hexamer was isolated by gel filtration chromatography (Figure 29D). This finding indicates a lack of specificity of Scm3 for interaction with Cse4 octamers *in vitro.* A molecular size standard was run on the same column and used it to verify correct molecular weight of the purified hexameric complex (Figure 29E). Using purified Scm3-Cse4-H4 hexamers from Figure 29C, we attempted to

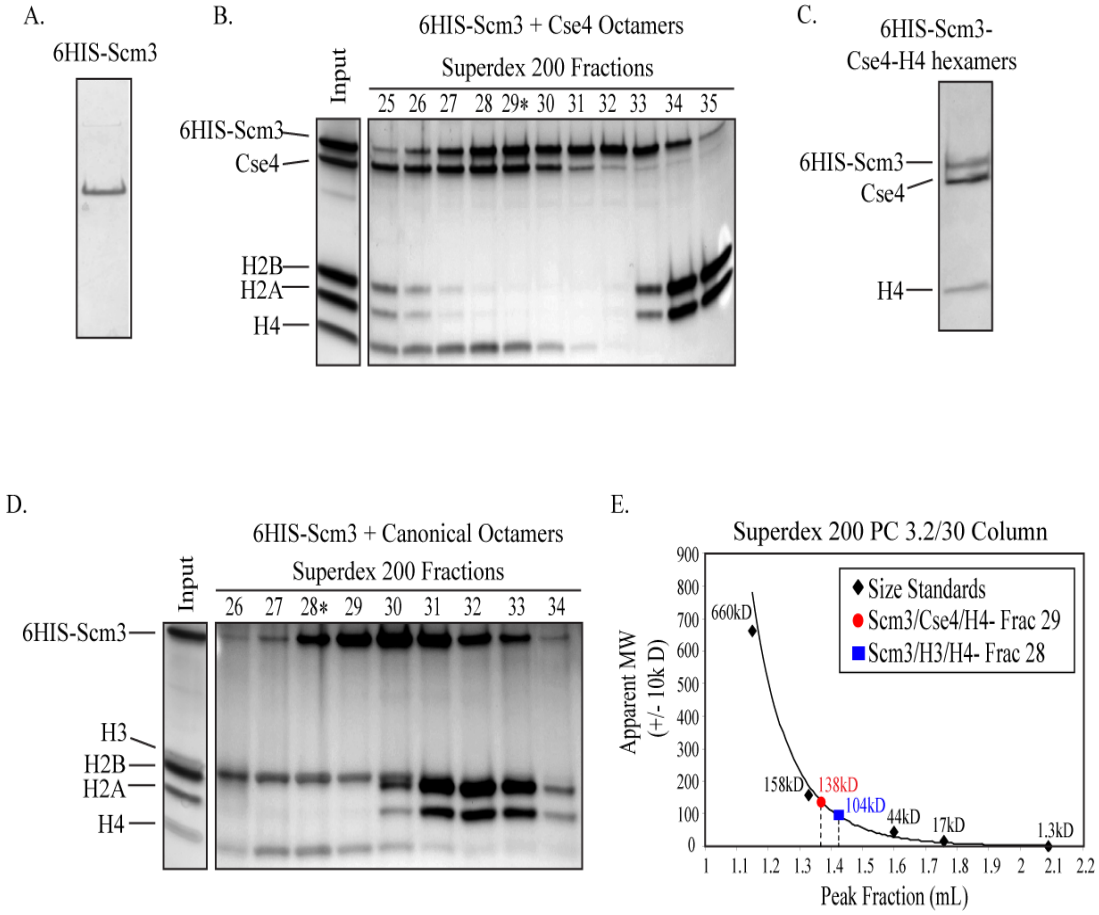

Figure 29. Reconstitution of Scm3 hexamers *in vitro*.
A) Recombinant six histidine-tagged Scm3 (6HIS-Scm3) was purified from *E. coli*. B) 6HIS-Scm3 was mixed with Cse4 octamers at a 1:1 ratio in 2 M salt, incubated for 2 hours at 30° C, and subjected to gel filtration chromatography. Fractions collected were subjected to PAGE followed by silver staining. The asterisk indicates the fraction used for molecular weight (MW) determination. C) Fractions from (B) containing Scm3-Cse4-H4 hexamers were pooled. D) 6HIS-Scm3 was mixed with canonical octamers at a 1:1 ratio in 2 M salt, incubated for 2 hours at 30°C, and subjected to gel filtration chromatography. Fractions collected were subjected to PAGE followed by silver staining. 6HIS-Scm3 facilitates removal of H2A-H2B dimers from canonical octamers and forms a complex consistent with Scm3-H3-H4 hexamers. The asterisk indicates the fraction used for MW determination. E) A molecular size standard was run on the same column used for hexamer reconstitutions, and an apparent MW standard curve was created. Error is estimated to be +/- 10 kD. The MW of a Scm3-Cse4-H4 hexamer is calculated to be ~131 kD and the apparent MW of fraction 29 from B is 138 kD. The MW of a Scm3-H3-H4 hexamer is ~106 kD and the apparent MW of fraction 28 from D is 104 kD.

reconstitute a hexameric nucleosome. Using the same salt dialysis protocol used to reconstitute Cse4 octameric nucleosomes, we attempted to reconstitute a hexameric Scm3-containing nucleosome using both 601 and CEN3 DNA. Unfortunately, we were unable to reconstitute hexameric nucleosomes *in vitro* using this method (data not shown).

7. Scm3 chaperone activity in vitro

It has been proposed that Scm3 may be a Cse4-specific histone chaperone which facilitates the deposition of Cse4-containing nucleosome onto centromeric DNA [118]. Previous work on *Drosophila* CID (CENP-A) has identified RbAp48 as a possible CenH3 chaperone protein. RbAp48 immunopurifies with CID, and was shown to possess chaperone activity *in vitro* using a plasmid supercoiling assay [112]. Similar to RbAp48, Scm3 is comprised of a large percentage of acidic residues, and binds Cse4-H4 *in vitro* [117]. To test for Scm3 chaperone activity *in vitro* we performed the same plasmid supercoiling assay used for RbAp48. In this assay, Scm3-mediated nucleosome deposition onto a fully relaxed, circular plasmid substrate will lead to a positive supercoiling of the plasmid. Using recombinant 6HIS-Scm3, recombinant histone chaperone Nap1 (GST-Nap1), and pre-assembled canonical and Cse4 octamers we performed the plasmid supercoiling assay. In the control reaction using GST-Nap1 as the chaperone we find that Cse4 octamers readily assemble onto the plasmid substrate, with nearly 100% of the plasmid returning to a fully supercoiled state (Figure 30A). With Scm3 as the chaperone, very little

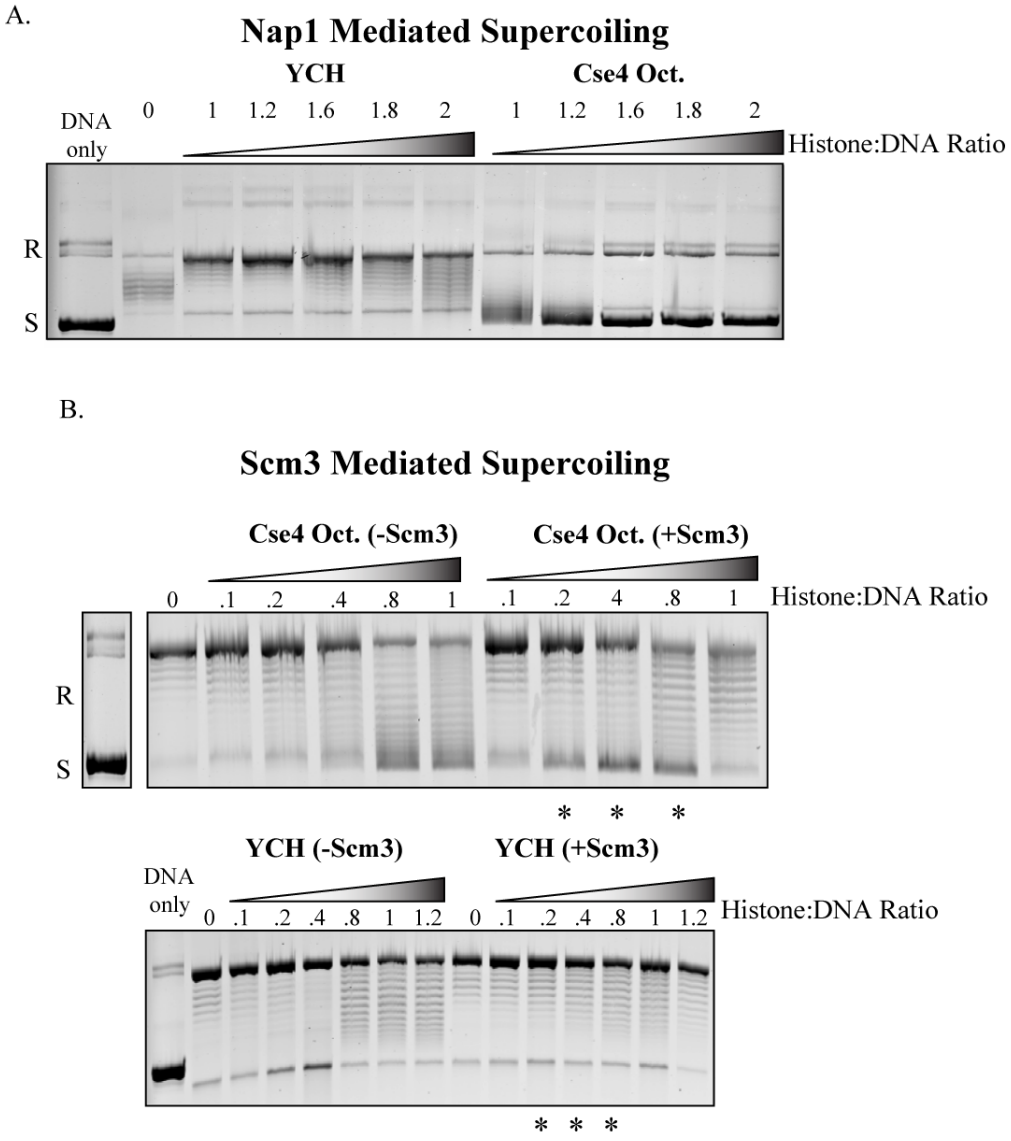

Figure 30. Plasmid supercoiling assay.
A plasmid supercoiling assay was performed using plasmid pG5E3, which contains ~25 repeats of the "601" nucleosome positioning sequence. pG5E3 was fully relaxed using recombinant Topoisomerase I (Topo I), and mixed with chaperone incubated with increasing amounts of pre-assembled octamers. A) Using GST-NapI as the chaperone, strong reversion to a supercoiled state is observed when pG5E3 was mixed with Cse4 octamers. Yeast canonical histone octamer (YCH) do not assemble onto DNA as efficiently. B) Using 6HIS-Scm3 as the chaperone, a slight increase in supercoiled species is observed when pG5E3 is incubated with Cse4 octamers at .2, .4, an .8 ratios of octamers:DNA (asterisks). When compared to the reaction where 6HIS-Scm3 is incubated with canonical octamers, no increase in supercoiled species is observed at these same ratios (asterisks).

supercoiling was observed when compared to a reaction without Scm3, although there was a slight increase when the Histone:DNA ratio was between 0.2-0.8.:1 (Figure 30B). Although we do not observe significant chaperone activity using the plasmid supercoiling assay, we can not rule out that Scm3 is not a Cse4-specific chaperone. The weak chaperone activity seen may be a direct result of improper experimental conditions, or Scm3 may require a centromeric DNA sequence on the template plasmid for full chaperone activity *in vitro*.

8. Dimerization of Cse4 in vivo

To determine which individual amino acids are essential for Cse4 function we have performed single residue alanine scanning mutagenesis across the entire Cse4 open reading frame. Each mutant was tested for its ability rescue growth in a *cse4Δ* strain. Using this unbiased approach we have identified 6 single amino acid residues that are essential for Cse4 function *in vivo* (Figure 31A). All 6 lethal mutants are located at the C-terminal end of Cse4, in the evolutionarily conserved HFD. This finding is consistent with previous reports that the N-terminus of Cse4 is dispensable for Cse4 function [103]. Using the predicted crystal structure of the Cse4-containing nucleosome as a guide [131], we have mapped the location of each of the 6 essential residues (Figure 31B). We find that 5 of the 6 essential residues are located in close proximity to the Loop II-Helix III transition. Mutations in this region would be predicted to interfere with the structure and folding of Helix III, disrupting the dyad axis and subsequently the Cse4-Cse4 dimer interface at the four-helix bundle.

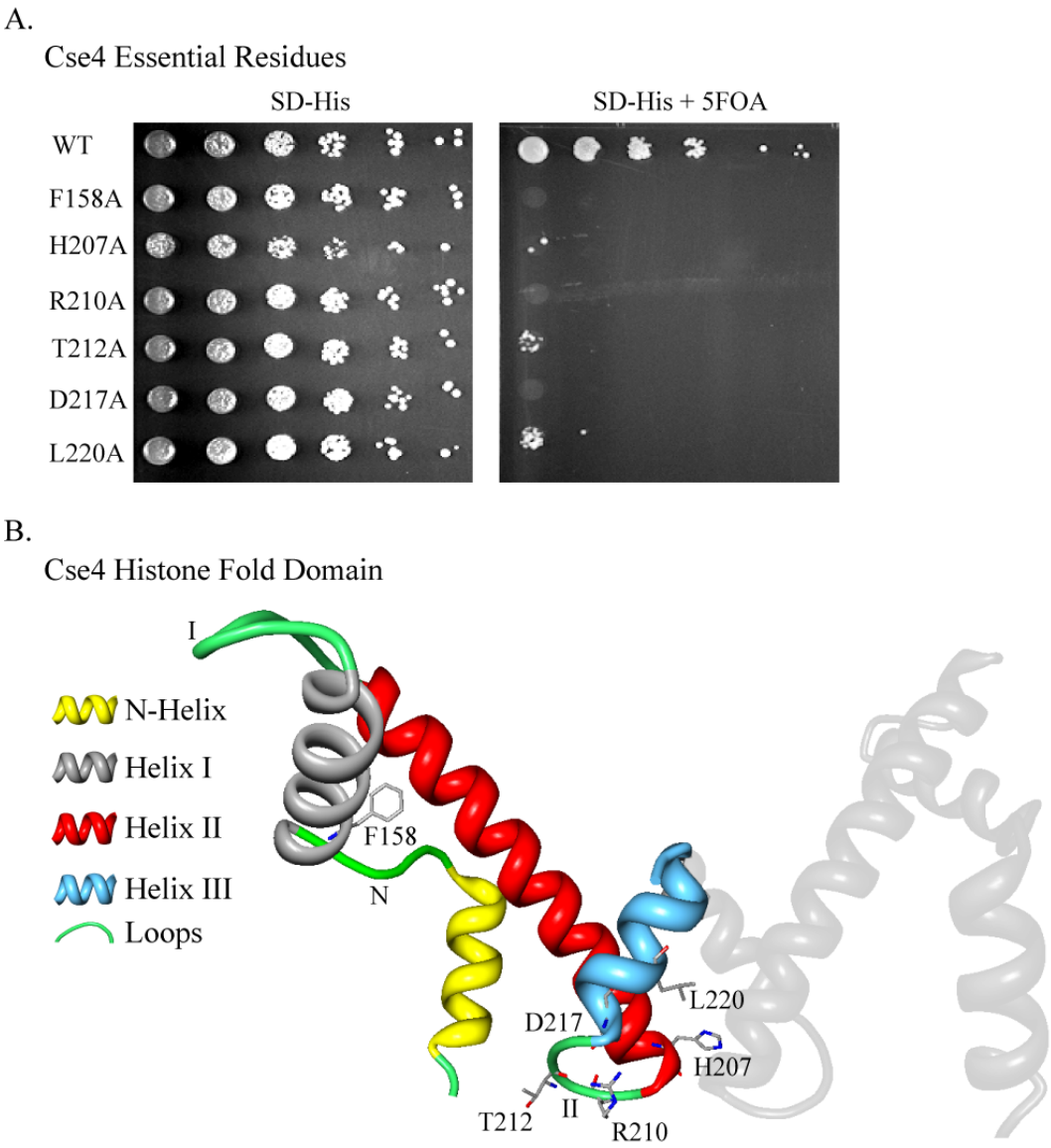

Figure 31. Single residue alanine scanning mutagenesis of Cse4.
Cse4 was cloned into pRS413 and subjected to site directed mutagenesis which mutated each individual amino acid to an alanine. Each mutated plasmid in the collection was transformed into a haploid *cse4Δ* strain containing another plasmid with a wild type copy of Cse4, and a plasmid-shuffle assay was performed. A) Growth on 5-FOA identified six single alanine substitutions that do not support growth in the *cse4Δ* background. B) Using the modeled Cse4 crystal structure as a guide [131], the location of each of the 6 lethal point mutants was mapped. One molecule of Cse4 histone fold domain from the predicted Cse4 octamer crystal structure is shown in color and the essential residues are indicated. The second molecule of Cse4 is shown in grey. Five of six of the lethal point mutations lie in close proximity in either Loop II or Helix III.

Although the results of the alanine scanning mutagenesis strongly suggest that Cse4-Cse4 dimers are required for Cse4 function, this experiment did not directly address whether multimers of Cse4 are actually found *in vivo*. In order to do this, we created a yeast strain that co-expressed two differentially epitope-tagged Cse4 proteins, Cse4-12Myc and FLAG-Cse4. Using this strain we performed co-immunoprecipitation to detect an interaction between the two epitope-tagged Cse4 proteins. We found that in whole cell extracts we were able to detect a physical interaction between Cse4-FLAG and Cse4-12Myc (Figure 32A). To test whether this interaction occurs in the context of the Cse4-containing centromeric nucleosome, we performed quantitative sequential chromatin immunoprecipitation (SeqChIP) [132] using the differentially-tagged Cse4 strain. We find that when we ChIP with an antibody against the Myc epitope, followed by ChIP using an antibody against the FLAG epitope, we see significant enrichment of Cse4 specifically at the centromere (CEN3) (Figure 32B). Coupled with the alanine scanning mutagenesis data, these compelling results strongly suggest that Cse4-Cse4 dimers are required for Cse4 function, and indicate that the centromeric nucleosome contains two copies of Cse4.

IV. Discussion

To address the composition of centromeric chromatin in budding yeast, we have performed a number of *in vivo* and *in vitro* experiments. When we treat bulk chromatin with MNase *in vivo* we find that unlike Cse4 and the core histones, Scm3 is not solubilized. Co-immunoprecipitation from the MNase-solubilized chromatin

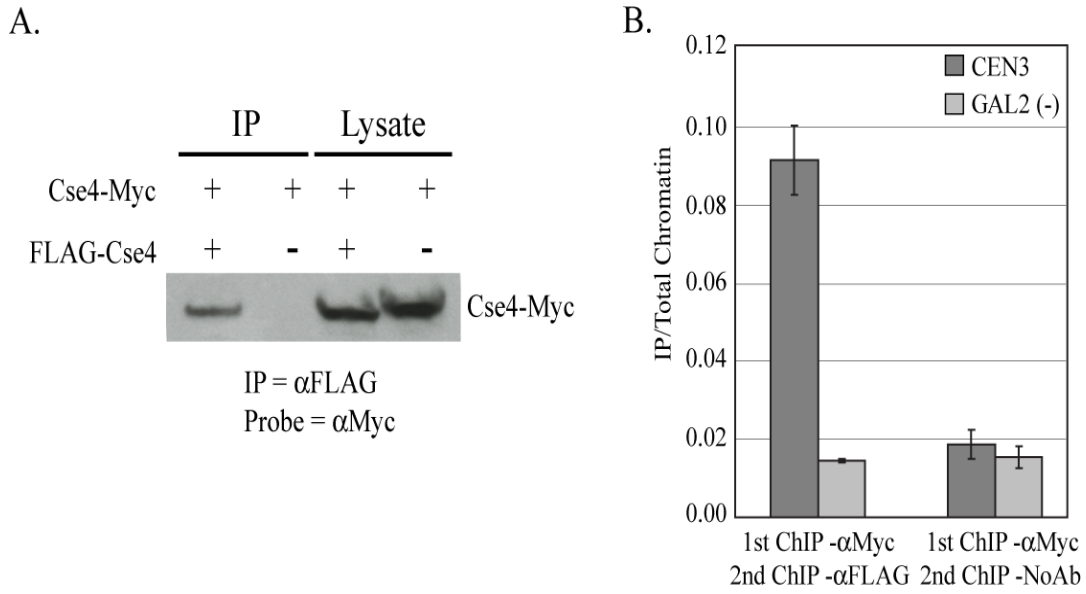

Figure 32. Co-immunoprecipitation and sequential ChIP of differentially tagged Cse4 proteins.

A) Co-immunoprecipitation was performed using whole cell extracts (WCE) isolated from a strain which expresses both Cse4-12Myc and FLAG-Cse4. αFLAG-conjugated beads were used to pulldown FLAG-Cse4 from WCE, and the pulldown was probed by Western blotting with the αMyc antibody. The negative control pulldown was performed using chromatin from a strain lacking FLAG-Cse4. B. SeqChIP was performed using sheared chromatin isolated from the same strain as in (A). αMyc antibody was used for the 1st round of ChIP, followed by ChIP using either the αFLAG antibody or no antibody. The signal from each ChIP has been divided by the signal obtained with total chromatin. The centromeric primer pair spans ~ 350bp across CEN3. The *GAL2* gene serves as a negative control for Cse4 localization. Error bars represent +/- the average deviation of biological replicates.

reveals that Cse4 physically associates with histones H2A, H2B, and H4. In MNase-solubilized chromatin we cannot detect an interaction between Cse4 and either H3 or Scm3. These results strongly suggest that the Cse4-containing nucleosome contains Cse4, H2A, H2B, and H4, but not H3 or Scm3. Overexpression of Cse4 can bypass the requirement for Scm3 in kinetochore formation. Furthermore, Cse4 can localize properly to the centromere even in the absence of Scm3. These results are a strong indication that a Scm3-containing nucleosome is not essential for chromosome segregation in budding yeast.

To further study the properties of the Cse4-containing nucleosome we have reconstituted Cse4 mononucleosomes *in vitro*. We can efficiently reconstitute Cse4 octamers and nucleosomes. Using comprehensive alanine scanning mutagenesis we have identified a number of Cse4 residues that are essential for protein function *in vivo*. The large majority of these mutations are located at the Cse4-Cse4 dimer interface, underscoring the importance of this domain for Cse4 function *in vivo*. Additionally, using co-expression of differentially epitope-tagged Cse4 proteins and sequential ChIP, we have verified the presence of a Cse4 nucleosome at the centromere which contains multiple copies of Cse4. Taken together our results suggest that Cse4 is found in an octameric nucleosome *in vivo*, which also contains histones H2A, H2B, and H4.

1. Putting the hexamer to the test

It has been proposed that in budding yeast, Scm3 is a component of a

specialized hexameric centromeric nucleosome [117] which lacks histones H2A and H2B. This model is based partly on experiments *in vitro* in which Scm3 was shown to evict H2A and H2B from preassembled Cse4-containing octamers. Based on our experimental evidence we hypothesize that Scm3-Cse4-H4 hexamer may be some type of intermediate in the formation of the centromeric nucleosome, but not the actual complex that is found in the centromeric nucleosome. We find that Cse4/H4 tetramers are poorly reconstituted. One possibility is that Scm3 may stabilize the Cse4/H4 tetramer *in vivo* but is not maintained as an actual component of the centromeric nucleosome. The hexameric nucleosome model is also difficult to reconcile with previous work that shows H2A is required for proper centromere function [133], and that the inner kinetochore protein Mif2 physically interacts with Cse4, H2A, H2B, and H4, but not H3 [80, 133]. High resolution mononucleosome ChIP reveals that the localization pattern of Cse4 differs from that of Scm3. Cse4 appears to localize directly over the entire length of the centromeric DNA sequence, while Scm3 localizes with a bias towards the CDE III end of the centromere. This result is consistent with the observed interaction between Ndc10 and Scm3 [116], given that Ndc10 has been shown to interact directly with CDE II-III [65].

Similar to a previous report [117] we were also unable to ChIP H2A and H2B to the centromere. However, we do not think this reflects their absence at this site. Reciprocal Co-IP of both Cse4 and H2A from mononucleosomes reveals that these proteins physically interact with one another, as well as histones H2B and H4. Based on this result, we hypothesize that the formation of the kinetochore over the

centromeric nucleosome precludes antibody accessibility to the histone epitopes for ChIP, some of which are buried within the core of the nucleosome.

Another compelling result is that Cse4 can rescue a complete deletion of *SCM3*. Based on this result it seems likely that Scm3 is only required for the formation of the centromeric nucleosome when Cse4 protein levels are limited. We were unable to find evidence for a Scm3-containing centromeric nucleosome *in vivo*. Therefore, we favor a model in which Scm3 is not an actual component of the centromeric nucleosome, but rather intimately associates with it at the inner kinetochore. This model is consistent with Scm3 being a Cse4-specific chaperone. While we did detect slight chaperone activity in the Scm3 plasmid supercoiling assay, our data was inconclusive. It is important to note that in previous supercoiling assays done using *Drosophila* Cid and RbAp48 [112], strong chaperone activity was only observed when a plasmid containing large tandem repeats (several kb) of Drosophila centromeric DNA was used. Unfortunately, the budding yeast centromeric sequence will only accommodate a single nucleosome, therefore a plasmid containing a single yeast centromere would not be feasible to use in a supercoiling assay, when multiple nucleosomes must be deposited on a single plasmid template in order to quantify the chaperone activity.

2. Cse4 nucleosomes are likely octamers in vivo

Another proposed model for centromeric chromatin is that a single molecule of each Cse4, H2A, H2B, and H4, form a structure at centromeres called a hemisome [114].

Hemisomes were observed in interphase *Drosophila* cells [115], but have not been observed in any other organism. Unlike both CENP-A and CID [112, 113], Cse4-containing nucleosomes had not been reconstituted *in vitro*. When we reconstituted Cse4 complexes *in vitro*, we find that Cse4 readily forms an octameric complex with the core histones. We did not detect any population by gel-filtration chromatography that would be consistent with a hemisome. We also show that the reconstituted Cse4 octamer can wrap DNA to form an octameric nucleosome similar in structure to a canonical H3-containing nucleosome. In addition, using comprehensive alanine scanning mutagenesis we find that 6 single amino acids are required for Cse4 function *in vivo*. Unlike previous Cse4 mutagenesis studies that identified functional regions of the HFD in the context of multiple mutations across the region [40, 134], we have identified single residues essential for Cse4 function. The fact that 5 of 6 lethal mutants fall either in Loop II or Helix III is indicative of the importance of this region in Cse4 function. By analogy to H3, the Loop II-Helix III transition is the location of the dyad axis, which forms the Cse4-Cse4 four-helix bundle. Mutation in this region would be predicted to disrupt two heterodimers of Cse4-H4 coming together to form a tetramer, which would occur at the Cse4-Cse4 dimerization interface. If Cse4 was found in a hemisome, one would predict that this dimerization event would be unnecessary. Additionally, the results of sequential ChIP using a strain expressing two differentially-tagged Cse4 proteins provides direct *in vivo* evidence that the budding yeast centromeric nucleosome contains more than one copy of Cse4. Therefore, it is hard to reconcile these data with the requirement for a Cse4-

containing hemisome *in vivo*. The sum of all of our experiments strongly suggests that the CenH3 variant Cse4 is found at a single octameric nucleosome at the budding yeast centromere.

Chapter 4.

Conclusions and Future Directions

Although much is understood about the formation of the budding yeast kinetochore, little is known about how exactly the inner kinetochore recognizes and assembles at centromeric DNA. Additionally, the exact composition of the centromeric nucleosome is a subject of strong debate. The data presented in this dissertation represents a large step forward in understanding when and where this nucleosome forms, how it forms, and what additional protein components are required. We have provided evidence that *SCM3* encodes a previously uncharacterized inner kinetochore protein which functions in localizing both Ndc10 and Cse4 to the centromere. Our work demonstrates that Scm3 is vital for formation of centromeric chromatin, the inner kinetochore, and subsequent chromosome segregation. Additionally we believe that Scm3 is not an integral component of a specialized centromeric nucleosome, but rather intimately associates with it at the inner kinetochore. Based on our findings, we support a model in which a single octameric nucleosome forms at budding yeast centromeres. This nucleosome is comprised of Cse4, H2A, H2B, and H4 and forms early in S-phase after centromeres are replicated, with Scm3 and Ndc10 acting as a specificity factors for its centromeric location (Figure 33). In addition to its role in the formation of the centromeric nucleosome, Scm3 is also required throughout the cell cycle to maintain a segregation-competent kinetochore. Future investigation into the role of Scm3 in

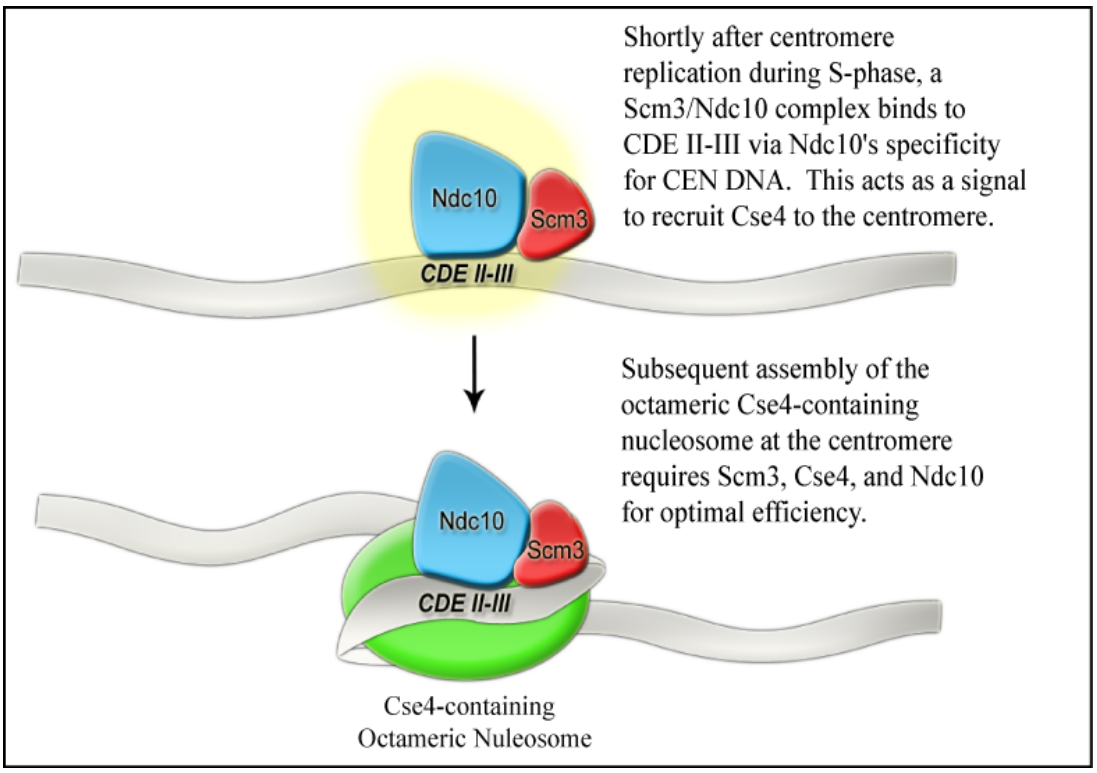

Figure 33. Model for the formation of centromeric chromatin.
A complex containing Ndc10 and Scm3 localizes to centromeric DNA early in S-Phase following centromere replication by virtue of the ability of Ndc10 to bind to the CDE II-III sequences specifically. After Ndc10 and Cse4 localize to the centromere, a single octameric nucleosome containing Cse4, H2A, H2B, and H4 forms at this site. The localization of Ndc10, Scm3 and Cse4 is interdependent and establishes functional centromeric chromatin.

kinetochore function should aim to further elucidate the molecular mechanism by which this protein helps to demarcate the centromere, and to pinpoint its role in maintenance of a functional kinetochore.

I. The mechanism of Scm3 function in formation of the Cse4 nucleosome

Previous experiments have suggested that Ndc10 binding to CDE II-III is the nucleating step of kinetochore formation [84, 87-89]. This hypothesis is strongly based on previous work that shows a lack of localization of several kinetochore components in a *ndc10-1* temperature sensitive mutant. Also, no proteins have been identified that are required for Ndc10 localization to the centromere. We have shown that Scm3 is required for the localization of Ndc10 to the centromere during S-phase. Conversely, Ndc10 is required for proper localization of Scm3 to the centromere. These findings strongly suggest a reciprocal relationship between Ndc10 and Scm3 in nucleation of the kinetochore. Future studies should focus on the relationship between Ndc10 and Scm3. It would be helpful to understand which domain of Scm3 actually interacts with Ndc10. One would predict that the Ndc10-interacting domain would be essential. Other key experiments could include looking at the relationship between Scm3, Ndc10, and centromeric DNA *in vitro* using purified components.

Although we know that Scm3 is required for formation of the Cse4-containing centromeric nucleosome, we have not as of yet identified the precise molecular mechanism of action of Scm3 at the inner kinetochore. Future experiments should focus on the identification of this mechanism. We have confirmed that Scm3 can

displace H2A and H2B from pre-assembled Cse4 octamers. However, the relevance of this reaction to the formation of the centromeric nucleosome *in vivo* is not clear. Also we observed that Cse4-H4 tetramers do not readily form *in vitro*. These findings suggest that Scm3 may facilitate formation and maintenance of Cse4-H4 tetramer pools *in vivo,* or may be a Cse4-H4 specific histone chaperone, involved in nuclear import, chromatin formation, or both. These hypotheses are consistent with the finding that Scm3 can form a stoichiometric complex with Cse4 and H4 [117] and that overexpression of Cse4 can rescue a *scm3Δ* strain, presumably through high levels of Cse4 in the cell driving the Cse4-H4 interaction. Although the result of the supercoiling assay using recombinant Scm3 and Cse4 octamers was inconclusive, we can not rule out the possibility that Scm3 is indeed a Cse4-specific chaperone. It is possible that Scm3 chaperone activity would only be observed when using a plasmid substrate possessing an actual centromeric sequence. Although technically challenging, it would be possible to create a plasmid with multiple copies of a yeast centromeric sequence. This plasmid could then be utilized in the plasmid supercoiling assay in conjunction with recombinant Scm3, and pre-assembled Cse4 octamers.

II. The role of Scm3 in maintenance of a functional kinetochore.

Another function for Scm3 besides initiation of kinetochore formation is maintenance of kinetochore function throughout the rest of the cell cycle. When cells are released from a metaphase arrest after Scm3 is depleted, they cannot enter

anaphase, and remain arrested at the spindle checkpoint. Based on the fact that Dam1-GFP appears to localize properly when Scm3 is depleted, we do not think this failure to rescue chromosome segregation in Scm3 depleted cells is due to a lack of localization of the outer kinetochore proteins. It is possible that Scm3 somehow is responsible for signaling to the spindle checkpoint that the kinetochore is formed. It seems unlikely that the same Scm3 molecule which interacts with Ndc10 and Cse4 at the inner kinetochore is later responsible for signaling to the spindle checkpoint. This function most likely is independent from its role in kinetochore formation, and would suggest dynamic loading/unloading of Scm3 at the centromere during the cell cycle. Isolation of Scm3 separation of function mutants would be an important step in identifying its role in kinetochore maintenance. Comprehensive alanine scanning mutagenesis, or further large-scale mutagenesis studies would be helpful in identifying these mutants.

CHAPTER 5.

Materials and Methods

I. Bacterial Methodology

1. Bacteria culturing and strains

The *Escheria coli* strain DH5α was used for all standard cloning and plasmid preparation techniques. One Shot library efficiency chemically competent *E. coli* (Invitrogen) were used for all standard plasmid transformations. All E. *coli* strains were grown in Luria Bertani (LB) growth media supplemented with appropriate antibiotics at 37°C. Ampicillin and Kanamycin were used at 100 μg/ml and 25 μg/ml respectively.

2. Plasmid manipulation

Standard restriction digest cloning was performed using techniques found in Molecular Cloning: A Laboratory manual [135]. All restriction enzymes, calf intestinal phosphatase (CIP) and T4 DNA ligase were obtained from New England Biolabs (NEB) and used with supplied buffers at recommended concentrations. Constructs for cloning were amplified from genomic or plasmid DNA using standard polymerase chain reaction (PCR). Phusion polymerase (Finnzymes) was used for high fidelity PCR as per supplied protocol. Primers for cloning and sequencing were synthesized by Integrated DNA Technologies (IDT). Plasmid sequencing was performed in the Stowers Institute for Medical Research molecular biology facility

using ABI 3730 48-capillary DNA analyzers. The reactions were performed by PCR according to Applied Biosystems protocols (Big Dye Terminator ver. 3.1). Unincorporated nucleotides were removed by exclusion columns from Edge Biosystems or by SPRI technology from Agencourt. Sequencing results were analyzed using VectorNTI Contig Express (Invitrogen). To make the Gal4BD-Scm3 fusion, *SCM3* was cloned into the Gal4BD vector pGBKT7 (Clontech Laboratories). Gal4BD-Scm3 was subcloned into pESC-*HIS3* (Stratagene).

3. Recombinant protein expression and purification

The expression vector pET15-HIS-Scm3 encodes a N-terminal 6-Histidine tagged Scm3 protein (6HIS-Scm3), and was a gift of Carl Wu (NIH, Bethesda, MD). For expression of recombinant 6-HIS Scm3, pET15-HIS-Scm3 was transformed into One Shot BL21 Codon Plus competent *E. coli* (Invitrogen). Recombinant 6HIS-Scm3 expression was induced by addition of IPTG (0.3 mM final). Cultures were induced at 25°C for 4-6 hours. Expression of 6HIS-Scm3 was monitored by polyacrylamide gel electrophoresis and subsequent Coomasie Brilliant Blue staining (Bio-Rad). 6L cultures were used for each round of expression. *E. coli* were lysed by sonication in the presence of high salt lysis buffer (1X PBS, 500 mM NaCl, 10 mM imidazole) supplemented with protease inhibitors (Complete tablets, Roche) and lysozyme (1 mg/ml) and Benzonase (25 U/ml, Novagen). Lysates were cleared via ultracentrufigation, and 6HIS-Scm3 was isolated using Talon metal affinity resin (BD Biosciences). After several hours of incubation with the lysate, Talon resin was

collected in an disposable chromatography column (Bio-Rad), washed with several column volumes (CVs) of wash buffer (1X PBS, 500 mM Nacl, 20 mM imidazole), and protein was eluted from the resin with several CVs of elution buffer (1X PBS, 500 mM NaCl,150 mM imidazole). Lysate, flow-through, wash, elution and bead-bound fractions were all subjected to PAGE and Coomasie blue staining. To further polish the 6HIS-Scm3 prep and to remove any contaminating proteins the eluate from the talon beads was subjected to fast pressure liquid chromatography (FPLC). The eluate was diluted ten fold with FPLC running buffer (50 mM NaPO4, 10% glycerol) and loaded onto a HiTrap MonoQ anion-exchange column (Amersham) using an AKTA FPLC system (Amersham). Bound 6HIS-Scm3 was eluted from the column using an increasing gradient of NaCl from 0-500 mM. 6HIS-Scm3 elutes at ~300 mM NaCl. All collected fraction were subjected to PAGE and Coomasie blue staining. Yeast recombinant histones (H3, H4, H2A, H2B, Cse4) were individually expressed in *E. coli* and purified from inclusion bodies as previously described and were a kind gift from Bing Li (Stowers Institute) [136].

4. Octamer, hexamer, and nucleosome reconstitutions

Assembly of histone octamers was carried out as in [137] and octamers were purified on a HiLoad 16/600 Superdex 200 column (Amersham Biosciences) and an AKTA FPLC (GE Healthcare). Assembly of Scm3-Cse4-H4 hexamers was performed as previously described [117] by additions of 6HIS-Scm3 to preassembled octamers in hexamer reconstitution buffer (2 M NaCl, 10 mM Tris 7.5 pH) and gel

filtration was performed using a Superdex 200 PC 3.2/30 gel filtration column (Amersham Biosciences) on a SMART system (Pharmacia Biotech). PCR amplified DNA fragments for nucleosome reconstitution were ^{32}P 5' end-labeled and mixed with histone octamers in high salt (2 M) and subsequently subjected to ten dilutions to physiological salt concentrations (100 mM) to form mononucleosomes. Mononucleosome bands were purified from a 5% non-denaturing poly-acrylamide gel and subjected to DNase I digestion. Digested DNA was separated on an 8% denaturing poly-acrylamide gel.

The plasmid supercoiling assay was performed as previously described [112]. Recombinant Topoisomerase I was a kind gift from S. Venkatesh, Stowers Institute. Plasmid G5E4 used in the supercoiling assay contains 23 repeats of the 601 nucleosome positioning sequence.

II. Yeast Methodology

1. Yeast culturing and strains

All strains used were constructed in the W303 background unless otherwise noted. For a complete list of yeast strains used see appendix 1. In general yeast were grown at 30°C for wild type (WT) strains. For temperature sensitive strains (ts), permissive temperature was 25°C and non-permissive temperature was 37°C. The various epitope-tagged and knock-out strains were constructed by homologous integration using yeast transformation as previously described [138]. Yeast transformation was carried out using the standard LiOac transformation method.

Yeast growth on rich media was carried out on either yeast-peptone-dextrose (YPD) or YP-Galactose. When nutritional selection was required, yeast were grown on either synthetic dextrose or synthetic galactose (SD or SGal) media supplemented with the appropriate amino acid drop-out powder (Clontech). The antibiotics Geneticin (G418) and Hygromycin were used at 200 μg/ml and 300 μg/ml respectively. G1, S-phase and G2/M arrests were achieved using final concentrations of 5μM α-factor (Zymo Research), 0.2M Hydroxyurea (Sigma), or 15 μg/ml nocodazole (Sigma) respectively. The yeast HIP overexpression library was obtained from Harvard Proteomics and transformed into the "Magic Marker" yeast strain (Open Biosystems) as per standard high-throughput 96-well yeast protocols. Transformed diploids were selected on synthetic dropout medium lacking uracil (SD-Ura), sporulated, and then pinned in quadruplicate by hand to medium [139] that allowed the recovery of haploid yeast that contain both the $GAL_{1\text{-}10}$ overexpression plasmid and the deletion of interest (SGal glutamate, -Leu, -His-,-Ura, -Arg, +G418, 6 μg/ml +L-Canavanine) [140].

2. Chromatin immunoprecipitation

For chromatin immunoprecipitation (ChIP), 220-500 ml yeast cultures were grown to mid-log phase prior to any cell cycle arrest or harvest for ChIP. Cross-linking of cultures was done with formaldehyde (1% final) for 10 minutes and chromatin was harvested by beatbeating in the presence of lysis buffer (100 mM Tris pH 7.5, 150 mM NaCl, 0.1 mM EDTA, 1 mM DTT, 0.1% NP-40, 10% glycerol) plus

protease inhibitors (Complete tablets, Roche). For lower resolution ChIP studies, chromatin was sonicated to obtain fragments ~300-500 base pairs (bps) in size. For high-resolution mononucleosome ChIPs, $CaCl_2$ (3 mM final) and micrococcal nuclease (MNase) were added (~250-500 units, Worthington) to the chromatin after beatbeating and lysates were incubated at 37° for 30 min. in lieu of sonication. The MNase reaction was stopped by addition of EDTA and EGTA to 25 mM each and placing lysates at 4°C. Lysates were then cleared by sonication (15K rpm, 15 min.) and diluted 1:10 in IP dilution buffer (0.01% SDS, 1% Triton X-100, 1 mM EDTA, 20 mM Tris pH 7.5, 150 mM NaCl, protease inhibitors). Input samples and no antibody controls were taken at this time. Primary antibodies were all used at a 1:500 dilution unless otherwise noted. Antibodies used for ChIPs are as follows: αHA (12CA5, Roche), αMyc (Santa Cruz, 9E10), and αFlag M2 (Sigma), αH2B (gift from Carl Wu- NIH 1:1000, Lake Placid AR-0264), αH3 (Abcam 1791), αH4 (Abcam 31287, Millipore 05-858). Lysates were incubated with primary antibody overnight (ON) and harvested by incubation with Protein G sepharose (Amersham) for several hours-ON. Protein/DNA bound beads were extensively washed with TSE-150 (0.01% SDS, 1% Triton X-100, 1 mM EDTA, 20 mM Tris pH 7.5, 150 mM Nacl), LiCl detergent wash (1% NP-40, 1% DOC, 1 mM EDTA, 10 mM Tris, 250 mM LiCl) and TE (pH 8). In the case where cultures were not crosslinked the beads were washed several times with lysis buffer and TE. After the final TE wash ChIP samples were eluted with SDS lysis buffer (TE pH 8, 1% SDS) at 42°C for 30 min while shaking. For sequential ChIP, eluates from the 1st ChIP were diluted to .05% SDS

with lysis buffer and a 2nd ChIP was performed as above, using a different antibody. After elution, the crosslinks are then reversed by addition of NaCl to 300mM and incubation at 65ºC ON. Eluates were treated with RNase and Proteinase K for several hours, phenol-chloroform extracted and EtOH precipitated.

3. Immunoprecipitation, Co-Immunoprecipitation, and Western Blotting

Whole cell extracts for co-immunoprecipitation (Co-IP) were obtained by beadbeating in the presence of lysis buffer (100 mM Tris pH 7.5, 150 mM NaCl, 0.1 mM EDTA, 1 mM DTT, 0.1% NP-40, 10% glycerol, protease inhibitors). Chromatin fractionation was performed as previously described [141]. Co-IPs were performed with αMyc antibody (Santa Cruz, 9E10), αFlag M2 (Sigma) and αH3 (Abcam) and were all used at 1:500 dilution. IPs were harvested on proteinG sepharose beads. Beads were washed several times with lysis buffer and eluted in SDS buffer (1% SDS, TE). Denaturing PAGE was performed on the eluates using the Novex 4-12% bis-tris pre-cast PAGE gel system (Invitrogen) as per the manufacturer's protocol. Electrophoresed IPs were transferred to a nitrocellulose membrane and Western blots were performed using standard molecular biology protocols [135]. Primary antibodies for Western blots were as follows: αMyc antibody (Santa Cruz, 9E10, 1:5000), αFLAG M2 (Sigma, 1:5000), αH2B (Lake Placid Biologicals, 1:5000), αH3 (Abcam 1791, 1:1000), αH4 (Abcam 31827, 1:1000, Millipore 05-858, 1:1000), α-PGK (a-6457, Invitrogen), αDam1K233me^2 (gift from Sharon Dent, MD Anderson, 1:1000). Polyclonal rabbit antibodies against a c-terminal Scm3 peptide (aa210-223)

were generated and affinity purified by YenZym Antibodies, and used at 1:5000. For visualization of Western blots, a horseradish-peroxidase (HRP) coupled secondary antibody (αMouse-HRP, αRabbit-HRP, GE Healthcare) was used in conjunction with an ECL detection kit (Amersham). Westerns were exposed onto BioMax imaging film (Kodak) and developed using an X-O200A processor (Kodak).

4. Immunofluorescence and microscopy

For visualization of direct GFP fluorescence, cells were fixed in 4% paraformaldehyde/3.4% sucrose for 15 min. and stained with DAPI to visualize DNA (1 μg/ml final). Cultures for indirect immunofluorescence were fixed with 4% paraformaldehyde in 0.1 M sucrose for 20 min at room temperature (25°C), spheroplasted using zymolyase 100T (50 μg/ml final, Fisher), at 37ºC for 30 min.. Fixed, spheroplasted cultures are then fixed to poly-lysine coated slide via methanol/acetone fixation. The following primary antibody dilutions were used: for microtubules, 1:500 rat anti-tubulin antibody YOL 1/34 (Tub1) (Accurate Chemical & Scientific Corp.); for spindle pole bodies (SPBs), 1:500 affinity-purified anti-Tub4p antibodies (gift from Sue Jaspersen- Stowers Institute). Secondary antibodies included α-rat-FITC (1:500) and α-rabbit–alexa555 (1:20,000). After incubation with primary and secondary antibodies, DNA was visualized by staining with 1 μg/ml DAPI for 5 min immediately before mounting with Citifluor (Ted Pella Inc.). Wide-field microscopy was performed using the following setup: 63x PlanNeo oil objective on Zeiss Z1 fluorescent microscope equipped with filter set 488010 (BP450-490, 510-

580), DAPI filter, and an ORCA-ER digital camera. Image acquisition and analysis was performed using Axiovision 4.5.

5. Quantitative PCR

All Quantitative PCR (pPCR) was performed on an iCycler real-time PCR machine using IQ Sybr Green Supermix (Bio-Rad). Primers sets are listed in appendix 2. Low resolution primer sets span ~ 2 kb across the centromere of chromosome 3. PCR of ChIP DNA was quantified for biological replicates by comparing IP and total input samples against a standard curve established with PCRs of serial 10-fold dilutions of standard DNA. Dynamic well factors were used and cycling parameters were as follows: 94˚C/30 sec., 50˚C /30 sec., 72˚C /30 sec. repeated 40X. A melt curve analysis was performed starting at 50˚C /10 sec. and increasing 0.5˚C /cycle for 80 cycles, with all primers used exhibiting a single melt peak. Occupancy levels were determined by dividing the average of the ChIP DNA by the relative abundance of a control total chromatin sample. This ratio represents the enrichment of ChIP DNA over the input DNA for a specific target. All ratios for biological replicates routinely fell within 10% of each other for a given experiment. No antibody controls were performed for all qPCRs.

6. Flow cytometry

Fluorescence activated cell scanning (FACs) was performed to confirm all cell cycle arrests. For FACs analysis, cells were fixed in 70% EtOH followed by a wash

in FACS buffer (50 mM Na Citrate). Fixed cells were then resuspended in FACs buffer, treated with RNase (Sigma), stained with 1 μM final Sytox Green (Molecular Probes), and analyzed using a Cyan cytometer (Dako Cytomation). FACs data was analyzed using FlowJO cytometry software (Treestar Inc.)

7. DNA microarrays and statistical data analysis

Microarrays were printed in house and consist of over 13,000 PCR fragments representative of the entire yeast genome. Probes for high resolution tiling of yeast centromeres were designed by C. Seidel (Stowers Institute). Microarrays were competitively hybridized with fluorescently labeled immunoprecipitated and input DNA as previously described [125]. Microarray data analysis was carried out in Acuity, Microsoft Excel, and PeakFinder. For statistical analysis we first used Levene's test to determine if the variance of centromere or repetitive element probes were equal to the background. From this, no population variances (centromere or repetitive elements) tested were equal to the background. Correspondingly, we applied four different statistical tests (student t-test, welch t-test, Wilcox test and Kolmogorov-Smirnov test) for each comparison, with or without assuming equal variance. The results of the statistical tests are consistent with each other. Statistical analysis was performed by Dongxiao Zhu.

8. Alanine scanning mutagenesis and crystal structure analysis

Cse4 was cloned into pRS413 and site-directed mutagenesis was performed in 96-well plates using the QuickChange II Site-Directed Mutagenesis Kit (Stratagene) and plasmid manipulation was performed as previously described [142]. All mutants were confirmed by sequencing with T7 and T3 sequencing primers. Yeast were transformed using standard yeast protocols in 96-well format. Transformants were selected on SD-His-Ura. The plasmid shuffle to identify essential residues was performed as previously described [142]. 5-Fluoroortic Acid (5-FOA) was used at 500 μg/ml. Analysis of the predicted Cse4 crystal structure was performed with Sirius 1.2 structure visualization software (San Diego Supercomputer Center) and PDB 2FSB (Protein Data Bank) [131].

9. Mass Spectrometry

Protein samples for multi-dimensional protein identification technology (MudPIT) were isolated by affinity purification of 12Myc-Cse4 and Scm3-3FLAG, Scm3-13Myc and TAP-Scm3 from either asynchronous, alpha factor arrested, or nocodazole-arrested cells (Table 3). Proteins in the Scm3-3FLAG pull down were digested with endoproteinase Lys-C/trypsin, whereas, to improve sequence coverage on Cse4, the Myc-Cse4 pull-downs were independently digested with four enzymes of different specificities. To assess non-specific interactions, negative controls prepared from cells not expressing the epitope-tagged proteins of interest were analyzed in parallel. All MudPIT mass spectrometry (MS) was performed by the Stowers Institute proteomics facility using the following protocol.

First, TCA-precipitated protein samples were solubilized in 30µl of 100 mM Tris- HCl, pH 8.5, 8 M urea, reduced with 5 mM TCEP (Tris(2-Carboxylethyl)-Phosphine Hydrochloride; Pierce), and alkylated with 10 mM IAM (Iodoacetamide; Sigma). For the trypsin digestion, endoproteinase Lys-C (Roche) was added to an approximate enzyme to protein ratio of 1:100 (wt/wt), for at least 6 hours at 37°C. The sample was diluted to 2 M urea with 100 mM Tris-HCl, pH 8.5, and calcium chloride was added to 2 mM.Trypsin (Roche or Promega) was added to ca. 1:100 (wt/wt) and the reaction was let to proceed overnight at 37°C while shaking in an Eppendorf Thermomixer. For the subtilisin A digestion, urea was diluted to 4.8 M with 0.1 M Tris-HCl, pH 8.5, subtilisin A (Calbiochem) was added to ca. 1:50 (wt/wt) and left to incubate for 2 hours at 37°C. For the chymotrypsin digestion, urea was diluted to 2 M with 0.1 M Tris-HCl, pH 8.5, chymotrypsin (Roche) was added to ca. 1:100 (wt/wt) and left to incubate for 5 hours at 37°C. For the endoproteinase Asp-N digestion, urea was diluted to 2M with 0.1 M Tris-HCl, pH 7.5, Asp-N (Roche) was added to ca. 1:25 (wt/wt) and left to incubate for 5 hours at 37°C. All digestions were quenched by adding formic acid to 5%.

Peptide mixtures were loaded onto a 100µm fused silica microcapillary columnpacked with 8 cm of reverse phase material (Aqua, Phenomenex), follwed with 3 cm of 5-µm Strong Cation Exchange material (Partisphere SCX, Whatman), followed by 2cm of 5-µm C18 reverse phase. The loaded microcapillary columns were placed in-line with a Quaternary Agilent 1100 series HPLC pump. Overflow tubing was used to decrease the flow rate from 0.1 ml/min to about 200–300 nl/min.

Fully automated 7- or 10-step chromatography runs were carried out. Three different elution buffers were used: 5% acetonitrile, 0.1% formic acid (Buffer A); 80% acetonitrile, 0.1% formic acid (Buffer B); and 0.5 M ammonium acetate, 5% acetonitrile, 0.1% formic acid (Buffer C). Peptides were sequentially eluted from the SCX resin to the reverse phase resin by increasing salt steps, followed by an organic gradient.

The last two chromatography steps consist of a high salt wash with 100% Buffer C followed by the acetonitrile gradient. The application of a 2.5 kV distal voltage electrosprayed the eluting peptides directly into a ion trap mass spectrometers (either Deca-XP or LTQ) equipped with a nano-LC electrospray ionization source (ThermoFinnigan). Full MS spectra were recorded on the peptides over a 400 to 1,600m/z range, followed by five tandem mass (MS/MS) events sequentially generated in a data-dependent manner on the first to fifth most intense ions selected from the full MS spectrum (at 35% collision energy). Mass spectrometer scan functions and HPLC solvent gradients were controlled by the Xcalibur data system (ThermoFinnigan).

SEQUEST was used to match MS/MS spectra to peptides in a database of 12098 amino acid sequences, consisting of 5695 *S cerevisiae* proteins (NCBI on 2006-03-06 release), complemented with 177 usual contaminants such as human keratins, IgGs, and proteolytic enzymes. To estimate false discovery rates (FDR), each protein sequence was randomized (keeping the same amino acid composition and length) and the resulting 6049 "shuffled" sequences were added to the database

used for the SEQUEST searches. DTASelect was used to select and sort spectrum/peptide matches with cross-correlation scores (XCorr) and normalized difference in cross-correlation scores (DeltCn) above cut-off: matches were only retained if they had a DeltCn of at least 0.1, a maximum Sp rank of 10, and a minimum XCorr of 1.8 for singly-, 2.0 for doubly-, and 3.0 for triply-charged spectra. In addition, the peptides had to be at least 7 amino acids long and their ends had to conform to the enzymatic digestion used. Finally, combining all runs, proteins had to be detected by at least 2 such peptides, leading to an estimated false discovery rate of 1.5%. To estimate relative protein levels, spectral counts were normalized such as for each protein k detected in a particular MudPIT analysis.

Table 3. Mass spectrometry runs

Mass Spec ID	Bait	Cell Cycle	Culture	Elution	# Cse4 peptides	# Scm3 peptides
ScCse4-Myc_Meta_Ti_1_yeast-ncbi_2005-06-14	12Myc-Cse4	nocodozole	4L whole cell lysate	Myc peptide	3	1
ScCse4-Myc_G1_Ti_1_yeast-ncbi_2005-06-14	12Myc-Cse4	alpha factor	4L whole cell lysate	Myc peptide	0	0
ScMyc-Cse4_Sb_1_yeast-ncbi_2005-06-14	12Myc-Cse4	nocodozole	6L whole cell lysate	Myc peptide	3	0
ScHA-Cse4_Sb_1_yeast-ncbi_2005-06-14	Cse4-3HA	nocodozole	6L whole cell lysate	HA Peptide	0	0
ScMyc-Cse4_DN_1-Mp1Smn7y0ad.html	12Myc-Cse4	nocodozole	6L whole cell lysate	Myc peptide	3	2
Cse4_Myc-IP-Mp1Smn7y2asX	12Myc-Cse4	asynch	6L mnase treated nuclei	Myc peptide	8	0
ScSCM3-TAP_Ti_1_Scerevisiae_NCBI_2006-03-06	TAP-Scm3	nocodozole	4L whole cell lysate	EDTA	0	3
ScScm3-FLAG_Ti_1_Scerevisiae_NCBI_2006-03-06	Scm3-3FLAG	nocodozole	6L whole cell lysate	Flag Peptide	1	3
Scm3_Myc-IP-Mp1Smn7y2asX	Scm3-13Myc	asynch	6L mnase treated nuclei	Myc peptide	0	2

References

1. Hooke, R., *Observation XVIII.* Micrographia, 1865.
2. Goffeau, A., et al., *Life with 6000 Genes.* Science, 1996. **274**(5287): p. 546-567.
3. Human Genome Sequencing, C., *Finishing the euchromatic sequence of the human genome.* Nature, 2004. **431**(7011): p. 931-945.
4. Luger, K., et al., *Crystal structure of the nucleosome core particle at 2.8 A resolution.* Nature, 1997. **389**(6648): p. 251-60.
5. Allard, S., et al., *NuA4, an essential transcription adaptor/histone H4 acetyltransferase complex containing Esa1p and the ATM-related cofactor Tra1p.* Embo J, 1999. **18**(18): p. 5108-19.
6. Grant, P.A., et al., *Yeast Gcn5 functions in two multisubunit complexes to acetylate nucleosomal histones: characterization of an Ada complex and the SAGA (Spt/Ada) complex.* Genes Dev., 1997. **11**(13): p. 1640-1650.
7. Takeuchi, T., et al., *Roles of jumonji and jumonji family genes in chromatin regulation and development.* Dev Dyn, 2006. **235**(9): p. 2449-59.
8. Peckham, H.E., et al., *Nucleosome positioning signals in genomic DNA.* Genome Res, 2007. **17**(8): p. 1170-7.
9. Segal, E., et al., *A genomic code for nucleosome positioning.* Nature, 2006. **442**(7104): p. 772-8.

10. Lowary, P.T. and W. J, *Nucleosome packaging and nucleosome positioning of genomic DNA.* Proceedings of the National Academy of Sciences of the United States of America, 1997. **94**(4): p. 1183-1188.

11. Tagami, H., et al., *Histone H3.1 and H3.3 Complexes Mediate Nucleosome Assembly Pathways Dependent or Independent of DNA Synthesis.* Cell, 2004. **116**(1): p. 51-61.

12. Workman, J.L., *Nucleosome displacement in transcription.* Genes Dev., 2006. **20**(15): p. 2009-2017.

13. Wolffe, A.P., *Transcriptional Activation: Switched-on chromatin.* Current Biology, 1994. **4**(6): p. 525-528.

14. Flaus, A. and T. Owen-Hughes, *Mechanisms for ATP-dependent chromatin remodelling: farewell to the tuna-can octamer?* Current Opinion in Genetics & Development, 2004. **14**(2): p. 165-173.

15. Kireeva, M.L., et al., *Nucleosome Remodeling Induced by RNA Polymerase II: Loss of the H2A/H2B Dimer during Transcription.* Molecular Cell, 2002. **9**(3): p. 541-552.

16. Studitsky, V.M., et al., *Chromatin remodeling by RNA polymerases.* Trends in Biochemical Sciences, 2004. **29**(3): p. 127-135.

17. Lee, C.-K., et al., *Evidence for nucleosome depletion at active regulatory regions genome-wide.* Nat Genet, 2004. **36**(8): p. 900-905.

18. Adams, C.C. and J.L. Workman, *Nucleosome displacement in transcription.* Cell, 1993. **72**(3): p. 305-308.

19. David J. Steger, J.L.W., *Remodeling chromatin structures for transcription: What happens to the histones?* BioEssays, 1996. **18**(11): p. 875-884.

20. Workman, J.L. and R.E. Kingston, *Nucleosome core displacement in vitro via a metastable transcription factor-nucleosome complex.* Science, 1992. **258**(5089): p. 1780-4.

21. Bernstein, B.E., et al., *Global nucleosome occupancy in yeast.* Genome Biol, 2004. **5**(9): p. R62.

22. Schwabish, M.A. and K. Struhl, *Evidence for Eviction and Rapid Deposition of Histones upon Transcriptional Elongation by RNA Polymerase II.* Mol. Cell. Biol., 2004. **24**(23): p. 10111-10117.

23. Wirbelauer, C., O. Bell, and D. Schubeler, *Variant histone H3.3 is deposited at sites of nucleosomal displacement throughout transcribed genes while active histone modifications show a promoter-proximal bias.* Genes Dev., 2005. **19**(15): p. 1761-1766.

24. Belotserkovskaya, R. and D. Reinberg, *Facts about FACT and transcript elongation through chromatin.* Current Opinion in Genetics & Development, 2004. **14**(2): p. 139-146.

25. Shibahara, K.-i. and B. Stillman, *Replication-Dependent Marking of DNA by PCNA Facilitates CAF-1-Coupled Inheritance of Chromatin.* Cell, 1999. **96**(4): p. 575-585.

26. Gaillard, P.H., et al., *Chromatin assembly coupled to DNA repair: a new role for chromatin assembly factor I.* Cell, 1996. **86**(6): p. 887-96.

27. Green, E.M., et al., *Replication-independent histone deposition by the HIR complex and Asf1.* Curr Biol, 2005. **15**(22): p. 2044-9.

28. Loppin, B., et al., *The histone H3.3 chaperone HIRA is essential for chromatin assembly in the male pronucleus.* Nature, 2005. **437**(7063): p. 1386-1390.

29. Luger, K. and J.C. Hansen, *Nucleosome and chromatin fiber dynamics.* Curr Opin Struct Biol, 2005. **15**(2): p. 188-96.

30. Zlatanova, J., C. Seebart, and M. Tomschik, *Nap1: taking a closer look at a juggler protein of extraordinary skills.* FASEB J., 2007. **21**(7): p. 1294-1310.

31. Reinberg, D. and R.J. Sims, III, *de FACTo Nucleosome Dynamics.* J. Biol. Chem., 2006. **281**(33): p. 23297-23301.

32. Belotserkovskaya, R., et al., *FACT Facilitates Transcription-Dependent Nucleosome Alteration.* Science, 2003. **301**(5636): p. 1090-1093.

33. Kamakaka, R.T. and S. Biggins, *Histone variants: deviants?* Genes Dev., 2005. **19**(3): p. 295-316.

34. Buttinelli, M., et al., *The role of histone H1 in chromatin condensation and transcriptional repression.* Genetica, 1999. **106**(1): p. 117-124.

35. Meneghini, M.D., M. Wu, and H.D. Madhani, *Conserved Histone Variant H2A.Z Protects Euchromatin from the Ectopic Spread of Silent Heterochromatin.* Cell, 2003. **112**(5): p. 725-736.

36. Chadwick, B.P. and H.F. Willard, *A Novel Chromatin Protein, Distantly Related to Histone H2A, Is Largely Excluded from the Inactive X Chromosome.* J. Cell Biol., 2001. **152**(2): p. 375-384.

37. Stoler, S., et al., *A mutation in CSE4, an essential gene encoding a novel chromatin- associated protein in yeast, causes chromosome nondisjunction and cell cycle arrest at mitosis.* Genes Dev., 1995. **9**(5): p. 573-586.

38. Poccia, D.L. and G.R. Green, *Packaging and unpackaging the sea urchin sperm genome.* Trends in Biochemical Sciences, 1992. **17**(6): p. 223-227.

39. Black, B.E. and E.A. Bassett, *The histone variant CENP-A and centromere specification.* Current Opinion in Cell Biology, 2008. **20**(1): p. 91-100.

40. Chen, Y., et al., *The N terminus of the centromere H3-like protein Cse4p performs an essential function distinct from that of the histone fold domain.* Mol Cell Biol, 2000. **20**: p. 7037-48.

41. Wieland, G., et al., *Functional Complementation of Human Centromere Protein A (CENP-A) by Cse4p from Saccharomyces cerevisiae.* Mol. Cell. Biol., 2004. **24**(15): p. 6620-6630.

42. Pearson, C.G., et al., *Stable kinetochore-microtubule attachment constrains centromere positioning in metaphase.* Curr Biol, 2004. **14**(21): p. 1962-7.

43. Shelby, R.D., O. Vafa, and K.F. Sullivan, *Assembly of CENP-A into centromeric chromatin requires a cooperative array of nucleosomal DNA contact sites.* J Cell Biol, 1997. **136**(3): p. 501-13.

44. Jansen, L.E., et al., *Propagation of centromeric chromatin requires exit from mitosis.* J Cell Biol, 2007. **176**(6): p. 795-805.

45. Fujita, Y., et al., *Priming of centromere for CENP-A recruitment by human hMis18alpha, hMis18beta, and M18BP1.* Dev Cell, 2007. **12**(1): p. 17-30.

46. Hayashi, T., et al., *Mis16 and Mis18 are required for CENP-A loading and histone deacetylation at centromeres.* Cell, 2004. **118**(6): p. 715-29.

47. Takahashi, K., E.S. Chen, and M. Yanagida, *Requirement of Mis6 Centromere Connector for Localizing a CENP-A-Like Protein in Fission Yeast.* Science, 2000. **288**(5474): p. 2215-2219.

48. Takahashi, K., et al., *Two distinct pathways responsible for the loading of CENP-A to centromeres in the fission yeast cell cycle.* Philos Trans R Soc Lond B Biol Sci, 2005. **360**(1455): p. 595-606; discussion 606-7.

49. Chi, Y.H. and K.T. Jeang, *Aneuploidy and cancer.* J Cell Biochem, 2007. **102**(3): p. 531-8.

50. Petersen, M.B. and M. Mikkelsen, *Nondisjunction in trisomy 21: origin and mechanisms.* Cytogenet Cell Genet, 2000. **91**(1-4): p. 199-203.

51. Alberts, B., Lewis, J., Raff, M., Walter, P. , *Molecular Biology of the Cell*. 4th ed. 2002: Garland Science.

52. Fitzgerald-Hayes, M., L. Clarke, and J. Carbon, *Nucleotide sequence comparisons and functional analysis of yeast centromere DNAs.* Cell, 1982. **29**(1): p. 235-244.

53. McGrew, J., B. Diehl, and M. Fitzgerald-Hayes, *Single base-pair mutations in centromere element III cause aberrant chromosome segregation in Saccharomyces cerevisiae.* Mol Cell Biol, 1986. **6**(2): p. 530-8.

54. Cumberledge, S. and J. Carbon, *Mutational analysis of meiotic and mitotic centromere function in Saccharomyces cerevisiae.* Genetics, 1987. **117**(2): p. 203-12.

55. Gaudet, A. and M. Fitzgerald-Hayes, *Alterations in the adenine-plus-thymine-rich region of CEN3 affect centromere function in Saccharomyces cerevisiae.* Mol Cell Biol, 1987. **7**(1): p. 68-75.

56. Wood, V., et al., *The genome sequence of Schizosaccharomyces pombe.* Nature, 2002. **415**(6874): p. 871-80.

57. Clarke, L., et al., *Structure and function of Schizosaccharomyces pombe centromeres.* Cold Spring Harb Symp Quant Biol, 1993. **58**: p. 687-95.

58. Baum, M., V.K. Ngan, and L. Clarke, *The centromeric K-type repeat and the central core are together sufficient to establish a functional Schizosaccharomyces pombe centromere.* Mol Biol Cell, 1994. **5**(7): p. 747-61.

59. Malik, H.S. and S. Henikoff, *Conflict begets complexity: the evolution of centromeres.* Curr Opin Genet Dev, 2002. **12**(6): p. 711-8.

60. Sun, X., et al., *Sequence analysis of a functional Drosophila centromere.* Genome Res, 2003. **13**(2): p. 182-94.

61. Schueler, M.G., et al., *Genomic and genetic definition of a functional human centromere.* Science, 2001. **294**(5540): p. 109-15.

62. Cheeseman, I.M., D.G. Drubin, and G. Barnes, *Simple centromere, complex kinetochore: linking spindle microtubules and centromeric DNA in budding yeast.* J. Cell Biol., 2002. **157**(2): p. 199-203.

63. Rodrigo-Brenni, M.C., et al., *Sgt1p and Skp1p Modulate the Assembly and Turnover of CBF3 Complexes Required for Proper Kinetochore Function.* Mol. Biol. Cell, 2004. **15**(7): p. 3366-3378.

64. Meluh, P.B. and D. Koshland, *Budding yeast centromere composition and assembly as revealed by in vivo cross-linking.* Genes Dev., 1997. **11**(24): p. 3401-3412.

65. Espelin, C.W., et al., *Binding of the Essential Saccharomyces cerevisiae Kinetochore Protein Ndc10p to CDEII.* Mol. Biol. Cell, 2003. **14**(11): p. 4557-4568.

66. Euskirchen, G.M., *Nnf1p, Dsn1p, Mtw1p, and Nsl1p: a new group of proteins important for chromosome segregation in Saccharomyces cerevisiae.* Eukaryot Cell, 2002. **1**: p. 229-40.

67. De Wulf, P., A.D. McAinsh, and P.K. Sorger, *Hierarchical assembly of the budding yeast kinetochore from multiple subcomplexes.* Genes Dev., 2003. **17**(23): p. 2902-2921.

68. Kapoor, T.M., *Chromosome Segregation: Correcting Improper Attachment.* Current Biology, 2004. **14**(23): p. R1011-R1013.

69. McAinsh, A.D., J.D. Tytell, and P.K. Sorger, *Structure, Function, and Regulation of budding Yeast Kinetochores.* Annual Review of Cell and Developmental Biology, 2003. **19**(1): p. 519-539.

70. Biggins, S. and A.W. Murray, *The budding yeast protein kinase Ipl1/Aurora allows the absence of tension to activate the spindle checkpoint.* Genes Dev., 2001. **15**(23): p. 3118-3129.

71. Goshima, G. and M. Yanagida, *Establishing Biorientation Occurs with Precocious Separation of the Sister Kinetochores, but Not the Arms, in the Early Spindle of Budding Yeast.* Cell, 2000. **100**(6): p. 619-633.

72. Amon, A., *The spindle checkpoint.* Current Opinion in Genetics & Development, 1999. **9**(1): p. 69-75.

73. Bhalla, N., S. Biggins, and A.W. Murray, *Mutation of YCS4, a budding yeast condensin subunit, affects mitotic and nonmitotic chromosome behavior.* Mol Biol Cell, 2002. **13**: p. 632-45.

74. Walfridsson, J., et al., *The CHD remodeling factor Hrp1 stimulates CENP-A loading to centromeres.* Nucleic Acids Res, 2005. **33**: p. 2868-79.

75. Hayashi, T., et al., *Mis16 and Mis18 Are Required for CENP-A Loading and Histone Deacetylation at Centromeres.* Cell, 2004. **118**(6): p. 715-729.

76. Meraldi, P., et al., *Phylogenetic and structural analysis of centromeric DNA and kinetochore proteins.* Genome Biol, 2006. **7**: p. R23.

77. Meluh, P.B., et al., *Cse4p Is a Component of the Core Centromere of Saccharomyces cerevisiae.* Cell, 1998. **94**(5): p. 607-613.

78. Brown, M., L. Goetsch, and L. Hartwell, *MIF2 is required for mitotic spindle integrity during anaphase spindle elongation in Saccharomyces cerevisiae.* J. Cell Biol., 1993. **123**(2): p. 387-403.

79. Goh, P. and J. Kilmartin, *NDC10: a gene involved in chromosome segregation in Saccharomyces cerevisiae.* J. Cell Biol., 1993. **121**(3): p. 503-512.

80. Westermann, S., et al., *Architecture of the budding yeast kinetochore reveals a conserved molecular core.* J. Cell Biol., 2003. **163**(2): p. 215-222.

81. Scharfenberger, M., et al., *Nsl1p is essential for the establishment of bipolarity and the localization of the Dam-Duo complex.* Embo J, 2003. **22**: p. 6584-97.

82. Li, Y., et al., *The mitotic spindle is required for loading of the DASH complex onto the kinetochore.* Genes Dev., 2002. **16**(2): p. 183-197.

83. Hofmann, C., et al., *Saccharomyces cerevisiae Duo1p and Dam1p, Novel Proteins Involved in Mitotic Spindle Function.* J. Cell Biol., 1998. **143**(4): p. 1029-1040.

84. Janke, C., et al., *Four new subunits of the Dam1-Duo1 complex reveal novel functions in sister kinetochore biorientation.* Embo J, 2002. **21**: p. 181-93.

85. Kang, J.-s., et al., *Functional cooperation of Dam1, Ipl1, and the inner centromere protein (INCENP)-related protein Sli15 during chromosome segregation.* J. Cell Biol., 2001. **155**(5): p. 763-774.

86. Hoyt, M.A., *A new view of the spindle checkpoint.* J. Cell Biol., 2001. **154**(5): p. 909-912.

87. Ortiz, J., et al., *A putative protein complex consisting of Ctf19, Mcm21, and Okp1 represents a missing link in the budding yeast kinetochore.* Genes Dev., 1999. **13**(9): p. 1140-1155.

88. Kaplan, K.B., A.A. Hyman, and P.K. Sorger, *Regulating the Yeast Kinetochore by Ubiquitin-Dependent Degradation and Skp1p-Mediated Phosphorylation.* Cell, 1997. **91**(4): p. 491-500.

89. Janke, C., et al., *The budding yeast proteins Spc24p and Spc25p interact with Ndc80p and Nuf2p at the kinetochore and are important for kinetochore clustering and checkpoint control.* Embo J, 2001. **20**: p. 777-91.

90. Espelin, C.W., K.B. Kaplan, and P.K. Sorger, *Probing the architecture of a simple kinetochore using DNA-protein crosslinking.* J Cell Biol, 1997. **139**: p. 1383-96.

91. Giaever, G., et al., *Functional profiling of the Saccharomyces cerevisiae genome.* 2002. **418**(6896): p. 387-391.

92. Hajra, S., S.K. Ghosh, and M. Jayaram, *The centromere-specific histone variant Cse4p (CENP-A) is essential for functional chromatin architecture at the yeast 2-{micro}m circle partitioning locus and promotes equal plasmid segregation.* J. Cell Biol., 2006. **174**(6): p. 779-790.

93. Measday, V., et al., *Ctf3p, the Mis6 budding yeast homolog, interacts with Mcm22p and Mcm16p at the yeast outer kinetochore.* Genes Dev., 2002. **16**(1): p. 101-113.

94. Poddar, A., et al., *Differential kinetochore requirements for establishment and maintenance of the spindle checkpoint are dependent on the mechanism of checkpoint activation in Saccharomyces cerevisiae.* Cell Cycle, 2004. **3**: p. 197-204.

95. Fraschini, et al., *Role of the kinetochore protein Ndc10 in mitotic checkpoint activation in Saccharomyces cerevisiae.* Molecular Genetics and Genomics, 2001. **266**(1): p. 115-125.

96. Feng, W., et al., *Genomic mapping of single-stranded DNA in hydroxyurea-challenged yeasts identifies origins of replication.* Nat Cell Biol, 2006. **8**: p. 148-55.

97. Pinsky, B.A., et al., *An Mtw1 Complex Promotes Kinetochore Biorientation that Is Monitored by the Ipl1/Aurora Protein Kinase.* Developmental Cell, 2003. **5**(5): p. 735-745.

98. Biggins, S., et al., *Genes involved in sister chromatid separation and segregation in the budding yeast Saccharomyces cerevisiae.* Genetics, 2001. **159**: p. 453-70.

99. Biggins, S., et al., *The conserved protein kinase Ipl1 regulates microtubule binding to kinetochores in budding yeast.* Genes Dev, 1999. **13**: p. 532-44.

100. Eckert, C.A., D.J. Gravdahl, and P.C. Megee, *The enhancement of pericentromeric cohesin association by conserved kinetochore components promotes high-fidelity chromosome segregation and is sensitive to microtubule-based tension.* Genes Dev, 2007. **21**(3): p. 278-91.

101. Weber, S.A., et al., *The kinetochore is an enhancer of pericentric cohesin binding.* PLoS Biol, 2004. **2**: p. E260.

102. Zhang, K., et al., *The Set1 methyltransferase opposes Ipl1 aurora kinase functions in chromosome segregation.* Cell, 2005. **122**(5): p. 723-34.

103. Morey, L., et al., *The Histone Fold Domain of Cse4 Is Sufficient for CEN Targeting and Propagation of Active Centromeres in Budding Yeast.* Eukaryotic Cell, 2004. **3**(6): p. 1533-1543.

104. Tanaka, T.U., M.J.R. Stark, and K. Tanaka, *Kinetochore capture and bi-orientation on the mitotic spindle.* 2005. **6**(12): p. 929-942.

105. Bouck, D.C. and K.S. Bloom, *The kinetochore protein Ndc10p is required for spindle stability and cytokinesis in yeast.* PNAS, 2005. **102**(15): p. 5408-5413.

106. Waye, J.S. and H.F. Willard, *Structure, organization, and sequence of alpha satellite DNA from human chromosome 17: evidence for evolution by unequal crossing-over and an ancestral pentamer repeat shared with the human X chromosome.* Mol Cell Biol, 1986. **6**: p. 3156-65.

107. Cleveland, D.W., Y. Mao, and K.F. Sullivan, *Centromeres and kinetochores: from epigenetics to mitotic checkpoint signaling.* Cell, 2003. **112**: p. 407-21.

108. Hegemann, J.H. and U.N. Fleig, *The centromere of budding yeast.* Bioessays, 1993. **15**: p. 451-60.

109. Henikoff, S. and Y. Dalal, *Centromeric chromatin: what makes it unique?* Current Opinion in Genetics & Development

Chromosomes and expression mechanisms, 2005. **15**(2): p. 177-184.

110. Furuyama, S. and S. Biggins, *Centromere identity is specified by a single centromeric nucleosome in budding yeast.* Proc Natl Acad Sci U S A, 2007. **104**(37): p. 14706-11.

111. Vafa, O. and K.F. Sullivan, *Chromatin containing CENP-A and [alpha]-satellite DNA is a major component of the inner kinetochore plate.* Current Biology, 1997. **7**(11): p. 897-900.

112. Furuyama, T., Y. Dalal, and S. Henikoff, *Chaperone-mediated assembly of centromeric chromatin in vitro.* Proc Natl Acad Sci U S A, 2006. **103**(16): p. 6172-7.

113. Yoda, K., et al., *Human centromere protein A (CENP-A) can replace histone H3 in nucleosome reconstitution in vitro.* Proc Natl Acad Sci U S A, 2000. **97**(13): p. 7266-71.

114. Dalal, Y., et al., *Structure, dynamics, and evolution of centromeric nucleosomes.* Proceedings of the National Academy of Sciences, 2007. **104**(41): p. 15974-15981.

115. Dalal, Y., et al., *Tetrameric Structure of Centromeric Nucleosomes in Interphase Drosophila Cells.* PLoS Biology, 2007. **5**(8): p. e218.

116. Camahort, R., et al., *Scm3 Is Essential to Recruit the Histone H3 Variant Cse4 to Centromeres and to Maintain a Functional Kinetochore.* Molecular Cell, 2007. **26**(6): p. 853-865.

117. Mizuguchi, G., et al., *Nonhistone Scm3 and histones CenH3-H4 assemble the core of centromere-specific nucleosomes.* Cell, 2007. **129**(6): p. 1153-64.

118. Stoler, S., et al., *Scm3, an essential Saccharomyces cerevisiae centromere protein required for G2/M progression and Cse4 localization.* Proc Natl Acad Sci U S A, 2007. **104**(25): p. 10571-6.

119. Meluh, P.B., et al., *Cse4p is a component of the core centromere of Saccharomyces cerevisiae.* Cell, 1998. **94**: p. 607-13.

120. Collins, K.A., S. Furuyama, and S. Biggins, *Proteolysis contributes to the exclusive centromere localization of the yeast Cse4/CENP-A histone H3 variant.* Curr Biol, 2004. **14**: p. 1968-72.

121. Pearson, C.G., et al., *Stable kinetochore-microtubule attachment constrains centromere positioning in metaphase.* Curr Biol, 2004. **14**: p. 1962-7.

122. Collins, K.A., S. Furuyama, and S. Biggins, *Proteolysis Contributes to the Exclusive Centromere Localization of the Yeast Cse4/CENP-A Histone H3 Variant.* Current Biology, 2004. **14**(21): p. 1968-1972.

123. Ahmad, K. and S. Henikoff, *Histone H3 variants specify modes of chromatin assembly.* Proc Natl Acad Sci U S A, 2002. **99 Suppl 4**: p. 16477-84.

124. Van Hooser, A.A., et al., *Specification of kinetochore-forming chromatin by the histone H3 variant CENP-A.* J Cell Sci, 2001. **114**(19): p. 3529-3542.

125. Glynn, E.F., et al., *Genome-wide mapping of the cohesin complex in the yeast Saccharomyces cerevisiae.* PLoS Biol, 2004. **2**: p. E259.

126. Cohen, R.L., et al., *Structural and Functional Dissection of Mif2p, a Conserved DNA-binding Kinetochore Protein.* Mol Biol Cell, 2008.

127. Espelin, C.W., K.B. Kaplan, and P.K. Sorger, *Probing the Architecture of a Simple Kinetochore Using DNA-Protein Crosslinking.* J. Cell Biol., 1997. **139**(6): p. 1383-1396.

128. Almer, A., et al., *Removal of positioned nucleosomes from the yeast PHO5 promoter upon PHO5 induction releases additional upstream activating DNA elements.* Embo J, 1986. **5**(10): p. 2689-96.

129. Anderson, J.D. and J. Widom, *Sequence and position-dependence of the equilibrium accessibility of nucleosomal DNA target sites.* Journal of Molecular Biology, 2000. **296**(4): p. 979-987.

130. Li, B., et al., *Preferential occupancy of histone variant H2AZ at inactive promoters influences local histone modifications and chromatin remodeling.* Proc Natl Acad Sci U S A, 2005. **102**(51): p. 18385-90.

131. Bloom, K., S. Sharma, and N.V. Dokholyan, *The path of DNA in the kinetochore.* Current Biology, 2006. **16**(8): p. R276-R278.

132. Geisberg, J.V. and K. Struhl, *Quantitative sequential chromatin immunoprecipitation, a method for analyzing co-occupancy of proteins at genomic regions in vivo.* Nucleic Acids Res, 2004. **32**(19): p. e151.

133. Pinto, I. and F. Winston, *Histone H2A is required for normal centromere function in Saccharomyces cerevisiae.* Embo J, 2000. **19**(7): p. 1598-612.

134. Keith, K.C., et al., *Analysis of Primary Structural Determinants That Distinguish the Centromere-Specific Function of Histone Variant Cse4p from Histone H3.* Mol. Cell. Biol., 1999. **19**(9): p. 6130-6139.

135. Sambrook, J. and D.W. Russell, *Molecular cloning : a laboratory manual*. 3rd ed. 2001, Cold Spring Harbor, N.Y.: Cold Spring Harbor Laboratory Press.

136. Luger, K., et al., *Crystal structure of the nucleosome core particle at 2.8 A resolution.* Nature, 1997. **389**: p. 251-60.

137. Li, B., et al., *Preferential occupancy of histone variant H2AZ at inactive promoters influences local histone modifications and chromatin remodeling.* Proc Natl Acad Sci U S A, 2005. **102**: p. 18385-90.

138. Longtine, M.S., et al., *Additional modules for versatile and economical PCR-based gene deletion and modification in Saccharomyces cerevisiae.* Yeast, 1998. **14**: p. 953-61.

139. Tong, A.H., et al., *Systematic genetic analysis with ordered arrays of yeast deletion mutants.* Science, 2001. **294**(5550): p. 2364-8.

140. Pan, X., et al., *A robust toolkit for functional profiling of the yeast genome.* Mol Cell, 2004. **16**(3): p. 487-96.

141. Zhang, H., D.N. Roberts, and B.R. Cairns, *Genome-wide dynamics of Htz1, a histone H2A variant that poises repressed/basal promoters for activation through histone loss.* Cell, 2005. **123**(2): p. 219-31.

142. Nakanishi, S., et al., *A comprehensive library of histone mutants identifies nucleosomal residues required for H3K4 methylation.* Nat Struct Mol Biol, 2008. **15**(8): p. 881-888.

Appendix 1- Yeast Strains

SBY617	MATa ura3-1 leu2,3-112 his3-1 trp1-1 ade2-1 can1-100 Δbar1 CSE4-12myc::URA3
SBY1071	MATa *ura3-1 leu2,3-112 his3-1 trp1-1 ade2-1 can1-100 Δbar1* $pGAL_{1-10}$-CSE4-12myc::URA3
SBY2562	MATa *ura3-1 leu2,3-112 his3-1 trp1-1 ade2-1 can1-100 Δbar1* $pGAL_{1-10}$-*cse4-351*::URA3
MM5	MATa *ura3-1 leu2,3-112 his3-1 trp1-1 ade2-1 can1-100 Δbar1* PDS1-18myc::LEU2 *ipl1-321* $pGAL_{1-10}$-3HA-SCM3::KAN his3::CUP1-GFP-LacI:HIS3 cenIV::256lacOR::TRP1
JMH311	MATa *ura3-1 leu2,3-112 his3-1 trp1-1 ade2-1 can1-100 Δbar1* $pGAL_{1-10}$-3HA-SCM3::KAN MCD1-18Myc::TRP1
JG595	MATa *ura3-1 leu2,3-112 his3-1 trp1-1 ade2-1 can1-100 Δbar1* CSE4-12Myc::URA3 SCM3-3Flag::KAN
RC82	MATa *ura3-1 leu2,3-112 his3-1 trp1-1 ade2-1 can1-100 Δbar1* CSE4-12myc::URA3 SCM3-3HA::KAN
RC96	MATa *ura3-1 leu2,3-112 his3-1 trp1-1 ade2-1 can1-100 Δbar1* NDC10-13myc::KAN
RC100	MATa *ura3-1 leu2,3-112 his3-1 trp1-1 ade2-1 can1-100 Δbar1* CSE4-13myc::URA3 $pGAL_{1-10}$-3HA-SCM3::KAN
RC101	MATa *ura3-1 leu2,3-112 his3-1 trp1-1 ade2-1 can1-100 Δbar1*
RC111	MATa *ura3-1 leu2,3-112 his3-1 trp1-1 ade2-1 can1-100 Δbar1* CSE4-13myc::URA3 $pGAL_{1-10}$-3HA-SCM3::KAN Δ*mad1*::HIS3
RC111	MATa *ura3-1 leu2,3-112 his3-1 trp1-1 ade2-1 can1-100 Δbar1* CSE4-13myc::URA3 $pGAL_{1-10}$-3HA-SCM3::KAN Δ*mad1*::HIS3
RC117	MATa *ura3-1 leu2,3-112 his3-1 trp1-1 ade2-1 can1-100 Δbar1* $pGAL_{1-10}$-3HA-SCM3::KAN MIF2-13myc::HYG
RC123	MATa *ura3-1 leu2,3-112 his3-1 trp1-1 ade2-1 can1-100 Δbar1 ndc10-1*::LYS SCM3-3HA::KAN
RC128	MATa *ura3-1 leu2,3-112 his3-1 trp1-1 ade2-1 can1-100 Δbar1* $pGAL_{1-10}$-3HA-SCM3::TRP1 NDC10-13myc::KAN
RC130	MATα *ura3-1 leu2,3-112 his3-1 trp1-1 ade2-1 can1-100 Δbar1* $pGAL_{1-10}$-3HA-SCM3::KAN TUB1-GFP::TRP1
RC145	MATa *ura3-1 leu2,3-112 his3-1 trp1-1 ade2-1 can1-100 Δbar1* CSE4-3HA::KAN GAL1-UAS-YOL118c::URA3 pESC::HIS3
RC146	MATa *ura3-1 leu2,3-112 his3-1 trp1-1 ade2-1 can1-100 Δbar1* CSE4-3HA::KAN GAL1-UAS-YOL118c::URA3 pESC-Gal4BD-Myc-Scm3-Myc::HIS3
RC147	*ura3-1 leu2,3-112 his3-1 trp1-1 ade2-1 can1-100 Δbar1cse4-1* SCM3-3Flag::KAN NDC10-13Myc::TRP1
RC149	MATa *ura3-1 leu2,3-112 his3-1 trp1-1 ade2-1 can1-100 Δbar1* $pGAL_{1-10}$-3HA-SCM3::KAN MCD1-18Myc::TRP1 *cdc16-1*
RC151	MATa *ura3-1 leu2,3-112 his3-1 trp1-1 ade2-1 can1-100 Δbar1* DAM1-9Myc::TRP1 NDC10-HA::URA3
RC152	MATa *ura3-1 leu2,3-112 his3-1 trp1-1 ade2-1 can1-100 Δbar1* DAM1-9Myc::TRP1 NDC10-HA::URA3 pESC-Gal4BD-Myc-Scm3-Myc::HIS3
RC156	MATa *ura3-1 leu2,3-112 his3-1 trp1-1 ade2-1 can1-100 Δbar1* $pGAL_{1-10}$-3HA-SCM3::KAN Dam1-GFP::URA3
RC175	MATa/α *ura3-1 leu2,3-112 his3-1 trp1-1 ade2-1 can1-100 Δbar1* SCM3::SCM3 *scm3Δ*::TRP1

Appendix 1 (cont). Yeast Strains

RC176	MATa/α *ura3-1 leu2,3-112 his3-1 trp1-1 ade2-1 can1-100 Δbar1* CSE4::CSE4 cse4Δ::KAN
RC177	MATa *ura3-1 lys2Δ::hisG trp1-1 his3-11,15 leu2-3,112 can1-100* HTA1-Flag:LoxP/HTA2-3FLAG:KAN
RC188	MATa *ura3-1 leu2,3-112 his3-1 trp1-1 ade2-1 can1-100 Δbar1* $pGAL_{1-10}$-3HA-SCM3::TRP1 CSE4-12Myc::URA3 HTA1-Flag:LoxP/HTA2-3FLAG:KAN
RC192	MATa *ura3-1 leu2,3-112 his3-1 trp1-1 ade2-1 can1-100 Δbar1 scm3Δ*::TRP1 pHIP(pBY011)-Myc-Cse4::URA3 HTA1-Flag:LoxP/HTA2-3FLAG:KAN
RC193	MATa *ura3-1 leu2,3-112 his3-1 trp1-1 ade2-1 can1-100 Δbar1* $pGAL_{1-10}$-3HA-SCM3::TRP1 pRS316::URA3 pRS425-prCUP1-CSE4::LEU2
RC194	MATa *ura3-1 leu2,3-112 his3-1 trp1-1 ade2-1 can1-100 Δbar1* $pGAL_{1-10}$-3HA-SCM3::TRP1 pRS316-SCM3::URA3 pRS425-prCUP1-CSE4::LEU2
RC197	MATa *ura3-1 leu2,3-112 his3-1 trp1-1 ade2-1 can1-100 Δbar1 cse4Δ*::KAN pRS413-Cse4::HIS3
RC201	MATa *ura3-1 lys2Δ::hisG trp1-1 his3-11,15 leu2-3,112 can1-100* $pGAL_{1-10}$-3HA-SCM3::TRP1 HTA1-Flag:LoxP/HTA2-3FLAG:KAN pHIP(pBY011)-Myc-Cse4::URA3
RC203	MATa/α *ura3Δ0 leu2Δ0 his3Δ1 lys2Δ0/LYS met15Δ0/MET15 can1Δ::LEU2-MFA1pr-HIS3/CAN1 cse4Δ::kanMX/*CSE4 (Magic Marker-BY4743)
RC204	MATa/α *ura3Δ0 leu2Δ0 his3Δ1 lys2Δ0/LYS met15Δ0/MET15 can1Δ::LEU2-MFA1pr-HIS3/CAN1 scm3Δ::kanMX/*SCM3 (Magic Marker-BY4743)

Appendix 2. Primers

CEN1 high resolution			
Forward Primers	sequence	Reverse Primers	sequence
cen1L2F	GTACGTTTATCACCTAAACGGAGC	cen1L2R	CGATTTATCCTGACGAACTC
cen1L1.5F	GAAGCAATTTTATCAGACAC	cen1L1.5R	CTTGCCATAAGAGAGAAGAG
cen1L1F	CTTGTGGCTAGTTGGCTTCAACC	cen1L1R	CATCATAAAGGGCGGCGCTT
cen1L0.5F	GTTATATGTGTGACTGGTTGTT	cen1L0.5R	GCAAATCTGCATTTTCAAAT
cen1L0.4F	GCCGCCCTTTATGATGCAAA	cen1L0.4R	CGAGTTATTGAAGCTGGTAA
cen1L0.3F	CAGATTTGCAGAAATAAAAG	cen1L0.3R	TTCAATGTCAAAGTCAATAT
cen1L0.2F	AGCTTCAATAACTCGATTTGCATA	cen1L0.2R	TGTCATGTGACAAGACTTAAATCA
CDEI-II-IIIcen1F	TGACATTGAACTTCAAAACCTTT	CDEI-II-IIIcen1R	GGCGCTTGAAATGAAAGCTC
cen1R0.2F	GAAGCAGTCAAAGTATTTTA	cen1R0.2R	ATAATAATTTATCTTGATCG
cen1R0.3F	TTACACATAATACGATCAAGAT	cen1R0.3R	ATACATGGACTGACTCAAGATT
cen1R0.4F	CGGTGGACCTTATTAGCTCAATCT	cen1R0.4R	CAGTAACAGTACTTCAATGGAA
cen1R0.5F	AGCACTTTCTTTAATAAATATTCC	cen1R0.5R	TAAACAATGATTGATTTCTGGC
cen1R1F	AGAATGTAGAAATGGCGCCAGA	cen1R1R	GCAATCACTCGAATAACTATCT
cen1R1.5F	TTCAGCAGGTAAATTAAGAT	cen1R1.5R	GAACAATTAACGACACCTTC

Appendix 2 (cont). Primers

cen1R2F	ATTAATTTTTTCATAATGAAG	cen1R2R	AAAGTATACATTTAGCTTTT
CEN3 high resolution			
Forward Primers	sequence	Reverse Primers	sequence
cen3.640	AAATATACCATCCAATACCTT	cen3.640	TGACAAGTGTTAGATAAAAAG
cen3.680	TCAACATTAACTTCGAATT	cen3.680	AATAGAAGTGGTAGCAATA
cen3.720	ATCTAACACTTGTCAAACA	cen3.720	AGCTATTGAAACTATTGTG
cen3.760	TTGTCTTCTTTGCTACATAT	cen3.760	TGAGTGATTTAGATAAATTT
cen3.800	TCAATAGCTTGCAGCGTAGC	cen3.800	TATAAGCGGAAGGGGAAGG
cen3.840	AAATTTATCTAAATCACTCA	cen3.840	CATGTTTATGAAATGTATAG
RC 1/2	CATAAACATGGCATGGCG	RC 1/2	TCAAATATCATCATGTGA
cen3 CDE I-II-III	AAATAGTACAAATAAGTCACAT	cen3 CDE I-II-III	CCATTCAATGAAATATATATTTC
cen3.1080	GAAATAGTAAGAAATATATATT	cen3.1080	AATAATAATATATGAGCA
cen3.1120	ATGAAACGTTTACTGGTGGAAG	cen3.1120	AGTTGCTTTACCAACTTTTTCTTT
cen3.1160	GGAAGTTTTGCTCATATA	cen3.1160	TAGCTTAGATGTTCAAAA
cen3.1200	AGCAACTTAACAGTAAAA	cen3.1200	ATAGGCATGAGTACTAAT
cen3.1240	TTGATGGGTTTACAATTTTACCA	cen3.1240	TGATTGCTCTAAATCGCGG
cen3.1320	TGTCCGCGATTTAGAGCA	cen3.1320	AATGGGGCGGAAATTC

Appendix 2 (cont). Primers

cen3.1360	CATTTTAGCCAGAGAGGACTCG	cen3.1360	TGTTATTTGGGGTATATGAATGGG
Low Res CEN3			
Forward Primers	sequence	Reverse Primers	sequence
PM70	AGTGTCTTCGCATAAAATCCAG	PM71	CATCTATTTACTGCTATTAAGCG
PM72	CATACCATGCTTTGTTATCGTC	PM73	ATTTTATGCGAAGACACTGCTG
PM74	CATCTTTGAAAAGTTCATCAAGG	PM75	CGATAACAAAGCATGGTATGGC
PM76	ATATTGTTTGGCGCTGATCGC	PM77	CTTGATGAACTTTTCAAAGATGAC
PM22	GATCAGCGCCAAACAATATGG	PM48	AACTTCCACCAGTAAACGTTTC
PM78	GTCAACGAGTCCTCTCTGGC	PM79	TTTACTGGTGGAAGTTTTGCTC
PM80	GAATATGATAATGGTTACACCAG	PM81	GAGAGGACTCGTTGACGTAG
PM82	GATTTAATGCACGTTATGTTTCG	PM83	TGTAACCATTATCATATTCATGAC
PM84	GTAAGAGGTAGGTTTTGCAGG	PM85	ATAACGTGCATTAAATCTCACTG
EMP46F	ATAAGTTGGGAGAGAGCGTGA	EMP46R	AAACGATTCTTTGGATGCATC
GAL2	CGAACTCAGTTCAATGGAGAGT	GAL2	TACCGGCCATGATCAGATCT
FMP32F	AATGACAGATGCAATTAGGG	FMP32R	GATCAAGTTTGAAACCGGCGT
CEN3+5Kb F	GCTCAACTCCTTTCCATTTGGTTGC	CEN3+5Kb R	GTGATGATATTTCTGCCCTGCC

Appendix 2 (cont). Primers

CEN3-5Kb F	AGACATCAAAGCAAAACTGCTGG	CEN3-5Kb R	GCATCATTTTTATCACGAGCGG
Non-centromeric sites repetitive sites			
Forward Primers	sequence	Reverse Primers	sequence
YNL284c-b Ty F	CATTTCTCATGGTAGCGCCTGT	YNL284c-b Ty R	TGATGAAGCAGGTGTTGTTGTC
YGR038c-a F	TCACATATATCTCATGGTAGCGCC	YGR038c-a R	GCAGGTGTTGTTGTCTGTTGAG
rDNA37 NTS2-1 F	AGTTTGTCCAAATTCTCCGCTC	rDNA37 NTS2-1 R	ACGTCCCTGCCCTTTGTACACA
rDNA37 NTS2-2 R	CAAACGGTGGAGAGAGTCGCTA	rDNA37 NTS2-2 F	ACGCAAAAGAAACACACTCTGGG
Nucleosome Reconstitution			
Forward Primers	sequence	Reverse Primers	sequence
Chr6-NB-F	TCGATACGCATAAACTAGC	Chr6-NB-R	TAACATTTGGATGCTCTGAC
601L-5'	ACAGGATGTATATATCTGACACGTGCC	601L-216-3'	TGACCAAGGAAAGCATGATTCT
Gal4 UAS			
Forward Primers	sequence	Reverse Primers	sequence
YOL118c-5 F	CTTTCATCTGTACCATTGGGAG	YOL118c-5 R	CCGTGTGCCAAGGAATATTT
Gal2UAS F	CAAGGAGGTTTACGGACCAG	Gal2UAS R	AACCGCCCCTTTCGAATATA

Appendix 3. Cse4 ChIP-chip

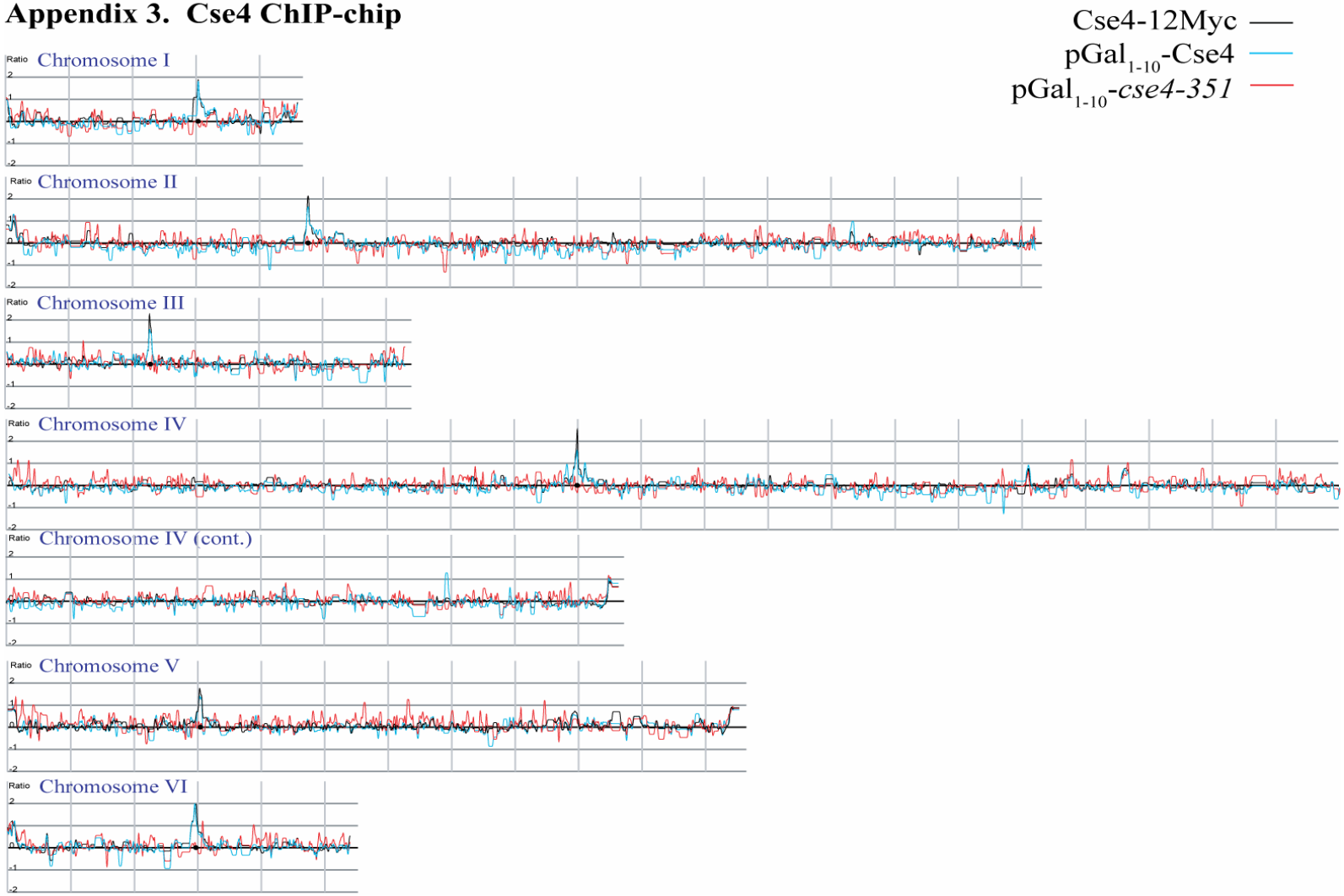

Appendix 3 (cont). Cse4 ChIP-chip

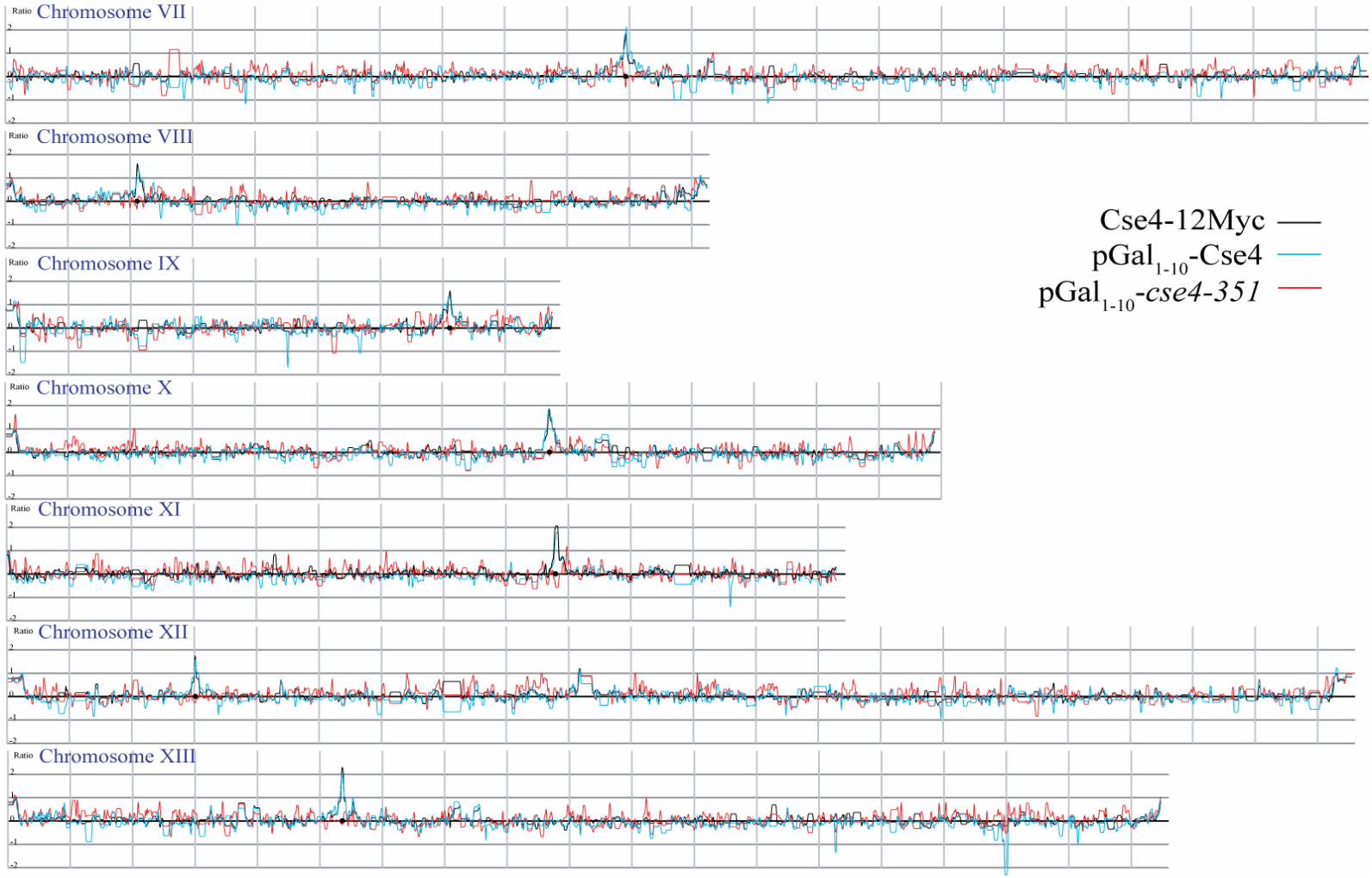

Appendix 3 (cont). Cse4 ChIP-chip

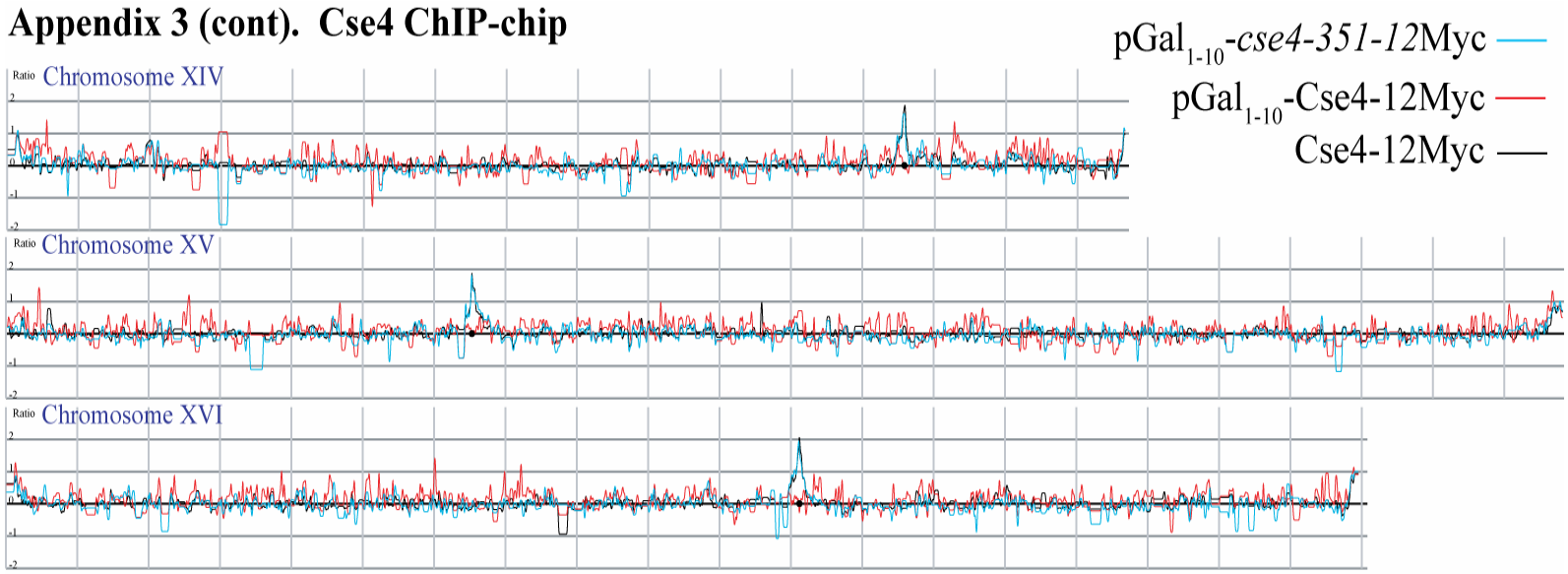

Appendix 3. Cse4 Chip-chip

Cultures expressing Cse4-12Myc, pGAL$_{1\text{-}10}$-Cse4-12Myc, or pGAL$_{1\text{-}10}$-*cse4-351*-12Myc were grown to mid-log phase and arrested in metaphase with nocodazole. ChIP-chip was performed using two independent biological samples and the results were averaged. PeakFinder display [26] of the pattern of Cse4-12Myc (black), pGAL$_{1\text{-}10}$-Cse4-12Myc (cyan), and pGAL$_{1\text{-}10}$-cse4-351-12Myc (red) on all 16 *S. cerevisiae* chromosomes. The centromere is indicated by a filled black circle. 50kb intervals on each chromosome are shown. Peaks were sujected to 8 rounds of Gaussian smoothing.

Appendix 4. Published papers and Meeting Abstracts

Publications

Camahort R., Mattingly, M., Li, B., Nakanishi, S., Zhu, D., Shilatifard, A., Workman, J.L., Gerton, J.L. Cse4 is part of an octameric nucleosome in budding yeast. (Submitted, *Genes and Development*).

Camahort, R., Li, B., Florens, L., Swanson, S.K., Washburn, M.P., and Gerton, J.L. Scm3 is essential to recruit the histone H3 variant Cse4 to centromeres and to maintain a functional kinetochore. *Molecular Cell*, 2007, **26**, 853-865. Commented on in: *Cell*, 2007. **129**(6): p. 1047-1049.; and *Nat Rev Mol Cell Biol*, 2007. **8**(8): p. 598-599.

Collins, K.A, Camahort, R., Seidel, C., Gerton, J.L., Biggins, S. The overexpression of a Saccharomyces cerevisiae centromeric histone H3 variant mutant protein leads to a defect in kinetochore biorientation. *Genetics*, 2007, **175**(2):513-25.

Henry, J.M., Camahort, R., Rice D.A., Florens, L., Swanson, S.K., Washburn, M.P., Gerton, J.L. Mnd1/Hop2 facilitates Dmc1-dependent interhomolog crossover formation in meiosis of budding yeast. *Mol. Cell. Biol*., 2006, **26**:2913-2923. (Work performed as a lab technician).

Meetings Abstracts and Presentations

Camahort, R., Gerton, J. Scm3 is a novel kinetochore protein required for formation and maintenance of a function kinetochore. Chromatin Structure and Function Meeting, Punta Cana, Dominican Republic, December, 2006 (poster).

Camahort, R., Gerton, J. Scm3p: A novel protein required for formation and maintenance of functional kinetochores in *S. cerevisiae*. NIH National Graduate Student Research Festival. National Institute of Health, Bethesda, MD., October, 2006 (poster).

Camahort, R., Gerton, J. Characterization of Scm3p: A Protein Required for Kinetochore Formation and Proper Chromosome Segregation in Budding Yeast. Stowers Institute for Medical Research Young Investigator's Research Day, Kansas City, April, 2006 (talk).

Camahort, R., Seidel, C., Gerton, J. Genome-Wide Localization of *Saccharomyces cerevisiae* Cse4p. Chromatin Structure and Function Meeting, Nassau, Bahamas, November, 2005 (poster).

Appendix 5. Collaborator's Contributions.

I would like to thank and acknowledge the collaborators listed below for their contributions to the following figures.

Figure 4 A. L. Florens, S. Swanson, and M. Washburn performed the mass spectrometry.

Figure 4 B. J. Gerton performed the chromatin fractionations and the salt challenge assay.

Figure 18 B-D. D. Zhu performed the statistical analysis and created the box plots.

Figure 22 A-C. J. Gerton performed the immunoprecipitations and the Western blots.

Figure 23 A. J. Gerton performed the knock-out suppression assay.

Figure 23 B. M. Mattingly performed the dilution assay.

Figure 25 A-C. B. Li performed the histone preparation and the octamer. reconstitutions.

Figure 26 A-B. B. Li performed the nucleosome reconstitution and the DnaseI assay.

Figure 29 A. The Stowers Institute Molecular Biology Facility performed the alanine scanning mutagenesis and S. Nakanishi performed the plasmid shuffle assay.